Central α-Klotho is a Novel Regulator of Arcuate Neurons and Peripheral Metabolism

By

Taylor Landry

May 2021

Director of Dissertation: Hu Huang

Major Department: Kinesiology

The arcuate nucleus of the hypothalamus (ARC) is a critical nexus of neuron populations that interpret peripheral signals of energy status and deliver diverse efferent outputs to metabolically active tissues. These neurons are critical to maintaining energy homeostasis, and disruption of their complex neurocircuitry results in metabolic disease phenotypes. The goals of this dissertation were to investigate the novel role for the circulating α-klotho protein to regulate neurons within the ARC to modulate peripheral metabolism.

Intracerebroventricular administration of a recombinant α-klotho in lean, obese, and type I diabetic mice for 1-12 days revealed a novel role for α-klotho to regulate whole body energy and glucose metabolism. α-Klotho-treated mice experienced suppressed food intake, increased energy expenditure, and improved glucose clearance. Central α-klotho-mediated regulation of peripheral glucose metabolism was determined to be independent from body weight and insulin sensitivity but may be due to reduced hepatic gluconeogenic gene expression and improved insulin secretion. Furthermore, cerebrospinal fluid collected from humans demonstrated body weight is strongly and negatively correlated to α-klotho concentrations, suggesting central α-klotho is also important to energy homeostasis in humans.

Experiments utilizing *ex vivo* patch clamp electrophysiology, immunohistochemical detection of the neuronal activation marker cFOS, and the immortal GT1-7 hypothalamic cell line demonstrated a novel role for α-klotho to regulate neurons in the ARC. α-Klotho decreased activity of the orexigenic neuropeptide Y/agouti-related peptide neuron population and increased activity of a subset of the anorexigenic proopiomelanocortin neuron population. α-Klotho was also shown to regulate the non-neuronal ARC astrocytes, which are involved in hormonal transport, nutrient-sensing, and neuronal health.

Mechanistically, ICV pretreatment with inhibitors of fibroblast growth factor receptors (FGFR's) or PI3kinase signaling attenuated the therapeutic effects of α-klotho, as well as its ability to modulate hypothalamic neuron activity. Overall, these studies identify a novel α-klotho→FGFR→PI3kinase signaling axis in ARC neurons that is critically involved in homeostatic regulation of energy and glucose metabolism. Identification of this molecular mechanism may facilitate the development of novel therapeutic approaches to metabolic disease and may also identify α-klotho as a preclinical marker of these disorders.

Central α-Klotho is a Novel Regulator of Arcuate Neurons and Peripheral Metabolism

A Dissertation

Presented to the Faculty of the Department of Kinesiology

East Carolina University

In Partial Fulfillment of the Requirements for the Degree

Doctorate of Philosophy in Bioenergetics and Exercise Science

By

Taylor Landry

May, 2021

Central α-Klotho is a Novel Regulator of Arcuate Neurons and Peripheral Metabolism

By,

Taylor Landry

APPROVED BY:

DIRECTOR OF DISSERTATION

_____

Hu Huang, PhD

COMMITTEE MEMBER:

_____

Joseph Houmard, PhD

COMMITTEE MEMBER:

_____

Ronald Cortright, PhD

COMMITTEE MEMBER:

_____

Srinivas Sriramula, PhD

CHAIR OF THE DEPARTMENT OF KINESIOLOGY

_____

JK Yun, PhD

DEAN OF THE GRADUATE SCHOOL

_____

Paul J. Gemperline, PhD

Acknowledgements

This dissertation is the product of countless individual efforts ranging from direct contributions from valuable colleagues and collaborators to indirect contributions from my beloved friends and family. Beginning with my mentor, Dr. Hu Huang, who took a chance on me when I had no background in neuroscience, benchwork, or animal studies. Dr. Huang provided me the tools, opportunities, and guidance to thrive during my doctoral studies. Second, Drs. Ron Cortright, Srinivas Sriramula, and Joe Houmard comprised my dissertation committee, providing priceless insight facilitating experimental development, data collection, analysis, and conclusions of my project. And then there were the many members of the East Carolina Diabetes and Obesity Institute who provided technical and emotional support daily. I'd like to name Alec Chaves specifically, for the coffee runs, gym time, evening beers, brainstorming sessions, and never-to-be-repeated venting periods, which were all integral to my sanity over the last four years.

I would also like to thank my mentors at James Madison University for providing guidance instrumental to my career choices thus far. Drs. Chris Womack, Mike Saunders, and Nick Luden, your passion, kindness, and wisdom are exceptional, and it is a big part of what makes the Kinesiology Department at JMU one of a kind.

Last but not least are my loved ones. Mom, Dad, and Nicole (sister), you all shaped and groomed me into the man I am today. Thank you for challenging me, pushing me outside my comfort zones, and giving me the freedom to forge my own path. And finally, Arieanne Creighton (fiancé), thank you for being my main confidant, my support, and my escape. Having you to come home to was always a brilliant light at the end of sometimes dark tunnels...and sorry for always vastly underestimating how long I'll be in lab. Thank you all.

Table of Contents

List of Tables.....vii

List of Figures.....viii

Abbreviations.....xi

CHAPTER 1: Introduction.....1

Chapter 1 Figures.....20

Statement of Problem.....23

Main Objective.....23

Hypothesis.....24

CHAPTER 2: Central α-klotho suppresses NPY/AgRP neuron activity and regulates metabolism in mice.....25

Abstract.....25

Introduction.....26

Methods.....27

Results.....33

Discussion.....37

Figures.....43

CHAPTER 3: Centrally circulating α-klotho inversely correlates with human obesity and modulates arcuate neuron populations in mice.....69

Abstract.....69

Introduction.....71

Methods.....72

Results.....78

Discussion.....82

Figures.....88

CHAPTER 4:

Conclusions.....112

Figures.....115

REFERENCES.....118

APPENDIX A: IACUC Approval – AUP 101.....136

APPENDIX B: IACUC Approval – AUP 085.....137

List of Tables

Chapter 2-

Supplemental Table 2.1: Primer Sequences Used for qPCR.....59

Chapter 3-

Supplemental Table 3.1: Human Subject Characteristics.....102

Supplemental Table 3.2: Primer Sequences Used for qPCR.....103

List of Figures

Chapter 1-

Figure 1.1: Arcuate Nucleus Control of Metabolism.....22

Chapter 2-

Figure 2.1: 7 Days Central Administration of α-Klotho Results in Weight Loss, Suppressed Food Intake, and Improved Glucose Regulation in DIO Mice.....51

Figure 2.2: Acute Central Administration of α-Klotho Improves Glucose Clearance and Suppresses Food Intake Independent of Body Weight in DIO Mice.....52

Figure 2.3: 7 Days Central α-Klotho Administration Attenuates the Progression of Diabetes in STZ-treated Mice.....53

Figure 2.4: Central α-Klotho Inhibition Impairs Glucose Tolerance.....54

Figure 2.5: α-Klotho Suppresses NPY/AgRP Neuron Activity, at least in part, by enhancing mIPSC's.....55

.Figure 2.6: α-Klotho-mediated cell signaling and regulation of NPY/AgRP neurons in the hypothalamus is dependent on FGFR's.....56

Figure 2.7: Central Inhibition of FGFR1 Blunts the Therapeutic Effects of 7 Days α-Klotho in DIO Mice.....57

Figure 2.8: Central Inhibition of PI3kinase Negates the Therapeutic Effects of a Single α-Klotho Injection in DIO Mice.....58

Supplemental Figure 2.1: Validation of ICV Cannulation Procedure.....60

Supplemental Figure 2.2: Effects of ICV α-Klotho in STZ-treated Mice.....61

Supplemental Figure 2.3: 12 days ICV α-Klotho Treatment does not Affect Insulin Sensitivity in Peripheral Tissues of DIO Mice.....62
Supplemental Figure 2.4: 12 days ICV α-Klotho Treatment Alters mRNA Levels of Key Metabolic Genes in the Liver.....63
Supplemental Figure 2.5: 7 Days ICV Treatment with Anti-α-Klotho Antibody has no Significant Effects on Hypothalamic Gene Expression, Liver Gene Expression, or Skeletal Muscle $pAKT^{ser473}$.....64
Supplemental Figure 2.6: α-Klotho Alters Cell Signaling and Neuronal Activity in the Hypothalamus.....65
Supplemental Figure 2.7: ICV α-Klotho does not Cause Additional Stress in Mice.....66
Supplemental Figure 2.8: 7 days ICV α-Klotho Treatment Improves Glucose Regulation and Suppresses Food Intake in Female DIO Mice.....67
Supplemental Figure 2.9: 7 Days ICV α-Klotho Treatment Suppresses Food Intake in Healthy Chow-Fed Mice.....68

Chapter 3-

Figure 3.1: Cerebrospinal Fluid α-Klotho Concentrations are Reduced in Overweight and Obese Adults.....94
Figure 3.2: Two Days ICV α-Klotho Treatment Increases Energy Expenditure in DIO Mice.....95
Figure 3.3: Acute ICV α-Klotho Treatment has no Effects on TH-expressing Neuron Activity in the ARC or PVN.....96
Figure 3.4: Acute ICV α-Klotho Treatment Increases ARC POMC Neuron Activity in Fasted Mice.....97

Figure 3.5: Central α-Klotho Increases ARC POMC Neuron Activity, at least in part, via FGFR's.....98
Figure 3.6: PI3kinase Inhibition Blunts α-Klotho-mediated ARC POMC Neuron Activation.....99
Figure 3.7: PI3kinase Inhibition Abolishes α-Klotho-mediated ARC NPY/AgRP Neuron Inhibition.....100
Figure 3.8: Acute ICV α-Klotho Treatment Stimulates Phosphorylated ERK$^{thr202/tyr204}$ in Astrocytes.....101
Supplemental Figure 3.1: Experimental Timeline of Indirect Calorimetry Experiments.....104
Supplemental Figure 3.2: Two Days ICV α-Klotho Treatment Decreases Food Intake and Reduces Body Weight in DIO Mice.....105
Supplemental Figure 3.3: POMC-expressing Neurons Exhibit a Heterogenous Response to α-Klotho Treatment.....106
Supplemental Figure 3.4: ICV α-Klotho Treatment has no Effects on POMC Neuron Activity in Fed Mice.....107
Supplemental Figure 3.5: Acute ICV α-Klotho Treatment Increases pSTAT3^{ser753} in NPY-Expressing Neurons.....108
Supplemental Figure 3.6: Twelve Days ICV α-Klotho Treatment Increases Ki67 Expression in the ARC of DIO Mice.....109
Supplemental Figure 3.7: Twelve Days ICV α-Klotho Treatment has no Effects on ARC Neurogenesis in DIO Mice.....110

Chapter 4-

Figure 4.1: Graphical Abstract.....11

List of Abbreviations

AAV -Adeno-associated virus
ACC – Acetyl coenzyme A carboxylase
aCSF – Artificial cerebrospinal fluid
ADAM - A disintegrin and metalloprotease
AgRP – Agouti-related peptide
AMPK – Adenosine monophosphate kinase
ANOVA – Analysis of variance
AUP – Animal use protocol
αMSH – α-melanocyte-stimulating hormone
APP – Amyloid precursor protein
ARC – Arcuate nucleus
ATP – Adenosine triphosphate
BACE-1 – β amyloid precursor protein converting enzyme 1
BAT – Brown adipose tissue
BBB – Blood-brain barrier
BMI – Body mass index
CAMKK – Calcium-calmodulin dependent protein kinase kinase
CCK – Cholecystokinin
C/EBPα - CCAAT/enhancer-binding protein α
CIDEA - Cell death activator CIDE-A
CNS – Central nervous system
CPT1 – Carnitine palmitoyl transferase 1
CSF – Cerebrospinal fluid
Dcx - Doublecortin
DIO – Diet-induced obesity
EE – Energy expenditure
ERK – Extracellular-regulated kinase
eWAT – Epididymal adipose tissue
ELISA – Enzyme-linked immunoabsorbant assay
FAS – Fatty acid synthase
FGF – Fibroblast growth factor
FGFR – Fibroblast growth factor receptor
FOXO – Forkhead box protein
G6Pase – Glucose 6 Phosphatase
GABA – Gamma-aminobutyric acid
GFAP – Glial fibrillary acid protein
GFP – Green fluorescent protein
GHSR – Growth hormone secretagogue receptor
GK - Glucokinase
GLUT – Glucose transporter
GPCR – G-protein coupled receptor
GTT – Glucose tolerance test
HCl – Hydrochloric acid
HDL – High-density lipoprotein

HMG-CoA - β-Hydroxy β-methylglutaryl coenzyme A
IACUC - Institutional animal care and use committee
ICV - Intracerebroventricular
IGF – Insulin-like growth factor
IGFR – Insulin-like growth factor receptor
IP - Intraperitoneal
IPSC – Inhibitory post-synaptic current
IR – Insulin receptor
ITT – Insulin tolerance test
KATP channel – ATP-sensitive potassium channel
LBPN – Lateral parabrachial nucleus
LiCl – Lithium chloride
MC4R – Melanocortin Receptor 4
mRNA – messenger ribonucleic acid
mTORC1 – Mammalian target of rapomyosin complex 1
NADPH – Oxidized Nicotinamide adenine dinucleotide phosphate
NPY – Neuropeptide Y
NRF1 – Nuclear respiratory factor 1
NTS – Nucleus of the solitary tract
PBS – Phosphate-buffered saline
PCR – Polymerase chain reaction
PEPCK – Phosphoenol-pyruvate carboxykinase
PGC1α - Peroxisome proliferator activated receptor γ coactivator alpha
PI3K – Phosphatidyl-inositol 3 kinase
PK – Pyruvate kinase
POMC – Proopiomelanocortin
PPARγ – Peroxisome proliferator activated receptor γ
PRDM16 – PR domain containing 16
Prx – Peroredoxin
Ptx – Picrotoxin
PVN – Paraventricular nucleus
qPCR – Quantitative polymerase chain reaction
RNA – Ribonucleic acid
ROS – Reactive oxygen species
SD – Standard deviation
SEM – Standard error of measurement
STAT3 – Signal transducer and activator of transcription 3
STZ – Streptozotocin
TBST – Tris-buffered saline with triton
TFAM – Mitochondrial transcription factor A
TG – triglyceride
TH – Tyrosine hydroxylase
TNFα – Tumor necrosis factor α
TRPV – Transient receptor potential cation channel subfamily V
Trx – Thioredoxin
Ttx – Tetrodotoxin

TXNIP – Thioredoxin interacting protein
UCP1 – Uncoupling protein 1
WAT – White adipose tissue

Chapter 1

Introduction

1.1. Diabetes and Obesity Epidemics

Metabolic diseases are increasingly prevalent in today's society, with the National Institute of Health estimating greater than 67% of adults in the United States are overweight or obese and approximately 10.5% suffer from diabetes [1]. These diseases are characterized by chronic energy surplus and dysfunctional substrate utilization, drastically increasing incidence and severity of various disorders including: cardiovascular disease [2], cancers [3], neurodegenerative diseases [4], psychiatric disorders [5], infection [6], liver disease [7], and kidney disease [8]. As a result, diabetes and obesity severely increase all-cause mortality and cause an estimated annual economic burden to the United States of $474-$537 billion [9].

The underlying causes of diabetes and obesity are a subject of debate in the scientific community, but these diseases are usually associated with disordered metabolism in one or more organ systems. The liver, skeletal muscle, adipose tissue, pancreas, kidneys, and heart are all intricately involved in homeostatic regulation of energy balance and substrate utilization. Interestingly, all these peripheral organs receive efferent inputs from the central nervous system (CNS) to modulate their function. Consequently, the CNS is a prominent focus of investigation for its potent ability to respond to nutritional and hormonal changes in the blood and regulate multiple organ system function accordingly.

1.2. The Arcuate Nucleus of the Hypothalamus Regulates Whole-Body Metabolism

The arcuate nucleus (ARC), located in the medio-basal hypothalamus, contains diverse neuron populations critically involved in metabolic regulation. ARC neuron populations are

located immediately adjacent to the third ventricle and cerebrospinal fluid (CSF), allowing for convenient nutrient- and hormone-sensing [10,11]. These neurons, including orexigenic (appetite-inducing) neuropeptide Y/agouti-related peptide (NPY/AgRP) and tyrosine hydroxylase (TH) neurons and anorexigenic (appetite-suppressing) proopiomelanocortin (POMC) neurons, then coordinate and project to various areas of the brain to ultimately deliver efferent signals to peripheral tissues.

1.2.1. POMC Neurons-

ARC POMC-expressing neurons release POMC neuropeptide, which is cleaved into α-melanocyte-stimulating hormone (αMSH) and subsequently binds to and stimulates CNS melanocortin 4 receptors (MC4R's) [12–16]. MC4R's are densely located in neurons within the paraventricular nucleus of the hypothalamus (PVN) that then project to various areas of the brain, including the nucleus of the solitary tract (NTS) and lateral parabrachial nucleus (LBPN), to ultimately regulate autonomic efferent signals to metabolically active tissues [15–19]. For example, POMC activity modulates sympathetic outflow to white adipose tissue (WAT), brown adipose tissue (BAT), and liver, which results in altered gene expression and covalent modification of key enzymes involved in substrate metabolism [12–14,20–22]. Through this neurocircuitry, POMC neuron activation is associated with satiety, increased locomotion, upregulated BAT thermogenesis, improved adipose insulin sensitivity, and reduced hepatic glucose output [12–14,20–22]. Consequently, insufficient POMC activity, or dysregulation of any of its downstream targets, results in metabolic disease phenotypes [11–13,23–25].

Notably, POMC-expressing neurons have been shown to be heterogenous in their neurotransmitter and cell surface receptor expression [26,27]. For example, while the canonical

POMC-expressing neuron expresses high POMC neuropeptide, about 28% of POMC neurons express low POMC and high AgRP. Additionally, POMC neurons differ in their expression of leptin and insulin receptors, identifying significant differences in regulatory mechanisms in this neuron population. Overall, the heterogeneity of this neuron population provides a challenge when characterizing their physiological and molecular functions.

1.2.2. NPY/AgRP Neurons-

NPY/AgRP neurons co-express both the NPY and AgRP neuropeptides, as well as the inhibitory neurotransmitter gamma-aminobutyric acid (GABA). These neurons play a corollary role to POMC neurons by directly antagonizing MC4R-expressing PVN neurons via Y receptors, as well as POMC neurons themselves via GABA [17–19,28,29]. As a result, NPY/AgRP neuron activation elicits rapid food intake, sedentary behavior, reduced thermogenesis, hepatic glucose output, hyperinsulinemia, skeletal muscle insulin resistance, and increased adipose glucose uptake [10,30–38]. Furthermore, overactivity of NPY/AgRP neurons results in hyperphagia, hyperglycemia, and obesity [34,35,39,40].

Neuronal crosstalk within the ARC is also very important to metabolic regulation. For example, NPY/AgRP neurons regulate TH neuron activity and subsequent BAT thermogenesis via NPY action on Y1 receptors [37,41]. Additionally, as previously mentioned, opto- or chemo-genetic NPY/AgRP activation elicits GABA-mediated POMC inhibition [28,42]. However, disrupted NPY/AgRP neuron activity or neurotransmitter release has no effects on POMC inhibitory post-synaptic currents (IPSC's) [28,43], resulting in the physiological relevance of NPY/AgRP→POMC connectivity being unclear.

1.2.3. TH Neurons-

TH is the rate limiting enzyme in dopamine and catecholamine synthesis [44]. Recently, ARC and PVN TH-expressing neurons have been shown to release dopamine and GABA to regulate energy balance [37,45]. Optogenetic ARC TH neuron activation elicits food intake, while disrupted release of these neurotransmitters has opposite effects [45], and PVN TH neurons increase sympathetic outflow to BAT to stimulate thermogenesis [37]. The neurocircuitry underlying ARC TH neuron function is still a new area of research, but TH projections have been observed in PVN neurons [45]. Furthermore, ARC TH neurons directly excite NPY/AgRP neurons via dopamine release and inhibit POMC neurons via both GABA and dopamine [45]. TH neurons may also be involved in the pathology of metabolic disease, demonstrated by overactivity of TH neurons resulting in hyperphagia and obesity [46].

1.2.4. Nutritional and Hormonal Control of the ARC-

Glucose-sensing and responsiveness in ARC neuron populations is critical to maintaining euglycemia and energy balance. Glucose and monocarboxylate transporters facilitate glucose, lactate, and pyruvate entry and metabolism in neurons, which increases ATP levels and alters neuronal firing [47]. More specifically, NPY/AgRP and POMC neurons are glucose-inhibited and glucose-excited, respectively [48,49]. Changes in ATP levels in these neurons modulates ATP-sensitive potassium channels (KATP), alters potassium flux, and therefore regulates membrane potential [48,49]. The importance of these glucose sensing mechanisms is underscored by studies observing mutant KATP channels specifically in NPY/AgRP or POMC neurons resulting in poor maintenance of glucose homeostasis [48].

Equally important to ARC neuron regulation are hormones released from peripheral organs. The plethora of metabolic hormones released from adipose, gut, and the pancreas allow for fine communication between peripheral and central metabolism. For example, ghrelin is a hunger-inducing hormone released primarily from the distal stomach in response to low glucose concentrations and decreased stomach distention [50,51]. While there is no known ghrelin receptor on POMC neurons, circulating ghrelin stimulates NPY/AgRP neuron activity via growth hormone secretagogue receptors (GHSR's), a subtype of G-protein coupled receptors (GPCR's) [52]. Mechanistically, ghrelin indirectly stimulates NPY/AgRP neuron activity by acting on presynaptic neurons to elicit Gq-coupled signaling and downstream CAMKK and AMPK activation, increased calcium flux, and glutamate release [53]. Ghrelin→GHSR signaling has also been shown to be critical to hunger and hepatic glucose output by directly increasing NPY/AgRP neuron activity and neuropeptide gene expression [52,54,55].

While ghrelin is the only known "hunger-inducing" hormone, there are many "satiety-inducing" neurons, including leptin, insulin, cholecystokinin (CCK), peptide YY, and glucagon-like peptide. Leptin is released from adipose tissue, is essential to promoting satiety, thermogenesis, and reduced glucose output, and has even been shown to be therapeutic in metabolic disease models [56–64]. Leptin's physiological functions are, in part, mediated by its role as a key negative regulator of NPY/AgRP and TH neurons and positive regulator POMC neurons [10,12,19,32,46,62,65,66]. Leptin binds to tyrosine kinase leptin receptors on these neurons and elicits downstream rho kinase 1-mediated phosphorylation of janus kinase 2, which stimulates dimerization and phosphorylation of signal transducer and activator of transcription 3 (STAT3) [66]. This phosphorylation of STAT3, as well as activation of PI3kinase (PI3K) signaling, regulates neuropeptide gene expression and KATP channel activity [19,23,67,68].

Notably, the leptin and leptin receptor deficient transgenic mice have become renowned models of extreme early onset obesity and reintroduction of leptin activity specifically in ARC neurons drastically rescues these phenotypes [12,58,69–72].

Insulin is another key regulatory hormone in ARC neurons, stimulating satiety, reduced glucose output, and increased energy expenditure [39,73]. Insulin is released from the pancreatic β cells in response to elevated glucose levels and binds to tyrosine kinase insulin receptors to inhibit or excite NPY/AgRP and POMC neurons, respectively. Downstream of insulin receptor is PI3K signaling, which regulates neuropeptide gene expression via forkhead box protein (FOXO) and modulates KATP channels [21,39,74,75].

Additional hormones with satiety functions in the central nervous system are CCK, peptide YY, and glucagon-like peptide, which are all released from the small intestine in response to changes in glucose and gut distention [76–80]. CCK and glucagon-like peptide act via GPCR's and peptide YY via inhibition of Y receptors to elicit similar physiological effects to insulin and leptin [76–80]. Overall, these gut hormones, insulin, and leptin coordinate to relay peripheral signals to the central nervous system and ultimately maintain energy and substrate homeostasis.

1.2.5. Resistance to satiety hormones and metabolic disease-

Considering the potent physiological functions of leptin, insulin, peptide YY, and CCK, studies have identified promising therapeutic effects in response to acute exogenous treatment with these hormones in metabolic disease models [61,72,81–84]. Unfortunately, chronic administration with these hormones has diminishing returns, largely due to metabolic disease pathologies resulting in resistances to satiety hormones' physiological effects, including in ARC

neurons [32,66,84–88]. Studies have implicated inflammation and reactive oxygen species to hormonal resistances observed in diabetes in obesity, but these phenomena are complex, multifaceted, and poorly understood [89]. Overall, the diminishing central functions of leptin, insulin, and other satiety hormones in metabolic disease states highlight the value of identifying novel hormonal regulators of ARC neuron populations. Furthermore, characterizing the molecular mechanisms underlying novel hormonal ARC regulators could facilitate the development of new therapeutic targets for diabetes and obesity.

1.3. α-Klotho: The Anti-Aging Protein

Approximately 24 years ago the α-klotho gene was discovered when a study revealed mutation of a single gene within Chromosome 13 results in a rapid, premature aging phenotype [90]. α-Klotho overexpression has since been researched for its ability to prolong the lifespan 20-30% in rodents [91], as well as its therapeutic potential in various neurological [92–96], metabolic [69,97–103], cardiorespiratory [104–113], osmolar, [114–117] and cancer-related diseases/disorders [118]. More recently, in an attempt to combat the unrelenting obesity and diabetes epidemics, studies have begun to elucidate the specific roles of α-klotho in the regulation of energy and substrate metabolism. Increasing evidence demonstrates reduced central and peripheral α-klotho concentrations in humans with metabolic disease, suggesting its involvement in the pathology of these disorders. However, the role of α-klotho in metabolic regulation is complex, in part due to α-klotho's diverse physiological functions and paradoxical effects on insulin activity [69,91,98,99,102]. Additionally, most studies utilize models involving whole-body α-klotho manipulation, which neglects its tissue-specific functions, especially considering α-klotho's inability to cross the blood-brain barrier (BBB) [92,119].

1.3.1. Structure of the α-Klotho Protein-

RNA-splice variants of the α-klotho gene encode either a transmembrane or secreted α-klotho protein [120,121]. Transmembrane α-klotho has ~1014 amino acids with a molecular weight of 130kD and is comprised of a signal sequence at its N-terminus, a single transmembrane helix domain near the C-terminus, two internal repeats (KL1 and KL2) between the two, and a small intracellular domain. Secreted α-klotho consists of only the KL1 domain and N-terminus, weighs 65kD, and has ~550 amino acids. Both transmembrane and secreted α-klotho exhibit enzymatic activity due to KL1 and KL2 domains possessing identical beta-glucuronidase and sialidase homology. Notably, the rodent α-klotho protein has ~86% homology with that of humans [120–122].

Transmembrane α-klotho can also undergo proteolytic cleaving between the KL1 domain and the transmembrane domain (α cut) or between the KL1 and KL2 domains (β cut) to release full or short form α-klotho into the circulation [123–125]. Similar to tumor necrosis factor α (TNFα) and amyloid precursor protein (APP), α-klotho is cleaved by members of the ADAM family (a disintegrin and metalloprotease) 10 and 17, as well as β APP converting enzyme 1 (BACE-1) [123,125,126]. Notably, while no specific α-klotho receptor has been discovered, both cleaved and secreted α-klotho exhibit diverse hormonal function in various tissues [124,127]. Little is known about what regulates the cleaving of transmembrane α-klotho, but insulin can augment this process via PI3kinase signaling [123]. Considering one of the first discovered metabolic functions of α-klotho was to inhibit insulin signaling [91,118,128,129], these findings may suggest a physiologically relevant negative feedback loop.

1.3.2. Regulation of α-Klotho Expression-

α-Klotho is primarily expressed in the kidneys and the choroid plexus of the brain; however low levels of expression are detected in many other tissues including: pituitary gland, placenta, skeletal muscle, adipose tissue, bladder, pancreas, testis, ovary, colon, and lungs [90,130]. Little is known about the regulation of α-klotho expression, but studies show it is upregulated by PPARy activity [131,132] and is downregulated by estradiol [133], HMG-CoA reductase [108], and angiotensin II (via an angiotensin 1 receptor) [127]. Studies investigating regulation of α-klotho expression are largely observational and produce mixed results. For example, one study determined plasma α-klotho concentrations fluctuate diurnally [134], with high concentrations around noon and low concentrations at midnight, while another observed no diurnal variations [135]. Sex differences in peripheral α-klotho expression are equally equivocal, with one study suggesting females have higher α-klotho levels [136] and another observing no differences [137]. Pedersen et. al. compared two popular commercially available α-klotho ELISA kits (Immuno-Biological Laboratories, Japan and Casabo, China) and discovered drastic variability between the two [136], suggesting the variability in results throughout the literature is likely due to unreliable α-klotho-detecting assays.

What is clearer in the literature is that peripheral α-klotho expression is inversely correlated with age in humans [105,134,136–138], as well as oxidative stress [99,109,139,140], endothelial dysfunction [141,142], and atherosclerosis [90] in rodents. Plasma α-klotho concentrations are also impaired in many human disease states, including cardiovascular disease [105] and diabetes [143–145], suggesting involvement in the pathology of these disorders. Additionally, human plasma α-klotho concentrations are positively correlated with HDL [105] and phosphate levels [137] and negatively correlated with triglycerides [138] and fibroblast

growth factor (FGF) 23 concentrations [137]. Currently, the relationship between plasma α-klotho concentrations and many vital physiological variables such as blood glucose, blood pressure, and calcium is unclear due to confounding medications commonly taken by the populations observed in these studies [105,136–138,146].

Notably, α-klotho functions as two independent pools in the CSF and the blood. In fact, there is no correlation between α-klotho concentrations in these pools, with significantly less in the CSF [147]. The few studies that have examined CSF α-klotho concentrations have determined no diurnal variations [148], decreased levels in females [147,148], an inverse correlation with age [148], and a positive correlation with FGF23 [147]. Additionally, human CSF α-klotho concentrations are reduced in some neurological disorders such as Alzheimer's disease [148] and Multiple Sclerosis [149].

1.3.3. Functions of α-Klotho-

While no specific α-klotho receptor has been discovered, a variety of α-klotho functions have been discovered throughout the body. Perhaps the most well-documented function of α-klotho is its role in the kidney regulating Vitamin D, phosphate, and calcium homeostasis. α-Klotho is a critical non-enzymatic scaffolding protein that tethers FGF23 to tyrosine kinase FGF receptors (FGFR's), without which FGF23/FGFR affinity is very low [150–152]. In the proximal renal tubule downstream α-klotho/FGF23/FGFR signaling decreases Vitamin D levels by decreasing gene expression of 25-hydroxyvitamin D 1-α-hydroxylase and increasing expression of 1,25-dihydroxyvitamin D 24-hydroxylase, the enzymes responsible for the synthesis and degradation of the bioactive form of Vitamin D, respectively [114,153]. This signaling mechanism is a negative feedback loop in response to elevated Vitamin D levels, and may also

be responsible for α-klotho-mediated downregulation of phosphate reabsorption and upregulation of calcium reabsorption [115,133,154–156]. Interestingly, FGF23 knockout mice exhibit a similar phenotype to α-klotho knockout mice, including growth impairment and premature death, highlighting the importance of α-klotho/FGF23/FGFR-mediated regulation of mineral homeostasis [157]. Furthermore, ablation of the enzyme responsible for Vitamin D synthesis, overexpression of the enzyme responsible for Vitamin D degradation, or dietary restriction of Vitamin D and phosphate markedly rescues the signature premature aging phenotype in these mutants [91,114,140,153].

α-Klotho also possesses β-glucuronidase enzymatic capabilities, which allow it to hydrolyze sugar residues on members of the "transient receptor potential cation channel subfamily V" (TRPV channels) and stabilize them on cell membranes [122,158]. Through this mechanism in TRPV5 channels, α-klotho increases calcium reabsorption in the distal renal tubules to promote calcium homeostasis [154–156,158]. Recently, α-klotho has also been observed to similarly regulate TRPV2 channels to promote calcium influx and insulin release in pancreatic beta cells [69,98].

Another mechanism through which α-klotho is involved in the aging process is via competitive inhibition of various Wnt ligands [139,159–161]. Wnt signaling is associated with stem cell proliferation, but overactivity of Wnt's is associated with aging and even tumorigenesis [159]. α-Klotho is an important competitive antagonist of many Wnt ligands and has even been shown to act as a tumor suppressor in human hepatocellular carcinoma and breast cancer via this mechanism [118,139,159–161].

Lastly, α-klotho is involved in various reactive oxygen species (ROS) buffering systems. α-Klotho interferes with insulin receptor autophosphorylation which relieves antagonism of

forkhead box (FOXO) transcription factors and increases transcription of antioxidative enzymes [140]. For example, α-klotho increases FOXO1, 3a, and 4 activity, augments superoxide dismutase and catalase transcription, and attenuates oxidative stress [103,140,162]. α-Klotho also upregulates the thioredoxin/peroxiredoxin (trx/prx) ROS buffering system and overall has been shown to improve resistance to the toxic effects of paraquat, streptozotocin, glutamate, and hydrogen peroxide [99,140,163].

1.4. Peripheral α-Klotho and Metabolism

1.4.1. Peripheral α-Klotho Inhibits Insulin Signaling, but does not Result in Clinical Insulin Resistance-

One of the first-identified metabolic functions of α-klotho was its ability, via unknown mechanisms, to interfere with autophosphorylation of the insulin/IGF1 receptor in myoblasts, adipocytes, and hepatocytes [91,118,128,129,164]. Consequently, α-klotho-knockout mice exhibit improved glucose clearance and GLUT4 expression, but also drastically stunted growth and premature death [90,100,128,164]. On the contrary, α-klotho overexpressing mice experience insulin resistance and prolonged lifespans with no differences in food intake, energy expenditure, or body weight, suggesting direct glucoregulatory action of α-klotho, independent of energy balance [91]. Since α-klotho-overexpressing mice do not experience hyperglycemia, adiposity, or hyperphagia associated with clinical insulin resistance [91,164], α-klotho is likely an important homeostatic modulator of insulin/IGF1 signaling to prevent hypoglycemia, regulate apoptosis, and enhance ROS buffering [94,95].

1.4.2. α-Klotho Facilitates Insulin Release and Glucose Uptake-

Despite α-klotho's role as a negative regulator of insulin signaling, α-klotho function is critical to homeostatic glucose clearance. Impaired α-klotho function exacerbates diabetic pathologies in various metabolic disease models [99,102,164–166], and many studies observe plasma α-klotho concentrations to be suppressed in humans with diabetes or obesity [143,145,167,168]. This documented inverse relationship between plasma α-klotho concentrations and incidence of metabolic disease suggests impaired α-klotho function may be directly involved in the development of these disorders, although some studies refute these findings and observe no correlation [169,170]. These mixed findings may be due to differing degrees of diabetes in the populations studied or, similar to leptin and insulin, α-klotho insensitivity may develop in some diabetic states. Nevertheless, recent studies have demonstrated encouraging therapeutic potential of α-klotho for diabetes and obesity.

Studies using the MIN6 β-cell line and α-klotho overexpression specifically in the pancreas have identified a prominent role of pancreatic α-klotho to increase insulin secretion, improve glucose tolerance, and reduce fasting glucose levels in mouse models of Type I and II diabetes [69,98,99]. Specifically the secreted/short form (~65kD, KL1 domain only) α-klotho hydrolyzes TRPV2 channels in pancreatic β-cells to increase calcium entry and facilitate insulin release [69,91,98,128]. Moreover, intraperitoneal (IP) injection with full length recombinant α-klotho also attenuates hyperglycemia, independent from insulin secretion [102,162,164], likely due to α-klotho's additional pancreatic role to preserve β-cell and islet health [69,99,102]. More specifically, α-klotho in the pancreas enhances β-cell proliferation, autophagy, and expression of insulin transcription factors, while attenuating oxidative stress, endoplasmic reticulum stress, and apoptosis [69,99]. α-Klotho inhibits caspase-3-mediated apoptosis in β-cells via integrin

β1→focal adhesion kinase→AKT signaling [99], while antioxidative action of α-klotho via inhibition of phosphorylated rac-1 and subsequent suppression of NADPH oxidase activity may also be involved [69]. Interestingly, there are no apparent effects of pancreatic α-klotho overexpression on insulin sensitivity in diabetic mice, and there is no glucoregulatory phenotype in lean mice [69,99].

A recent model using genetic overexpression or downregulation of soluble α-klotho in DIO mice reveals additional glucoregulatory functions of α-klotho in the liver [164]. Both *in vivo* and *in vitro* experiments demonstrate α-klotho increases hepatic glucokinase mRNA and decreases phosphoenolpyruvate carboxykinase mRNA, resulting in improved hepatic glucose uptake and glycogen storage, as well as reduced gluconeogenesis [100,164]. Consequently, while DIO mice experience reduced plasma α-klotho concentrations, further suppression of α-klotho exacerbates hyperglycemia, impaired insulin secretion, and insulin resistance [164]. Strikingly, rescuing α-klotho concentrations has opposite, therapeutic effects, although it is not clear if improved insulin sensitivity is indirectly a result of weight loss [164]. Mechanistically, α-klotho increases PPARy transcriptional activity by directly antagonizing insulin-like growth factor receptor 1 (IGFR1) and subsequently inhibiting downstream PI3kinase→AKT→mTORC1 signaling. Pharmacological inhibitor experiments have revealed this signaling pathway is critical to α-klotho-mediated glucose-lowering and modulation of hepatic gene expression.

1.4.3. Peripheral α-Klotho Increases Energy Expenditure and Increases Lipid Oxidation-

Increasing circulating α-klotho concentrations via IP injection or genetic manipulation attenuates weight gain and improves body composition in mouse models of metabolic disease, revealing a novel role of α-klotho in energy balance [97,162,164]. Food intake is unchanged in

these models, and α-klotho-knockout mice experience impaired thermogenesis, suggesting α-klotho is specifically involved in regulating energy expenditure [97,100,162,164]. Supporting this hypothesis, 4-weeks IP injection with α-klotho increases oxygen consumption in DIO mice; however, no changes in thermogenic gene expression are observed in BAT or epididymal white adipose tissue (WAT) [97]. Consequently, the mechanisms underlying α-klotho-mediated increases in energy expenditure require further research, including investigation into browning of other prominent WAT depots, such as inguinal WAT, and deciphering the molecular mechanisms involved.

While reduced lipid accumulation and improved body composition in DIO mice with experimentally increased α-klotho levels is, in part, due to increased energy expenditure, α-klotho also has a direct role in lipid metabolism in both liver and adipose tissue. α-Klotho modulates liver and WAT gene expression to favor lipid oxidation and decrease lipogenesis via a similar IGFR1→PI3kinase→AKT→mTORC1→PPARγ mechanism described above [97,164]. Paradoxically, one report using 3T3-L1 adipocytes observed α-klotho promotes adipocyte differentiation by inducing C/EBPα- and PPARγ gene expression [171]. One possible explanation for these findings is that DIO mice are in a status of energy surplus compared to healthy 3T3-L1 adipocytes; thus, α-klotho's predominant role in lipid metabolism may be dynamic and fluctuate with energy status. Overall, α-klotho's role in lipid metabolism is very recently discovered and requires further research.

1.4.4. The α-Klotho/FGF23/FGFR Complex-

The therapeutic potential of α-klotho in the treatment or prevention of metabolic disease is encouraging; however, the molecular mechanisms involved, ranging from target tissues, to cell

surface receptor, to intracellular signaling, remain poorly understood. α-Klotho's role as a scaffolding protein stabilizing the FGF23→FGFR complex to upregulate downstream signaling may be a promising avenue of future research [150–152]. While the FGF23→FGFR complex is primarily characterized for its role in regulation of mineral homeostasis, emerging evidence suggests potent antidiabetic and anti-obesogenic effects of FGFR activation, albeit via liver-derived FGF21 and intestine-derived FGF19 ligands [172–179]. Like the α-klotho→FGF23→ FGFR complex, FGF19 and FGF21 are tethered to FGFRs by the exclusively transmembrane β-klotho protein [180–182]. While the FGF ligands in these two complexes vary, the differences in downstream FGFR signaling and subsequent physiological effects are poorly understood. α-Klotho may elicit some of its metabolic effects by also activating FGFR's either via FGF23 or independently. This would shed significant light on the molecular mechanisms underlying α-klotho-mediated metabolic regulation, especially considering the metabolic effects of FGFR's have been popular topics in recent literature. For example, increased FGFR activity via FGF treatment, synthetic ligand, or β-klotho overexpression increases energy expenditure, promotes lipid oxidation, and improves glucose regulation [174–179,183–187], similar to the previously described roles of peripheral α-klotho. Future studies utilizing CrisprCas9 or inducible CreLoxP to perform tissue-specific genetic manipulation of different FGFR isoforms known to interact with α-klotho (FGFR's 1c, 3c, and 4 [151]) would be extremely valuable to deciphering the complex mechanisms underlying homeostatic and disordered α-klotho function in metabolism.

1.4.5. Summary of α-Klotho and Peripheral Metabolism-

To date, prominent roles of peripherally circulating α-klotho have been identified in the regulation of glucose metabolism, lipid metabolism, and energy expenditure; however, studies

utilizing whole-body α-klotho manipulation via genetic intervention or IP injection make drawing conclusions about α-klotho's tissue-specific metabolic functions and mechanisms challenging. Overall, various cell culture studies identify α-klotho as an important, ubiquitous, negative regulator of insulin signaling, but emerging evidence reveals α-klotho function is critical to homeostatic glucose clearance. For example, in the pancreas, α-klotho facilitates insulin release via TRPV channels and attenuates β cell apoptosis via integrin β1→focal adhesion kinase→AKT signaling. Furthermore, α-klotho promotes glucose uptake and glycogen synthesis, as well as suppresses gluconeogenesis in liver via IGFR1→PI3kinase→AKT→mTORC1→PPARγ signaling. Additional metabolic roles of peripheral α-klotho included increasing lipid oxidation in liver and WAT via similar IGFR1→PPARγ pathways and increasing whole-body energy expenditure through unknown mechanisms. Notably, blood α-klotho concentrations are reduced in metabolic disease models, and the most marked metabolic effects of α-klotho are observed in these disorders. This phenomenon suggests a possible direct role of impaired α-klotho function in the etiologies of diabetes and obesity. Overall, many questions surround α-klotho's metabolic functions and molecular mechanisms of action; however accumulating evidence implicates this circulating factor as a promising therapeutic target and preclinical marker in metabolic disorders.

1.5. Central α-Klotho-

Although high levels of α-klotho expression were observed in the choroid plexus during its discovery 24 years ago, little investigation has been made into its function in the brain [90]. To date, identified roles of brain α-klotho include regulation of baroreflex in rats [188],

myelination in cultured oligodendrocytes [95,189–191], and synaptic remodeling [192] and ROS buffering in hippocampal cells [94].

Similar to peripheral tissues, FGFR's have recently been popular subjects of metabolism research in the brain. ICV FGF19 and FGF21 elicit therapeutic effects via FGFR's, including decreased food intake, reduced weight, improved glucose clearance, inhibited NPY/AgRP neuron activity, and suppressed hepatic gluconeogenic gene expression [193–197]. Despite the encouraging evidence observing FGFR activation to elicit therapeutic effects in metabolic disease models, studies investigating FGFR involvement in the pathology of diabetes and obesity produce mixed results depending on animal model and experimental approach. ICV PD173074 (FGFR inhibitor) impairs glucose clearance in healthy rats, but is described as stress-related [198,199], and ICV PD173074 in DIO mice elicits no phenotype [193,200]. Furthermore, antibody-mediated inhibition of FGFR1 in rodents and monkeys increases energy expenditure, decreases food intake, and reduces body weight, while genetic deletion of FGFR1 in NPY/AgRP neurons also results in no metabolic phenotype [71,201,202]. Future studies should investigate the specific roles of FGFR's, their isoforms, and their neuronal effectors in central regulation of metabolism by performing selective deletion of FGFR isoforms in specific neurons of mature mice using the inducible Cre-LoxP system.

Brain-specific β-klotho knockout abolishes many of the weight-reducing and glucose-lowering effects of peripheral FGF19/21 administration [179,197,203]. Since β-klotho's role is to stabilize FGF19/21 interaction with FGFR's [180–182], this strongly indicates that brain FGFR's are the primary mediators of peripheral and central FGF19/21 metabolic function. Consequently, the potential involvement of an ARC α-klotho→FGFR signaling mechanism in

the regulation of metabolism would be valuable to understanding the pathologies of metabolic disease.

Chapter 1 Figures

Figure Legend:

Figure 1.1. Arcuate nucleus control of metabolism.

(A) Various circulating hormones relay signals from the periphery to the ARC and participate in ligand-mediated regulation of ARC neurons. **(B)** POMC neurons release αMSH to activate neuron populations in the PVN, commonly referred to as the satiety center. NPY/AgRP and dopamine neurons release their neurotransmitters to antagonize these neurons. **(C)** The PVN then communicates with different areas of the hindbrain, which then **(D)** deliver diverse efferent outputs to metabolic tissues regulating thermogenesis, glucose metabolism, and lipid metabolism.

Arcuate Control of Metabolism

B.

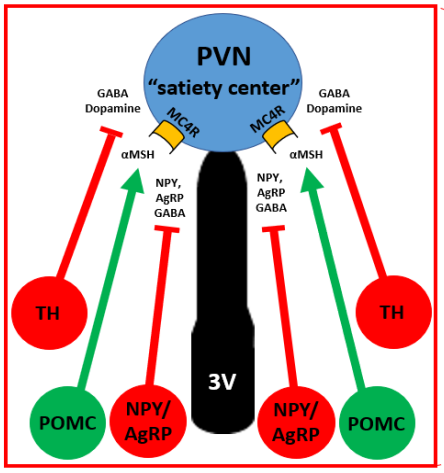

C.

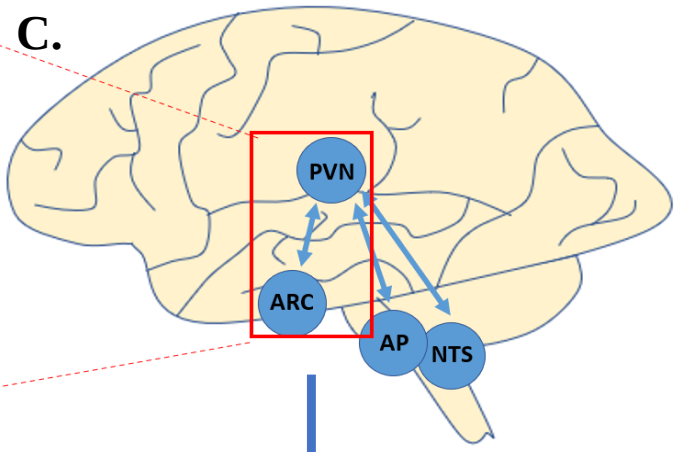

A.

Regulatory Hormones

Hormone and Source	Effects on NPY/AgRP Neurons	Effects on POMC Neurons
Insulin (pancreatic β cells)	-	+
Leptin (adipose tissue)	-	+
Ghrelin (stomach)	+	-
PYY (L cells of gut)	-	+
CCK (I cells of duodenum)	-	+
GLP-1 (L cells of gut)	-	+

D.

Efferent Signals

Behavioral Changes	Liver	Skeletal Muscle	White Adipose Tissue	Brown Adipose Tissue
• ↓ food intake • ↑ locomotor activity	• ↓ decreased gluconeogenesis • ↓ PEPCK • ↓G6P	• ↑ insulin sensitivity • ↓ lipogenesis • ↑ lipid oxidation • ↑ AMPK acitvity	• ↑ lipolysis via leptin • ↓ lipolysis via insulin	• ↑ thermogenesis • ↑UCP1 • ↑ glucose uptake

Legend

→ = regulates ↔ = 2-way regulation → = agonizes MC4R ⊣ = antagonizes MC4R

Abbreviations: PYY = peptide YY; CCK = cholecystokinin; GLP-1 = glucagon-like peptide 1; 3V = third ventricle; POMC = pro-opiomelanocortin neuron; AgRP = agouti-related peptide; NPY = neuropeptide Y; TH = tyrosine hydroxylase; GABA = gamma-aminobutyric acid; αMSH = α melanocortin-stimulating hormone; MC4R = melanocortin 4 receptor; PVN = periventricular nucleus; ARC = arcuate nucleus; AP = area postrema; NTS = nucleus of the solitary tract; PEPCK = phosphoenol-pyruvate carboxykinase; G6P = glucose 6 phosphatase; UCP1 = uncoupling protein 1

Statement of Problem

Obesity and diabetes are increasingly prominent diseases involving disordered energy balance and substrate metabolism in many metabolically active tissues throughout the body. The consequences of these metabolic diseases include decreased quality of life, increased mortality, and an overwhelming economic burden. As a result, investigation into homeostatic and disordered metabolic regulation is valuable to the discovery of novel therapeutic approaches to the prevention and treatment of these disorders.

The central nervous system is critical to metabolic regulation due to its ability to sense changes in nutrient status and deliver efferent outputs to peripheral tissues to maintain energy homeostasis. One specific area, the arcuate nucleus in the mediobasal hypothalamus, contains dense and diverse neuron populations that coordinate to regulate food intake, energy expenditure, locomotor activity, glucose metabolism, and lipid metabolism. These neurons have immediate proximity to the cerebrospinal fluid via the third ventricle, resulting in their fine regulation by changes in circulating hormones or nutrients. Unfortunately, in metabolic disease states, these neurons become decreasingly sensitive to circulating hormones like insulin and ghrelin, resulting in disordered metabolism including hyperphagia, hyperglycemia, and dyslipidemia. This phenomenon highlights the importance of identifying novel therapeutic regulators on neuron populations involved in metabolic regulation.

Main Objective

The circulating α-klotho protein has recently been identified to have metabolic functions in peripheral tissues including regulating lipid metabolism in liver and adipose, insulin secretion in pancreas, and glucose metabolism in liver. However, α-klotho cannot cross the blood brain

barrier and, to date, studies investigating potential metabolic functions of α-klotho in the central nervous system have been lacking. This dissertation aimed to identify and characterize the roles of α-klotho to regulate arcuate neuron populations critically involved in metabolic regulation.

Hypothesis

Considering α-klotho's documented structure and function in peripheral tissues, I hypothesize that centrally circulating α-klotho will inhibit NPY/AgRP and excite POMC neurons, thus promoting homeostatic energy and substrate metabolism.

Chapter 2

Central α-Klotho Suppresses NPY/AgRP Neuron Activity and Regulates Metabolism in Mice

ABSTRACT

α-Klotho is a circulating factor with well-documented anti-aging properties; however, the central role of α-klotho in metabolism remains largely unexplored. The current study investigated the potential role of central α-klotho to modulate NPY/AgRP neurons, energy balance, and glucose homeostasis. Intracerebroventricular (ICV) administration of α-klotho suppressed food intake, improved glucose profiles, and reduced body weight in mouse models of Type I and II diabetes. Furthermore, central α-klotho inhibition via an anti-α-klotho antibody impaired glucose tolerance. *Ex vivo* patch clamp electrophysiology and immunohistochemical analysis revealed that α-klotho suppresses NPY/AgRP neuron activity, at least in part, by enhancing mIPSC's. Experiments in hypothalamic GT1-7 cells observed α-klotho induces phosphorylation of AKT^{ser473}, $ERK^{thr202/tyr204}$, and $FOXO1^{ser256}$, as well as blunts AgRP gene transcription. Mechanistically, fibroblast growth factor 1 (FGFR1) inhibition abolished the downstream signaling of α-klotho, negated its ability to modulate NPY/AgRP neurons, and blunted its therapeutic effects. PI3 kinase inhibition also abolished α-klotho's ability to suppress food intake and improve glucose clearance. These results indicate a prominent role of hypothalamic α-klotho/FGFR1/PI3K signaling in the modulation of NPY/AgRP neuron activity and maintenance of energy homeostasis, thus providing new insight into the pathophysiology of metabolic disease.

T. Landry, B.T. Laing, P. Li, W. Bunner, Z. Rao, A. Prete, J. Sylvestri, H. Huang, Central α-Klotho Suppresses NPY/AgRP Neuron Activity and Regulates Metabolism in Mice, Diabetes. 69 (2020) db190941. doi:10.2337/db19-0941

2.1. Introduction

2.1.1. Background- α-Klotho, a well-documented anti-aging protein primarily produced in the kidney and choroid plexus [91,130], has recently been observed to have therapeutic potential in rodent models of metabolic disease [69,97–99]. Studies show α-klotho promotes lipid oxidation, protects pancreatic beta cells from oxidative damage, increases energy expenditure, and facilitates insulin release [69,97–100]. Furthermore, circulating α-klotho concentrations are decreased in patients with obesity and diabetes [145], suggesting a possible direct role in the pathophysiology of metabolic disorders. Notably, studies have primarily investigated peripheral α-klotho, which neglects the central function of α-klotho due to its impermeability to the blood-brain barrier [92]. The few studies investigating centrally circulating α-klotho demonstrate that α-klotho has antioxidative and anti-inflammatory properties [163], is involved in myelination [95], and can be therapeutic in models of hypertension [188]; however, the role of central α-klotho in the regulation of metabolism remains unexplored.

Neuropeptide Y/agouti-related peptide-expressing (NPY/AgRP) neurons are located within the arcuate nucleus (ARC) of the hypothalamus and are critical to homeostatic regulation of metabolism. NPY/AgRP neurons sense nutritional changes in the cerebrospinal fluid (CSF) to regulate feeding behavior [34], energy expenditure [39], and glucose metabolism [35,43,54]; however, disordered overactivity of these neurons results in phenotypes resembling diabetes and obesity [34,35]. Some circulating factors, such as leptin and insulin, also modulate NPY/AgRP neurons [31,65], but in metabolic disease states signaling of these hormones is disrupted. Therefore, identification of novel regulators of this neuron population could facilitate the development of therapeutic tools for the prevention and treatment of metabolic disease. For example, recent studies have identified several fibroblast growth factor (FGF) hormones that

activate FGF receptor (FGFR)-PI3kinase signaling to elicit antidiabetic effects and regulate NPY/AgRP neurons [73,193–195,198,204]. Interestingly, α-klotho serves as a critical scaffolding protein to the FGF23-FGFR complex to promote FGFR activity [151,205].

2.1.2. Main objective/hypothesis- The current study investigates the novel role of central α-klotho in the regulation of NPY/AgRP neurons and whole-body metabolism via a potential fibroblast growth factor receptor (FGFR)/PI3kinase mechanism.

2.2. Methods

2.2.1. Cell culture- Cell culture experiments were performed on immortal hypothalamic GT1-7 cells cultured in high glucose (4.5mg/dL) Dulbecco's Modified Eagle Medium, 10% fetal bovine serum, and 1% penicillin-streptomycin. Cells were treated with 3.65mM α-klotho (R&D Systems) [95,163,192], 100ng/mL FGF23 (R&D Systems) [192], and/or pretreated with 10nM FGFR1 antagonist PD173074 (Fisher Sci Co) [206] or 50nM PI3kinase inhibitor wortmannin (Fisher Sci Co) [25]. All experiments used vehicle-treated cells as controls.

2.2.2. Experimental animals- C57BL/6 and B6. Tg(NPY-hrGFP)1Lowl/J (NPY-GFP reporter) mice were cared for in accordance with the National Institutes of Health Guide for the Care and Use of Laboratory Animals and experimental protocols were approved by Institutional Animal Care and Use Committees of East Carolina University. Mice were housed at 20-22°C with a 12-hour light-dark cycle.

2.2.3. High fat diet-induced obesity (DIO)- 6-week old male C57BL/6 mice were given ad libitum access to high-fat diet with a kilocalorie composition of 58%, 25%, and 17% fat,

carbohydrate, and protein respectively for 10 weeks (D12331, Research Diets, New Brunswick, NJ) before undergoing intracerebroventricular (ICV) cannulation.

2.2.4. Intracerebroventricular (ICV) cannulation- Prior to the procedure, mice were given oral analgesic meloxicam and anesthetized with intraperitoneal (IP) injection of ketamine and xylazine. Mice were placed on a stereotaxic device, and a midline incision was made on the head. A hole was drilled (1.0mm lateral, -0.5mm posterior, 2.5mm deep to the bregma), and a cannula was placed into the lateral ventricle (Supplemental Fig. 2.1). Another hole was drilled, and a screw placed, approximately at the ipsilateral lambdoid structure to aid in supporting the cannula in the skull with 3M carboxylate dental cement. Mice recovered for 14 days before immunohistochemical experiments and 7 days before all other experiments. All ICV treatments were administered via Hamilton syringe as 2.0uL between 6:30-7:30pm.

2.2.5. 12 Day ICV Injection Timeline- In DIO mice, central administration of either 2.0ug recombinant α-klotho (R&D Systems) alone, 25.0ug PD173074 alone, 25.0ug PD173074 ten minutes before 2.0ug α-klotho [195], or vehicle was performed daily. On day 7, glucose tolerance tests (GTT's) or insulin tolerance tests (ITT's) were performed and on day 12, body composition analysis was performed using echo MRI (Echo Medical Systems Houston, USA). Mice were then euthanized, and tissues were collected. Food intake and body weight data were analyzed from the first 7 days to prevent confounding effects from additional assays.

2.2.6. Single ICV Injection Timeline- In DIO mice, ICV administration of either 2.0ug recombinant α-klotho (R&D Systems), 10ng wortmannin, 10ng wortmannin one hour before

2.0ug α-klotho [68], or vehicle was performed the night before a GTT or ITT. Food intake was measured for four days after the injection.

2.2.7. Streptozotocin-induced (STZ) diabetes- 8-9-week-old chow-fed, male mice underwent ICV cannulation before receiving three days IP injection of 100mg/kg STZ. Dose was determined by pilot studies yielding consistently elevated fed glucose levels between 250 and 600mg/dL (Supplemental Fig. 2.2A). 7 Days after STZ injection, mice received 7 days ICV treatment with either 2.0ug recombinant α-klotho (n=10) or vehicle (n=9). Food intake, body weight, and fed glucose levels were monitored daily. To identify the effects of α-klotho treatment on glucose levels independent from food intake, a pair-fed experiment was performed using the same protocols, and on day 7 fasting glucose levels were measured (n=8-9/group).

2.2.8. Central α-klotho inhibition via ICV anti-α-klotho antibody (ab-α-klotho)- 9-week-old male, chow-fed mice were ICV treated with 1.0ug ab-α-klotho (R&D Systems) or vehicle (n=8/group). Treatments were performed on the evening of day 1 and morning of day 2, while subsequent treatments were performed between 6:30-7:30pm for seven days. GTT's were performed on day 3, and on day 7 mice were euthanized, followed by tissue collection for further assays.

2.2.9. Food intake measurements- Food intake was measured daily by weighing food (8-9g) and subtracting from the total food. Bedding was inspected thoroughly for residual bits of food which were included in measurements. On day 4 in one cohort of DIO mice, food was removed from

cages during the light-phase and replenished at the beginning of the dark-phase (7:30pm). Food intake was measured at 0.5, 1, 1.5, 2, 3, 4, 8, 14, and 24 hours after food reintroduction.

2.2.10. Glucose and insulin tolerance tests- For GTT's, 20% glucose solution (1.0g/kg BW) was IP injected after an overnight fast, and for ITT's, 0.6U/kg insulin was IP injected after a four hour fast. Tail blood samples were collected 15, 30, 60, 90, and 120 minutes post-injections for analysis using a glucose meter (Relion Prime Blood Glucose Monitoring System, ARKRAY INC. Kyoto, JAPAN). Serum was isolated from clotted blood spun at 4^0C and 2000g for 30 minutes. Insulin levels were quantified using an insulin ELISA kit (Crystal Chem).

2.2.11. Insulin-stimulated signaling- On day 12 of ICV treatment, a weight-matched cohort of DIO mice was IP injected with 10U/kg insulin or saline. 7 minutes after the injection, hypothalamus, epididymal adipose tissue (eWAT), liver, and hindlimb skeletal muscle were flash frozen for future Western Blot analysis.

2.2.12. Immunohistochemistry- For immunofluorescent analysis, mice were intracardially perfused with PBS followed by 10% formalin before immunohistochemistry was performed as described previously [207]. Briefly, brains were sliced into 20um coronal sections using a freezing microtome (Leica VT1000 S) and incubated overnight in antibody to phosphorylated ERK (Cell Signaling 1:500, Danvers, MA, USA) or cFOS (Santa Cruz 1:500, Santa Cruz, CA), followed by incubation with Alexa-fluorophore secondary antibody for 2 hours. Stains were photographed using an optical microscope (Leica DM6000, Wetzlar, Germany), followed by

blind analysis using Image J. At least three anatomically matched images per mouse were quantified.

2.2.13. Western blot- Western blot was performed as described previously [207]. Briefly, equal protein samples were loaded into a 4-20% HCL gel, transferred to a nitrocellulose membrane, and incubated overnight in 1:500-1:1000 antibody dilutions in 5% milk+TBST for $pAKT^{ser473}$, total AKT, $pFOXO1^{ser256}$, total FOXO1, $pERK^{thr202/thr204}$ (Cell Signaling Technology), pIR^{tyr972} (Invitrogen), and total ERK (Santa Cruz). Image J software was used to quantify mean intensity of equal-area sections representing each sample.

2.2.14. Quantitative PCR- Cell and tissue RNA were extracted by Trizol (Thermo Fisher Scientific; Waltham, MA USA). The expressions of specific mRNA were analyzed using quantitative real-time PCR (RT-qPCR) (POWER SYBR GREEN PCR Master Mix; Applied Biosystems, Foster City, CA, USA). Reactions were performed in triplicate for each sample, while glyceraldehyde 3-phosphate dehydrogenase was used as a reference gene for normalization.

2.2.15. Patch clamp electrophysiology- We conducted cell attached voltage clamp recordings of NPY/AgRP neurons as described previously [208,209]. Briefly, mice were deeply anesthetized by isoflurane followed by intracardial perfusion with chilled n-methyl-D-glucamine solution and sliced into 200-300μm sections. Slices recovered for an hour in HEPES recovery solution and recordings were conducted in a normal aCSF bath. For whole cell recordings, gigaohm seals were obtained and the cells were broken into using negative pressure. Data was sampled at 10

kHz. Current clamp recordings were stabilized for repeated firing under the baseline condition. Equivalent length periods (0.5-5minutes) were set within each recording during perfusion of aCSF or α-klotho (3.65mM). Firing rate (Hz) was calculated by dividing the number of events by the number of seconds. Bath application of tetrodotoxin (TTX) (1.0uM) prior to α-klotho treatment was used to determine action potential independent effects on membrane potential. Voltage clamp whole cell recordings were conducted at a -70mV holding potential and a high KCl intracellular solution (in mM: 130 KCl, 5CaCl2, 10 EGTA, 10 HEPES, 2MgATP, .5NaGTP, 5 phosphocreatine) was used. For voltage clamp recordings of mini inhibitory post-synaptic currents (mIPSC's), glutamatergic blockade was induced using NMDA receptor blocker AP5 (50uM) and AMPA receptor blocker CNQX (10nM), followed by α-klotho administration, and then currents were abolished with picrotoxin (100uM) [210].

2.2.16. Statistical Analysis- Unpaired t-tests were used in *in vivo* mouse experiments to compare differences between groups in food intake, body weight, and body composition. To compare pre-post within-group changes over the course of the experiment, paired t-tests were performed. To compare differences at GTT or ITT timepoints, Two-Way ANOVA's with repeated measures for time and Bonferroni corrections for multiple comparisons were used. Unpaired t-tests or one-way ANOVA's with Tukey's correction for multiple comparisons were using in cell culture experiments when appropriate. Paired t-tests or repeated measures ANOVA with Tukey's correction for multiple comparisons were used in patch clamp electrophysiology experiments when appropriate. All analyses were performed using GraphPad Prism statistics software, and a P value < 0.05 was considered statistically significant.

2.2.17. Data and Availability Statement- The datasets generated during the current study are available from the corresponding author on reasonable request.

2.3. Results

2.3.1. 7 Days Central Administration of α-Klotho Results in Weight Loss, Suppressed Food Intake, and Improved Glucose Regulation in DIO Mice

7 days ICV α-klotho treatment in DIO mice significantly reduced body weight (4.9%) compared to vehicle treated controls (Fig. 2.1A-B). These changes were, at least in part, due to decreased food intake both daily (14.8%) and after a daytime food restriction (11.4%) (Fig. 2.1E-H). ICV α-klotho treatment also improved glucose clearance and insulin release during a GTT, as well as insulin sensitivity during an ITT (Fig. 2.1I-N).

2.3.2. A Single ICV α-Klotho Injection Improves Glucose Clearance and Suppresses Food Intake in DIO Mice

To determine if the effects of central α-klotho on glucose metabolism were independent from changes in body weight, a single ICV α-klotho injection was performed in DIO mice the night before a GTT or ITT. Acute ICV α-klotho treatment improved glucose clearance during a GTT (Fig. 2.2A-C) and even decreased food intake the following day (Fig. 2.2D). Interestingly, acute ICV α-klotho treatment had no effects on insulin sensitivity (Fig. 2.2E-H). These data suggest central α-klotho regulates glucose metabolism independent from changes in body weight and insulin sensitivity. Supporting this hypothesis, 12 days ICV α-klotho had no effects on insulin-stimulated signaling in hypothalamus, skeletal muscle, eWAT, nor liver in weight-matched DIO mice (Supplemental Fig. 2.3).

To begin to investigate alternative peripheral mechanisms through which central α-klotho improves glucose regulation, basal hepatic gene expression was analyzed. Hepatic phosphoenol pyruvate carboxykinase (PEPCK) mRNA was significantly reduced (0.75 fold) in DIO mice treated with α-klotho for 12 days, suggesting attenuated hepatic gluconeogenesis, despite no changes in pyruvate kinase (PK), glucose-6-phsophatase (G6Pase), or glucokinase (GK). α-Klotho-treated mice also had reduced hepatic lipid accumulation and upregulated ACC1 and ACC2 mRNA (Supplemental Fig. 2.4).

2.3.3. 7 Days Central α-Klotho Administration Attenuates the Progression of Diabetes in STZ-treated Mice

The therapeutic potential of α-klotho was also investigated in a model of type I diabetes induced by streptozotocin (STZ) treatment. Similar to DIO mice, ICV α-klotho decreased body weight (5.3%), suppressed food intake (27.8%), and attenuated hyperglycemia (20.2% reduction in fed glucose levels) in STZ-treated mice compared to vehicle-treated controls (Fig. 2.3A-G). Even in pair-fed STZ-treated mice, ICV α-klotho attenuated hyperglycemia and trended to improve fasting glucose levels (Fig 2.3K-M). These data further demonstrate glucoregulatory and anorexic action of central α-klotho in both type I and type II diabetes models.

2.3.4. Central α-Klotho Inhibition Impairs Glucose Tolerance

To determine the effects of central α-klotho inhibition on energy and glucose homeostasis, we performed central administration of anti-α-klotho antibody (ab-α-klotho). 2 days ab-α-klotho treatment significantly impaired glucose tolerance compared to vehicle-treated controls despite similar body weights (Fig. 2.4A-C). There were no differences in liver PEPCK or G6Pase,

however gene expression of GK and PK trended to be lower in ab-α-klotho mice (p=0.14 and 0.15 respectively) (Supplemental Fig. 2.5D). Surprisingly, 7 days of ab-α-klotho significantly decreased body weight with no changes in food intake (Fig. 2.4D-G). Taken together with ICV α-klotho experiments, these data suggest a distinct glucoregulatory role of central α-klotho independent of body weight and food intake.

2.3.5. α-Klotho Suppresses NPY/AgRP Neuron Activity, at least in part, by enhancing mIPSC's

We next aimed to investigate the effects of α-klotho on NPY/AgRP neurons considering their critical role in energy homeostasis. A single ICV α-klotho injection in NPY-GFP reporter mice before an overnight fast significantly reduced cFOS colocalization with NPY/AgRP neurons by 49.0% (Fig. 2.5A-C). Furthermore, electrophysiological recordings revealed α-klotho treatment decreases NPY/AgRP neuron firing rate and membrane potential (0.79 vs 0.22Hz. and -52.7 vs. -57.8mV respectively) (Fig. 2.5D-F).

To determine if α-klotho's suppressive effects on NPY/AgRP neurons are due to pre or post synaptic events, brain slices were pretreated with TTX (1.0uM) to block action potentials. In the presence of TTX, α-klotho still decreased membrane potential (-53.4 vs. -58.4mV), suggesting post-synaptic action of α-klotho on NPY/AgRP neurons (Fig. 2.5G-H). We also observed α-klotho to increase the magnitude, but not the frequency, of mIPSC's in NPY/AgRP neurons under glutamatergic blockade (25.9 vs. 34.4pA) (Fig. 2.5I-M), indicating α-klotho is directly antagonizing NPY/AgRP neurons by modulating receptor availability or intracellular signals [211]. Overall, these experiments illustrate that α-klotho directly suppresses NPY/AgRP neuron activity by, at least in part increasing receptor-mediated inhibitory signals.

2.3.6. α-Klotho induces cell-signaling, alters gene expression, and decreases NPY/AgRP neuron activity via FGFR's

To investigate the potential of α-klotho to alter cell signaling and gene expression in the hypothalamus, we first used the GT1-7 immortal hypothalamic cell line [212]. 30 minutes α-klotho treatment increased phosphorylation of $ERK^{thr202/tyr204}$, AKT^{ser473}, and $FOXO1^{ser256}$ (Supplemental Fig. 2.6A). Additionally, α-klotho treatment during both overnight and two hours serum starvation significantly reduced AgRP mRNA (by 28.5% and 30.3% respectively), suggesting hormonal action of α-klotho in GT1-7 cells (Supplemental Fig. 2.6C). To investigate if α-klotho has hormonal action in the hypothalamus *in vivo,* we performed acute ICV α-klotho administration in healthy, fed mice and observed elevated phosphorylated ERK after 90 minutes in the ARC compared to vehicle-treated controls (Supplemental Fig. 2.6B).

Previous studies demonstrate the importance of α-klotho as a scaffolding protein increasing the affinity of FGF23 to FGFR1 [151,205]. In hypothalamic GT1-7 cells, 30 minutes FGF23 (100ng/mL) treatment had no effects on phosphorylated ERK or AKT (Fig. 2.6A-C), while co-treatment with FGF23 and α-klotho had no synergistic effect compared with α-klotho alone. This suggests, at least in hypothalamic GT1-7 cells, α-klotho is independent of exogenous FGF23-mediated signaling. When cells were pretreated with FGFR1 inhibitor PD173074 (10nM), α-klotho-mediated cell-signaling and suppression of AgRP mRNA was abolished (Fig. 2.6A-D), indicating hypothalamic α-klotho action is dependent on FGFR1 activity. Moreover, immunofluorescent staining of cFOS revealed that ICV pretreatment with PD173074 also inhibited the ability of α-klotho to decrease NPY/AgRP neuron activity *in vivo* (Fig. 2.6E-G).

PI3 kinase is a downstream mediator of FGFR1 and is also an important negative regulator of NPY/AgRP neurons [73,213]. PI3 kinase inhibition using wortmannin (50nM) also eliminated α-klotho's ability to suppress AgRP gene expression (Fig. 2.6D). Taken together, these data demonstrate the importance of FGFR1/PI3kinase signaling in hypothalamic α-klotho function.

2.3.7. 7 Days central α-klotho treatment suppresses food intake and reduces body weight via FGFR and PI3kinase signaling in DIO Mice

To determine if the therapeutic effects of α-klotho in DIO mice were dependent on FGFR's, we centrally injected PD173074 to inhibit endogenous FGFR function. Mice receiving α-klotho treatment alone experienced significantly decreased food intake and body weight compared to all groups (Fig. 2.7A-D), while PD173074 treatment alone induced weight gain (Fig. 2.7A-B). PD173074 treatment blunted α-klotho-mediated reductions in food intake and body weight, suggesting the effects of central α-klotho on energy balance are mediated by FGFR signaling. Surprisingly, both α-klotho+FGFR inhibitor and α-klotho alone groups experienced improved glucose clearance compared to vehicle-treated controls (Fig. 2.7E-F), suggesting FGFR's may not be involved in central α-klotho-mediated glucose regulation.

Similar to FGFR antagonism, central inhibition of PI3kinase abolished α-klotho's ability to suppress food intake and improve glucose clearance (Figure 2.8). These data indicate PI3kinase is critical to α-klotho-mediated regulation of food intake and glucose metabolism. Overall, coupled with *in vitro* cell signaling experiments, these data demonstrate a novel α-klotho/FGFR/PI3kinase mechanism in the central regulation of metabolism.

2.4. Discussion

To our knowledge, this is the first study to provide evidence that α-klotho functions as a hypothalamic hormonal agent. ICV α-klotho administration improved glucose regulation, suppressed food intake, and reduced body weight in mouse models of Type I and II diabetes, illustrating the therapeutic potential of central α-klotho in metabolic disease states. Although deeper investigation is required to identify the direct connection between central α-klotho activity and peripheral glucose metabolism, the current study determined the glucose-lowering effects of α-klotho are independent from insulin-sensitivity, but rather, are mediated by augmented insulin secretion during a glucose challenge. However, STZ experiments revealed some of the glucoregulatory actions of α-klotho independent of insulin altogether. Basal hepatic PEPCK mRNA was decreased in α-klotho-treated DIO mice, suggesting decreased hepatic glucose output may an alternative mechanism.

The central and peripheral pools of α-klotho have distinct, independent functions due to α-klotho's inability to cross the blood-brain barrier [92]. While recent publications have demonstrated metabolic roles of α-klotho in the blood, including long-term α-klotho injection improving adiposity in DIO mice [97] and ameliorating diabetic cardiomyopathies in STZ-treated mice [106], the current study identifies distinct differences between central and peripheral α-klotho-mediated metabolic regulation. For example, α-klotho's effects on food intake and glucose metabolism seem to be mainly via central mechanisms, while peripherally circulating α-klotho regulates gene expression to promote lipid oxidation and energy expenditure [97,106]. Notably, whole-body α-klotho knockout and knockdown models have been previously utilized to investigate α-klotho's functions [91,100], but these approaches do not distinguish between peripheral and central α-klotho function.

ICV ab-α-klotho was used in this study as a novel approach specifically impairing central α-klotho signaling, and, as expected, ab-α-klotho treatment impaired glucose clearance. Although central α-klotho concentrations have yet to be quantified in diabetic patients, past studies show blood α-klotho concentrations to be decreased in some diabetic populations [144,145]. Thus, our data connecting central α-klotho impairment and disordered glucose regulation may provide new insight into the pathophysiology of metabolic disorders.

Contrary to our hypotheses, central α-klotho inhibition resulted in decreased body weight with no differences in food intake. α-Klotho knockout mice also experience weight loss, primarily due to atrophy of metabolically active organs, resulting in premature death [91,100]. These findings highlight the complicated and diverse metabolic functions of α-klotho. For example, while evidence from the current study and past literature describes α-klotho as an anti-diabetic agent [69,97–99,106], overexpression of α-klotho has been shown to elicit insulin resistance [91]. Notably, α-klotho-overexpressing mice do not experience hyperglycemia, adiposity, or hyperphagia associated with clinical insulin resistance [91]. Moreover, α-klotho is an important negative modulator of insulin and IGF-1 signaling to regulate apoptosis and ROS buffering [95,163]. The many complex physiological roles of α-klotho may explain the unexpected results in response to central α-klotho inhibition.

The current study identified central α-klotho as a novel antagonist of NPY/AgRP neurons. Considering NPY/AgRP neuron overactivity is associated disordered feeding, body weight and glucose regulation [34,36], our data provides encouraging evidence of α-klotho as a potential therapeutic target in metabolic disease prevention. At the present, it is unclear if NPY/AgRP neurons are the primary mediators of central α-klotho's regulation of metabolism, underscoring the importance of further investigation into the specific neuronal effectors and cell signaling

involved. However, the observed ICV α-klotho phenotype has many similarities to the previously described effects of NPY/AgRP neuron inhibition, including suppressed food intake, reduced body weight, improved glucose clearance and insulin release, and decreased hepatic gluconeogenic gene expression [34,35,43,54,214,215].

Similar to studies using hippocampal and oligodendrocyte progenitor cells [94,95,192], α-klotho induced phosphorylation of $ERK^{thr202/tyr204}$, AKT^{ser473}, and $FOXO1^{ser256}$ in hypothalamic GT1-7 cells; all of which are established signaling molecules involved in downregulating NPY/AgRP gene transcription and activity [65,216]. Furthermore, the observed ICV α-klotho phenotype resembles FGFR activation, which also results in suppressed food intake, improved glucose regulation, attenuated NPY/AgRP neuron activity, and decreased liver gluconeogenic gene expression [193–195,198,204]. α-Klotho serves as a non-enzymatic scaffold to increase FGF23 affinity to FGFR1 [151]; thus, we investigated the potential importance of a hypothalamic α-klotho-FGFR1 signaling mechanism. Similar to previous studies in hippocampal cells, our results show hypothalamic α-klotho-mediated signaling, and AgRP mRNA regulation in GT1-7 cells, were abolished when pre-treated with FGFR1 antagonist PD173074 [192]. Additional experiments determined that PI3kinase signaling, a downstream mediator of FGFR1 [213] and potent regulator of NPY/AgRP neurons [73], was also required for α-klotho-mediated AgRP mRNA suppression. Future studies should further investigate the possible involvement of a novel α-klotho/FGFR1/PI3kinase axis in the homeostatic modulation of NPY/AgRP neurons.

We further investigated the involvement of FGFR/PI3kinase signaling to central α-klotho-mediated regulation of metabolism. Central FGFR or PI3kinase inhibition blunted ICV α-klotho's effects on food intake and body weight, while only PI3kinase inhibition affected α-klotho-mediated glucose regulation. Overall, these data support the hypothesis that central

FGFR-PI3kinase signaling is critical to α-klotho-mediated regulation of metabolism; however, studies investigating the function of central FGFR's in metabolism yield mixed results depending on animal model and experimental approach. ICV PD173074 (FGFR inhibitor) impairs glucose clearance in healthy rats, but is described as stress-related [198,199], and ICV PD173074 in DIO mice elicits no phenotype [193,200]. Furthermore, antibody-mediated inhibition of FGFR1 in rodents and monkeys increases energy expenditure, decreases food intake, and reduces body weight, while genetic deletion of FGFR1 in NPY/AgRP neurons also results in no metabolic phenotype [71,201,202]. Additionally, the specificity for PD173074 *in vivo* is unclear, thus it likely has non-specific antagonism of other FGFR's. Future studies should investigate the specific roles of FGFR's, their isoforms, and their neuronal effectors in central regulation of metabolism by performing selective deletion of FGFR's in specific neurons of mature mice using the inducible Cre-LoxP system.

In addition to FGFR-PI3kinase signaling, there are likely unknown concurrent mechanisms underlying central α-klotho-mediated metabolic regulation. Other neuron populations, such as pro-opiomelanocortin (POMC) neurons, which are closely associated with NPY/AgRP neurons, may be involved. Our cell culture and immunohistochemistry data also may suggest ERK as an additional cell-signaling mechanism of hypothalamic α-klotho action. ERK signaling is downstream of α-klotho, negatively regulates NPY/AgRP neurons, possibly via kruppel-like factor 4, and is involved in hypothalamic FGF1- and FGF19-mediated glucose lowering [193,216,217].

To summarize, this study identifies α-klotho as a novel antagonist of NPY/AgRP neurons and demonstrates α-klotho's importance to central regulation of metabolism via an α-klotho-FGFR1-PI3kinase signaling axis. Our data revealed central administration of α-klotho to yield various

therapeutic effects in models of Type I and II diabetes, including improved glucose regulation, suppressed food intake, and reduced body weight. To our knowledge, this study provides the first evidence of α-klotho as a novel hypothalamic regulator of energy balance and glucose metabolism, thus providing new insight into the pathophysiology of metabolic disease.

Chapter 2 Figures

Figure Legend:

Figure 2.1. 7 Days Central Administration of α-Klotho Results in Weight Loss, Suppressed Food Intake, and Improved Glucose Regulation in DIO Mice. **(A)** Body weight**, (B)** Changes in body weight, **(C)** Fat mass, **(D)** Lean mass **(E)** Average daily food intake **(F)** Timeline of daily food intake, **(G)** Cumulative food intake after a daytime food restriction, **(H)** Timeline of food intake after a daytime food restriction, **(I)** Blood glucose levels during a GTT, **(J)** Area under the curve of the GTT, **(K)** Serum insulin levels 30min into the GTT, **(L)** Blood glucose during an ITT, **(M)** Area under the curve of the ITT, and **(N)** Fasting serum insulin in 17-18-week-old male DIO mice after 7 days ICV α-klotho or vehicle injections (n = 8-13/group). Data represented as mean ± SEM; *P < 0.05 vs. ICV control.

Figure 2.2. Acute Central Administration of α-Klotho Improves Glucose Clearance and Suppresses Food Intake Independent of Body Weight in DIO Mice. (A) Blood glucose during a GTT, **(B)** Area under the curve of the GTT, **(C)** Body weight before the GTT, **(D)** Daily food intake (including overnight fast before GTT on Day 1), **(E)** Blood glucose during an ITT, **(F)** Area under the curve of the ITT, **(G)** Food intake the night before the ITT, and **(H)** Body weight before the ITT in 17-18-week-old male DIO mice after a single ICV α-klotho or vehicle injection (n = 7-10/group). Data represented as mean ± SEM; *P < 0.05 vs. ICV control.

Figure 2.3. 7 Days Central α-Klotho Administration Attenuates the Progression of Diabetes in STZ-treated Mice. (A) Body weight, **(B)** Changes in body weight, **(C)** Average daily food intake, **(D)** Timeline of food intake **(E)** Fed blood glucose levels, **(F)** Timeline of fed blood glucose, and **(G)** Change in fed blood glucose levels in 9-10-week-old, STZ-treated, ad libitum

fed, mice after 7 days ICV α-klotho or vehicle injections (n = 9-10/group). **(H)** Body weight, **(I)** Changes in body weight, **(J)** Average daily food intake, **(K)** Fed blood glucose levels, **(L)** Change in fed blood glucose levels, and **(M)** Fasting blood glucose levels in pair-fed, STZ-treated mice (n=8-9/group). Data represented as mean ± SEM; *P < 0.05 vs. ICV control.

Figure 2.4. Central α-Klotho Inhibition Impairs Glucose Tolerance. (A) Blood glucose levels during a GTT, **(B)** Area under the curve of the GTT, **(C)** Fasting glucose levels, **(D)** Body weight, **(E)** Changes in body weight, **(F)** Daily food intake, and **(G)** Timeline of food intake in 9-week-old chow-fed male mice treated with anti-α-klotho antibody compared to vehicle-treated controls (n = 8/group). Data represented as mean ± SEM; *P < 0.05 vs. ICV control.

Figure 2.5. α-Klotho Suppresses NPY/AgRP Neuron Activity, at least in part, by enhancing mIPSC's. **(A)** Representative image of cFOS (red) colocalization with NPY/AgRP (green), **(B)** Number of NPY neurons, **(C)** Number of NPY neurons with cFOS colocalization in the ARC of mice ICV treated with 2.0 uL α-klotho or vehicle before an overnight fast (n = 4 mice/group), **(D)** Representative cell attached recording of an NPY/AgRP neuron, **(E)** Calculated firing rate (Hz) and **(F)** membrane potential (mV) during α-klotho administration (n = 8 neurons from 4 male mice). **(G)** Representative current clamp trace of an NPY/AgRP neuron, **(H)** Mean membrane potential induced by TTX or TTX and α-klotho. **(I)** Representative whole cell recording tracers with α-klotho, glutamatergic blockade, and GABAergic antagonist picrotoxin. **(J-K)** Mean amplitude, **(L)** Differences in cumulative probability of mIPSC amplitude, and **(M)** Mean frequency of IPSC's under glutamatergic blockade with and without α-klotho treatment. (n = 5 neurons from 3 male mice). Data represented as mean ± SEM; *P < 0.05 vs. aCSF.

Figure 2.6. α-Klotho-mediated cell signaling and regulation of NPY/AgRP neurons in the hypothalamus is dependent on FGFR's. (A) Representative western blot image, **(B)** Phosphorylation of ERK, **(C)** Phosphorylation of AKT, **(D)** AgRP mRNA expression in GT1-7 cells treated with α-klotho, FGF23, PD173074 and/or wortmannin. (n = 5-10/group). **(E)** Representative image of cFOS (red) colocalization with NPY/AgRP neurons (green), **(F)** Number of NPY neurons, and **(G)** Number of NPY neurons colocalized with cFOS in the arcuate nucleus of the hypothalamus of mice ICV treated with vehicle, FGFR inhibitor+vehicle, or FGFR inhibitor+α-klotho before an overnight fast (n = 3 mice/group). Data represented as mean ± SEM; *P < 0.05 vs. controls.

Figure 2.7. Central Inhibition of FGFR1 Blunts the Therapeutic Effects of 7 Days α-Klotho in DIO Mice. (A) Body weight, **(B)** Changes in body weight, (**C)** Average daily food intake, **(D)** Timeline of food intake, **(E)** Blood glucose levels during GTT and **(F)** Area under curve in DIO mice receiving 7 days ICV injection with vehicle, α-klotho, FGFR inhibitor, or inhibitor with α-klotho (n=7-11/group). Data represented as mean ± SEM; *P < 0.05 vs ICV Vehicle.

Figure 2.8. Central Inhibition of PI3kinase Negates the Therapeutic Effects of a Single α-Klotho Injection in DIO Mice. **(A)** Timeline of food intake (including overnight fast before GTT on Day 1), **(B)** Average 48 hour food intake, **(C)** Blood glucose during a GTT, and **(D)** Area under the curve of the GTT in DIO mice receiving a single injection with vehicle, α-klotho, wortmannin, or wortmannin with α-klotho (n=9/10/group). Data represented as mean ± SEM; *P < 0.05.

Supplemental Figure Legend:

Supplemental Figure 2.1. Validation of ICV cannulation procedure. (A) Observation of scar tissue path of the cannula and (B) 3.0ug ICV leptin treatment suppresses food intake after an overnight fast (n = 3-4 chow fed mice). Data represented as mean ± SEM; $P < 0.05$ indicates significant difference between groups.

Supplemental Figure 2.2. (A) Effects of different doses of STZ on fed blood glucose levels 7 days after injections. (B) Hypothalamic gene expression of agouti-related peptide (AgRP), neuropeptide Y (NPY), and pro-opiomelanocortin (POMC) in 9-10-week-old, STZ-treated, ad libitum fed, mice after 7 days ICV α-klotho or vehicle injections (n = 5-7/group). Data represented as mean ± SEM; *$P < 0.05$ vs. ICV control

Supplemental Figure 2.3. 12 days ICV α-klotho treatment does not affect insulin sensitivity in peripheral tissues of DIO mice. Insulin stimulated signaling (10U/kg 7 minutes before euthanasia) in (A) Skeletal muscle, (B) Liver, (C) Epididymal adipose tissue, and (D) Hypothalamus, and (E) Body weight in 17-18-week-old weight-matched male DIO mice after 12 days ICV α-klotho or vehicle injections (n = 4/group). Data represented as mean ± SEM; *$P < 0.05$ vs. ICV controls.

Supplemental Figure 2.4. 12 days ICV α-klotho treatment alters gene mRNA levels of key metabolic genes in the liver. (A) Hypothalamic gene expression of agouti-related peptide (AgRP), neuropeptide Y (NPY), pro-opiomelanocortin (POMC), and melanocortin-4 receptor (MC4R), (B) Western blot illustrating the effects of α-klotho on basal phosphorylation of AKT^{ser473} in skeletal

muscle, (C) Liver gene expression of pyruvate kinase (PK), phosphoenolpyruvate carboxykinase (PEPCK), glucose-6-phosphatase (G6Pase), and glucokinase (GK), (D) Liver gene expression of fatty acid synthase (FAS), carnitine palmitoyl transferase 1 (CPT1), and acetyl CoA carboxylase (ACC), and (E) Liver Oil Red O stains in 17-18-week-old male DIO mice after 12 days ICV α-klotho or vehicle injections (n = 4-5/group). Data represented as mean ± SEM; *P < 0.05 indicates significant difference between groups.

Supplemental Figure 2.5. 7 days ICV treatment with anti-α-klotho antibody has no significant effects on hypothalamic gene expression, liver gene expression, or skeletal muscle $pAKT^{ser473}$. (A) Western blot illustrating specificity of anti-α-klotho antibody to bind to α-klotho using kidney as a positive control. (B) Western blot illustrating the ability of anti-α-klotho antibody to suppress α-klotho-mediated cell signaling in GT1-7 cells. (C) Hypothalamic gene expression of AgRP, NPY, POMC, and melanocortin-4 receptor, (D) Liver gene expression of pyruvate kinase (PK), phosphoenolpyruvate carboxykinase (PEPCK), glucose-6-phosphatase (G6Pase), and glucokinase (GK), and (E) Representative Western Blot of basal phosphorylated AKTser473 in skeletal muscle in 9-week-old chow-fed male mice treated with anti-α-klotho antibody compared to vehicle-treated controls (n=8/group). Data represented as mean ± SEM; P < 0.05 indicates significant difference between groups.

Supplemental Figure 2.6. α-Klotho alters cell signaling and neuronal activity in the hypothalamus. **(A)** Representative Western Blot image and quantification illustrating the effects of 30 minutes 3.65mM α-klotho treatment on phosphorylation of $ERK^{thr202/tyr204}$, AKT^{ser473}, and $FOXO1^{ser256}$ in GT1-7 cells (n = 4 mice/group) **(B)** Representative immunofluorescence image

and quantification illustrating the effects of acute ICV administration of 2.0 uL of 1.0 ug/uL α-klotho compared to 2.0 uL vehicle on phosphorylation of $ERK^{thr202/tyr204}$ in the arcuate nucleus of the hypothalamus in 10 week old chow-fed mice (3V: third ventricle) (scale bar = 50 um) (n = 3/group) **(C)** The effects of α-klotho treatment (3.65mM) on AgRP mRNA during two hours and overnight serum starvation in GT1-7 cells (n = 4-6/group). Data represented as mean ± SEM; *P < 0.05 vs. controls.

Supplemental Figure 2.7. ICV α-klotho does not cause additional stress in mice. (A) Taste aversion to saccharin water after ICV treatment with 2.0 uL vehicle or 2.0 uL of 1.0ug/uL α-klotho in 13-week old chow-fed mice (n = 2-3/group). IP lithium chloride injection was used as a positive control to elicit an aversion to saccharin water. (B) Nest building behaviors in healthy 8-9-week-old chow-fed and 9-10 week old STZ-treated mice treated with 2.0 uL vehicle or 2.0 ug of 1.0 ug/uL α-klotho (n = 3-6/group). Data represented as mean ± SEM; P < 0.05 indicates significant difference between groups.

Supplemental Figure 2.8. 7 days ICV α-klotho treatment improves glucose regulation and suppresses food intake in female DIO mice. (A-B) Differences in body weight, (C) Average daily food intake, (D) Timeline of food intake, (E-F) Refeeding after daytime food restriction, and (G-H) Blood glucose levels during a glucose tolerance test (1 g/kgBW) after 7 days ICV α-klotho treatment in 17-18-week old DIO female mice (n=4/group). Data represented as mean ± SEM; P < 0.05 indicates significant difference between groups.

Supplemental Figure 2.9. 7 Days ICV α-klotho treatment suppresses food intake in healthy chow-fed mice. (A) Body weight, (B) Change in body weight, (C) Fed blood glucose levels, (D) Daily food intake, and (E) Timeline of food intake in 8-9-week old chow-fed mice (n=8-9/group). Data represented as mean ± SEM; $P < 0.05$ indicates significant difference between groups.

Supplemental Table 2.1. Primer sequences used for qPCR.

Figure 2.1

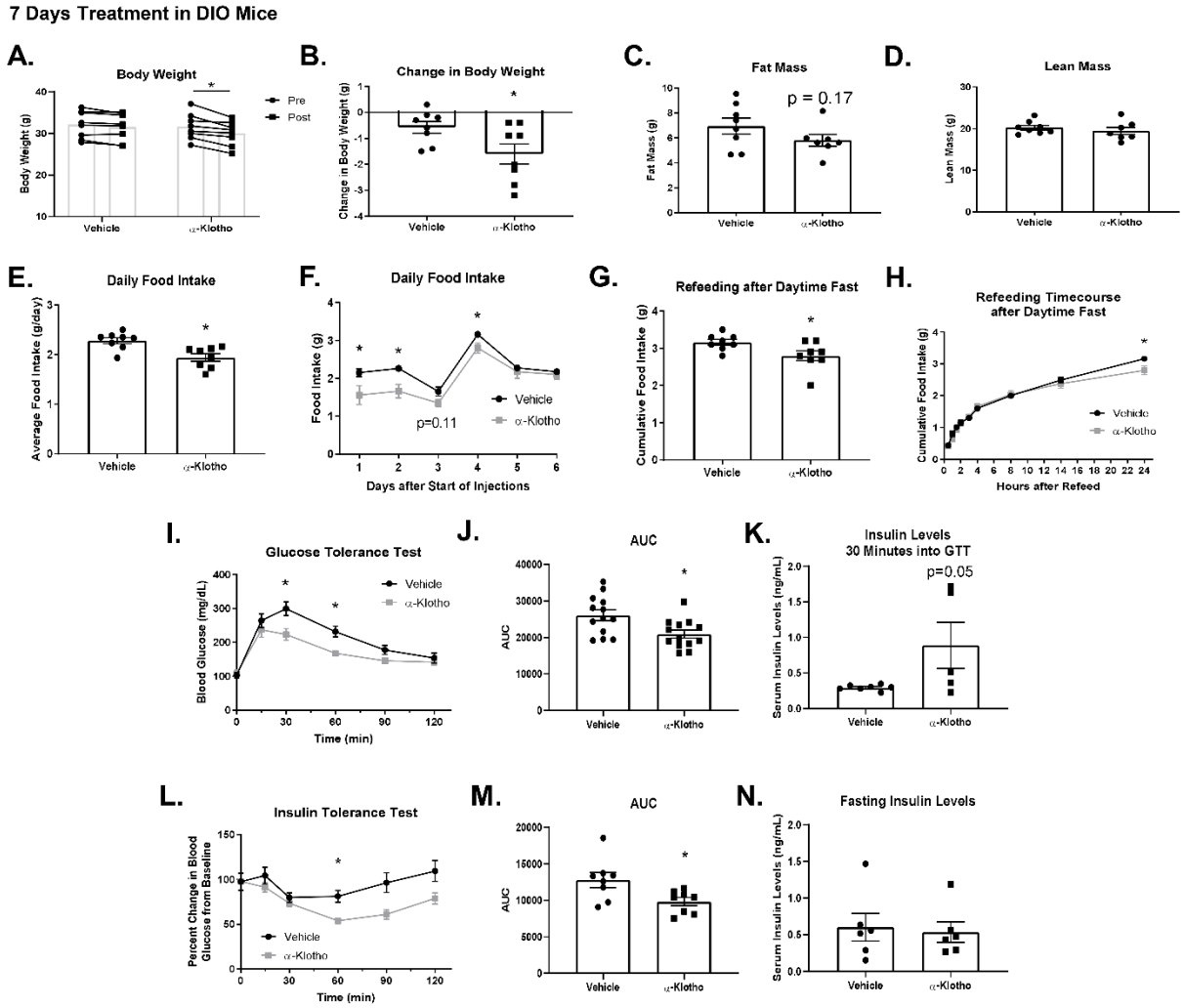
7 Days Treatment in DIO Mice
A.
Body Weight
Body Weight (g)
Pre
Post
Vehicle
α-Klotho
B.
Change in Body Weight
Change in Body Weight (g)
C.
Fat Mass
p = 0.17
Fat Mass (g)
D.
Lean Mass
Lean Mass (g)
E.
Daily Food Intake
Average Food Intake (g/day)
F.
Daily Food Intake
Food Intake (g)
p=0.11
Days after Start of Injections
G.
Refeeding after Daytime Fast
Cumulative Food Intake (g)
H.
Refeeding Timecourse after Daytime Fast
Cumulative Food Intake (g)
Hours after Refeed
I.
Glucose Tolerance Test
Blood Glucose (mg/dL)
Time (min)
J.
AUC
K.
Insulin Levels 30 Minutes into GTT
p=0.05
Serum Insulin Levels (ng/mL)
L.
Insulin Tolerance Test
Percent Change in Blood Glucose from Baseline
M.
AUC
N.
Fasting Insulin Levels

Figure 2.2

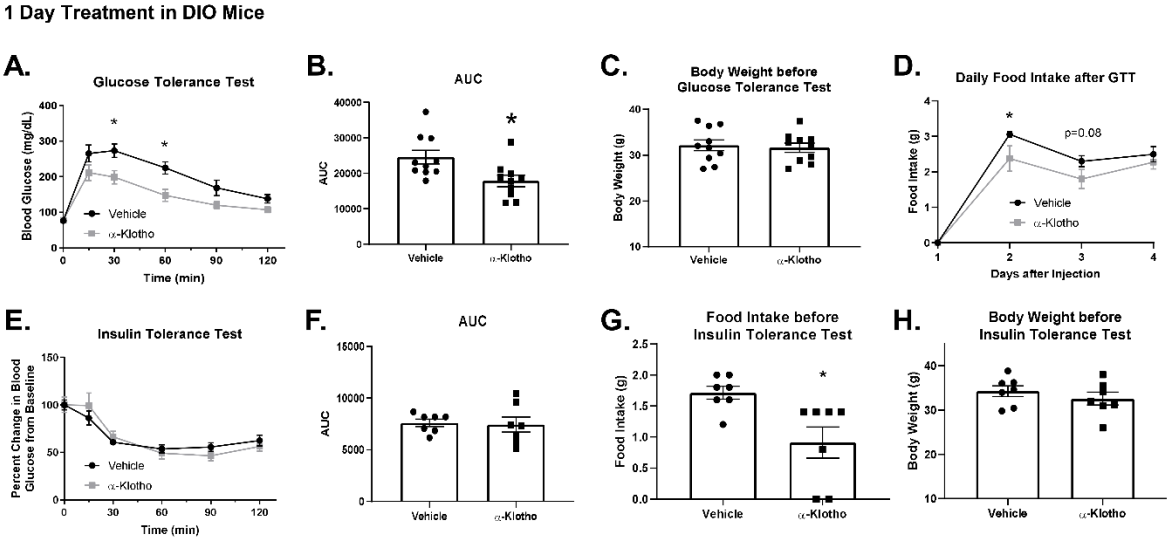
1 Day Treatment in DIO Mice
A.
Glucose Tolerance Test
Blood Glucose (mg/dL)
Time (min)
Vehicle
α-Klotho
B.
AUC
AUC
Vehicle
α-Klotho
C.
Body Weight before Glucose Tolerance Test
Body Weight (g)
Vehicle
α-Klotho
D.
Daily Food Intake after GTT
Food Intake (g)
p=0.08
Days after Injection
Vehicle
α-Klotho
E.
Insulin Tolerance Test
Percent Change in Blood Glucose from Baseline
Time (min)
Vehicle
α-Klotho
F.
AUC
AUC
Vehicle
α-Klotho
G.
Food Intake before Insulin Tolerance Test
Food Intake (g)
Vehicle
α-Klotho
H.
Body Weight before Insulin Tolerance Test
Body Weight (g)
Vehicle
α-Klotho

Figure 2.3

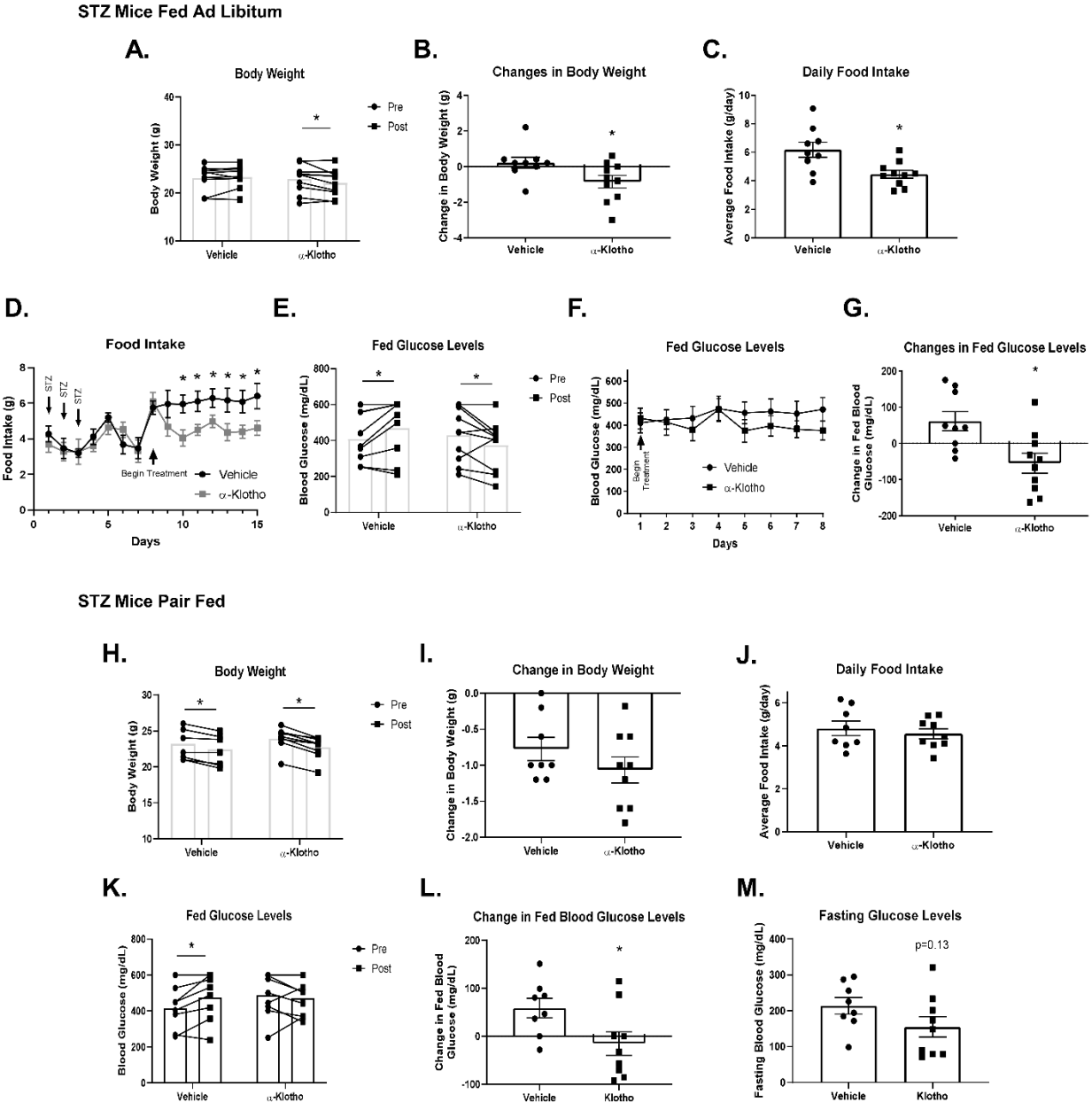
STZ Mice Fed Ad Libitum
A.
Body Weight
Body Weight (g)
Pre
Post
Vehicle
α-Klotho
B.
Changes in Body Weight
Change in Body Weight (g)
C.
Daily Food Intake
Average Food Intake (g/day)
D.
Food Intake
Food Intake (g)
STZ
STZ
STZ
Begin Treatment
Vehicle
α-Klotho
Days
E.
Fed Glucose Levels
Blood Glucose (mg/dL)
F.
Fed Glucose Levels
Begin Treatment
Days
G.
Changes in Fed Glucose Levels
Change in Fed Blood Glucose (mg/dL)
STZ Mice Pair Fed
H.
Body Weight
I.
Change in Body Weight
J.
Daily Food Intake
K.
Fed Glucose Levels
L.
Change in Fed Blood Glucose Levels
Klotho
M.
Fasting Glucose Levels
p=0.13

Figure 2.4

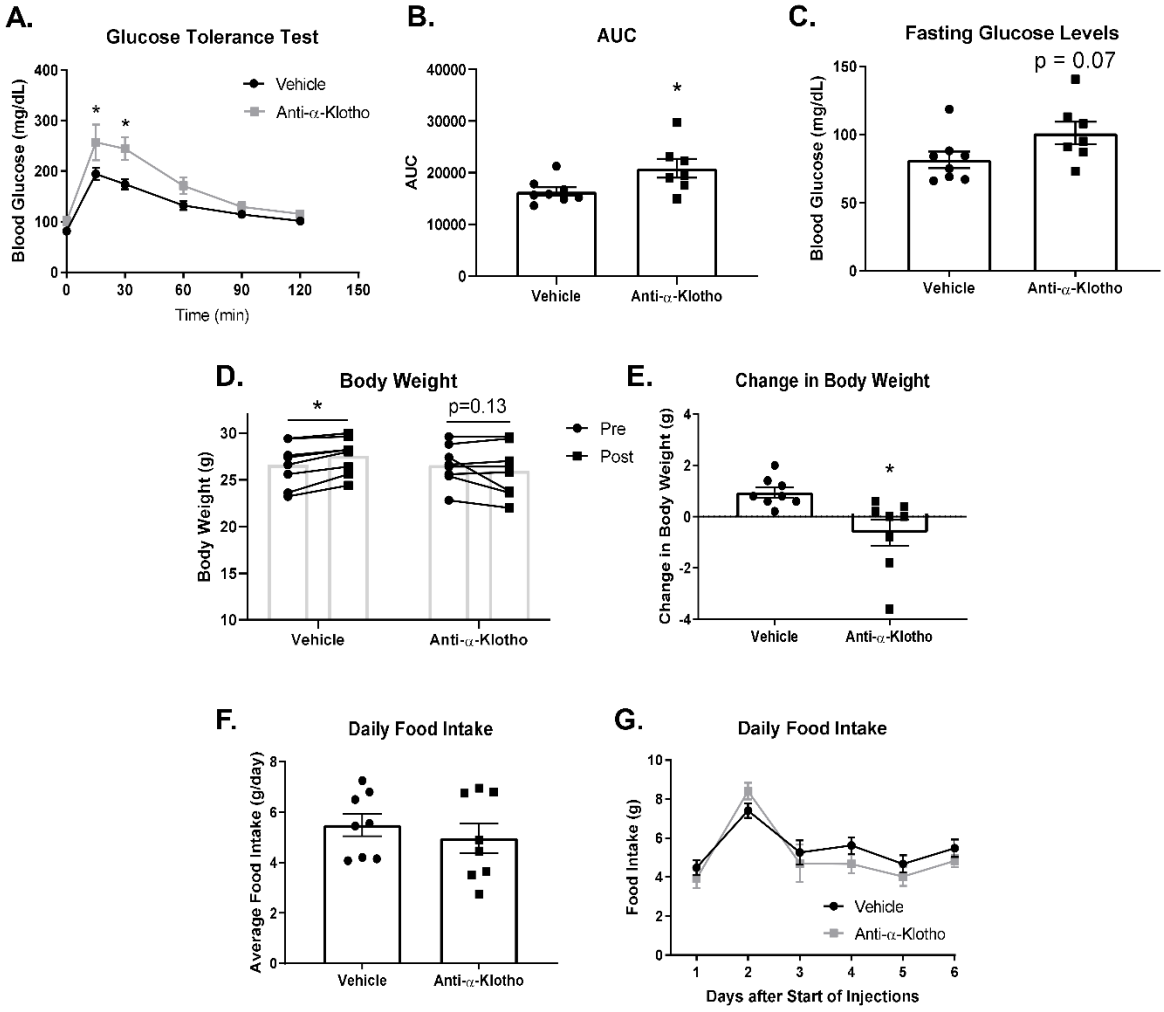
A.
Glucose Tolerance Test
Blood Glucose (mg/dL)
Time (min)
Vehicle
Anti-α-Klotho
B.
AUC
AUC
Vehicle
Anti-α-Klotho
C.
Fasting Glucose Levels
p = 0.07
Blood Glucose (mg/dL)
Vehicle
Anti-α-Klotho
D.
Body Weight
p=0.13
Body Weight (g)
Pre
Post
Vehicle
Anti-α-Klotho
E.
Change in Body Weight
Change in Body Weight (g)
Vehicle
Anti-α-Klotho
F.
Daily Food Intake
Average Food Intake (g/day)
Vehicle
Anti-α-Klotho
G.
Daily Food Intake
Food Intake (g)
Vehicle
Anti-α-Klotho
Days after Start of Injections

Figure 2.5

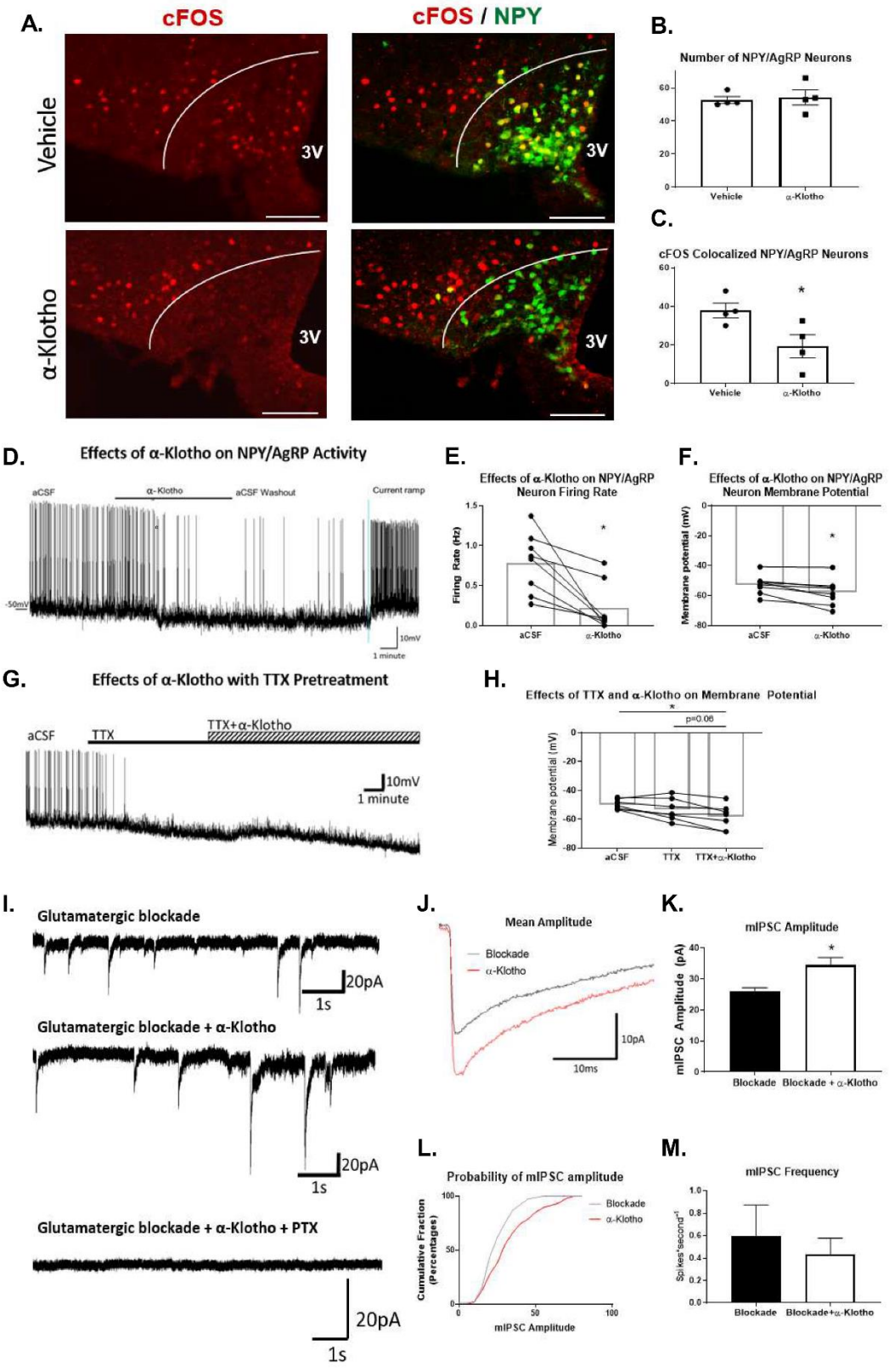
A.
cFOS
cFOS / NPY
Vehicle
α-Klotho
3V
B.
Number of NPY/AgRP Neurons
Vehicle
α-Klotho
C.
cFOS Colocalized NPY/AgRP Neurons
D.
Effects of α-Klotho on NPY/AgRP Activity
aCSF
α-Klotho
aCSF Washout
Current ramp
10mV
1 minute
E.
Effects of α-Klotho on NPY/AgRP Neuron Firing Rate
Firing Rate (Hz)
F.
Effects of α-Klotho on NPY/AgRP Neuron Membrane Potential
Membrane potential (mV)
G.
Effects of α-Klotho with TTX Pretreatment
TTX
TTX+α-Klotho
H.
Effects of TTX and α-Klotho on Membrane Potential
p=0.06
I.
Glutamatergic blockade
20pA
1s
Glutamatergic blockade + α-Klotho
Glutamatergic blockade + α-Klotho + PTX
J.
Mean Amplitude
Blockade
α-Klotho
10pA
10ms
K.
mIPSC Amplitude
mIPSC Amplitude (pA)
Blockade + α-Klotho
L.
Probability of mIPSC amplitude
Cumulative Fraction (Percentages)
mIPSC Amplitude
M.
mIPSC Frequency
Spikes*second-1

Figure 2.6

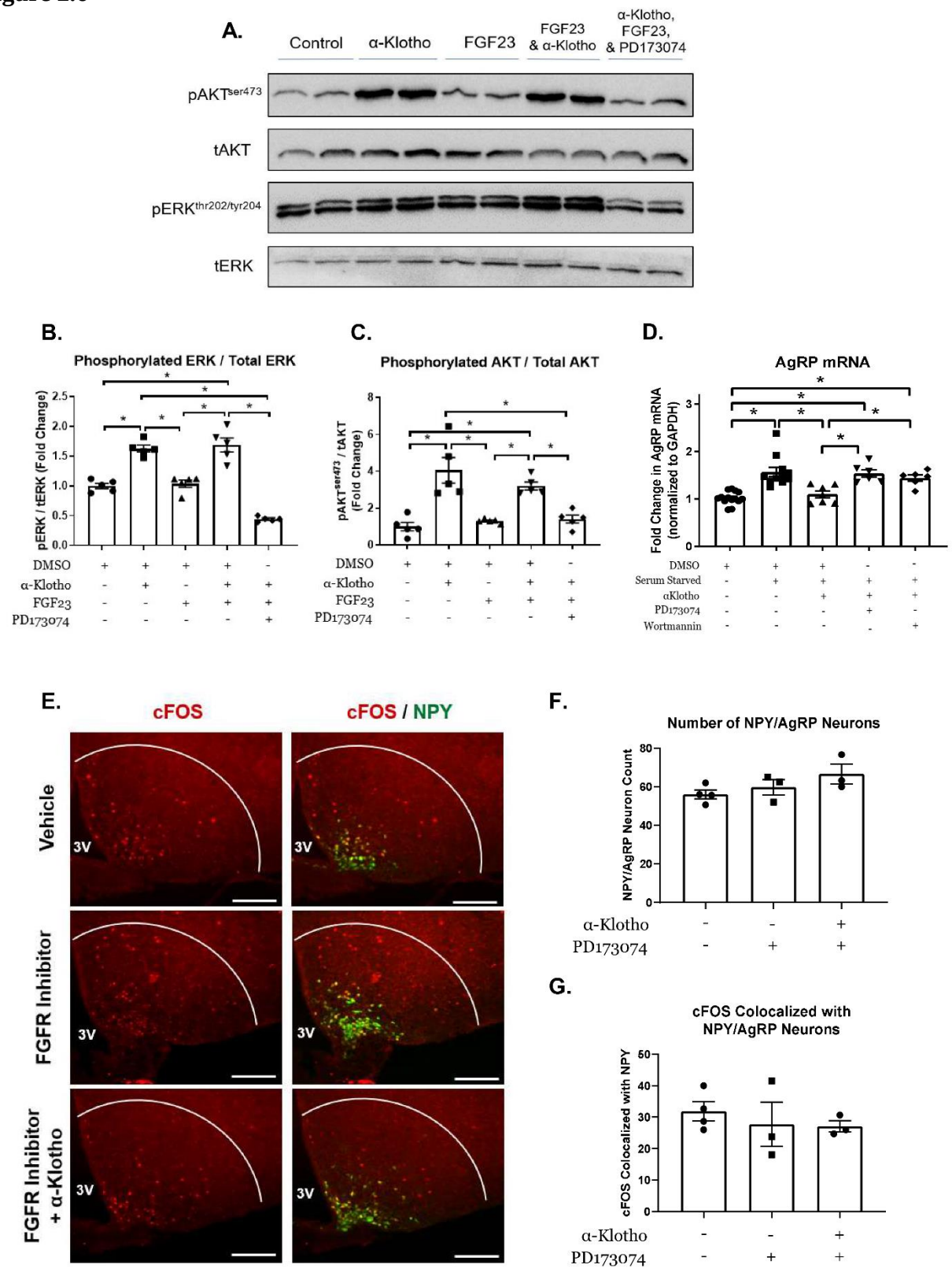
A.
Control
α-Klotho
FGF23
FGF23 & α-Klotho
α-Klotho, FGF23, & PD173074
pAKTser473
tAKT
pERKthr202/tyr204
tERK
B.
Phosphorylated ERK / Total ERK
pERK / tERK (Fold Change)
DMSO
α-Klotho
FGF23
PD173074
C.
Phosphorylated AKT / Total AKT
pAKTser473 / tAKT (Fold Change)
DMSO
α-Klotho
FGF23
PD173074
D.
AgRP mRNA
Fold Change in AgRP mRNA (normalized to GAPDH)
DMSO
Serum Starved
αKlotho
PD173074
Wortmannin
E.
cFOS
cFOS / NPY
Vehicle
FGFR Inhibitor
FGFR Inhibitor + α-Klotho
3V
F.
Number of NPY/AgRP Neurons
NPY/AgRP Neuron Count
α-Klotho
PD173074
G.
cFOS Colocalized with NPY/AgRP Neurons
cFOS Colocalized with NPY
α-Klotho
PD173074

Figure 2.7

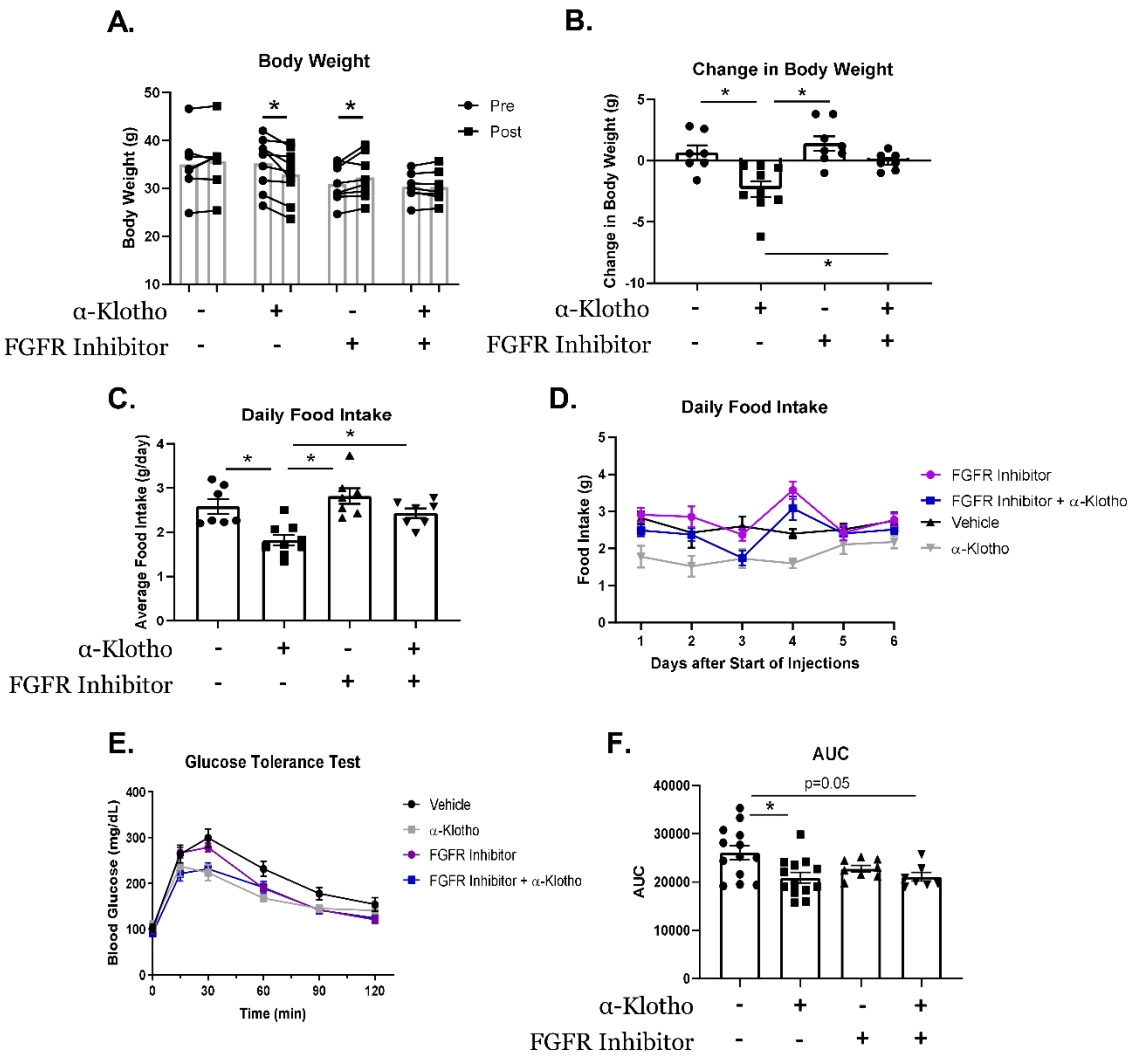
A.
Body Weight
Body Weight (g)
Pre
Post
α-Klotho - + - +
FGFR Inhibitor - - + +
B.
Change in Body Weight
Change in Body Weight (g)
α-Klotho - + - +
FGFR Inhibitor - - + +
C.
Daily Food Intake
Average Food Intake (g/day)
α-Klotho - + - +
FGFR Inhibitor - - + +
D.
Daily Food Intake
Food Intake (g)
Days after Start of Injections
FGFR Inhibitor
FGFR Inhibitor + α-Klotho
Vehicle
α-Klotho
E.
Glucose Tolerance Test
Blood Glucose (mg/dL)
Time (min)
Vehicle
α-Klotho
FGFR Inhibitor
FGFR Inhibitor + α-Klotho
F.
AUC
p=0.05
AUC
α-Klotho - + - +
FGFR Inhibitor - - + +

Figure 2.8

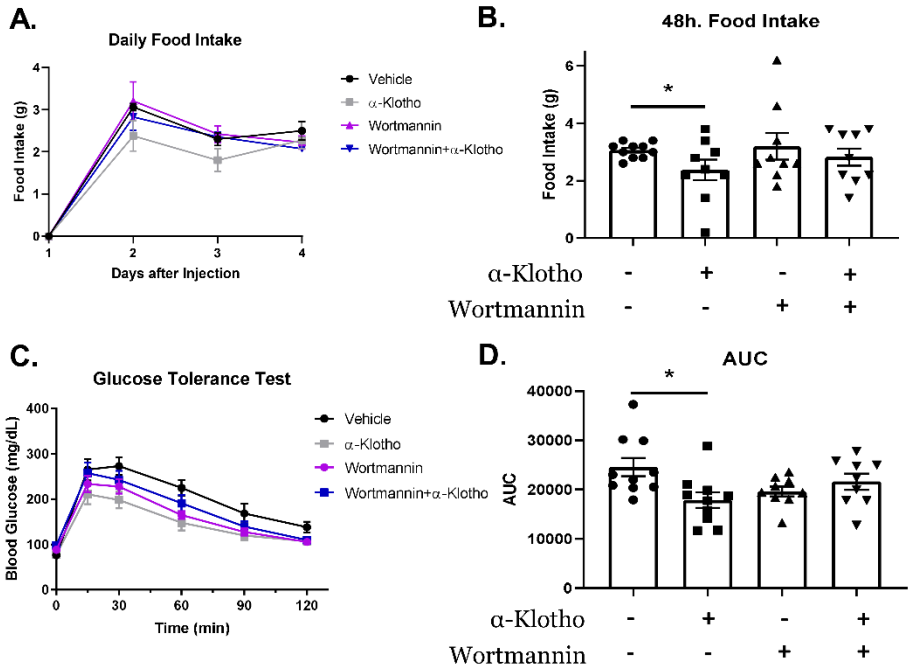
A.
Daily Food Intake
Food Intake (g)
Days after Injection
Vehicle
α-Klotho
Wortmannin
Wortmannin+α-Klotho
B.
48h. Food Intake
Food Intake (g)
*
α-Klotho - + - +
Wortmannin - - + +
C.
Glucose Tolerance Test
Blood Glucose (mg/dL)
Time (min)
Vehicle
α-Klotho
Wortmannin
Wortmannin+α-Klotho
D.
AUC
AUC
*
α-Klotho - + - +
Wortmannin - - + +

Supplemental Figure 2.1

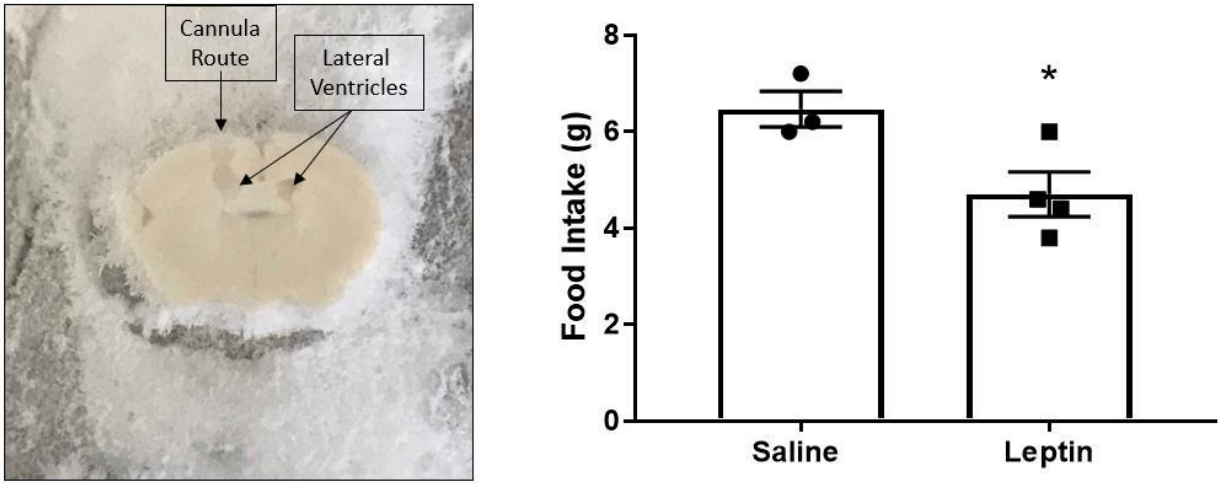

Supplemental Figure 2.2

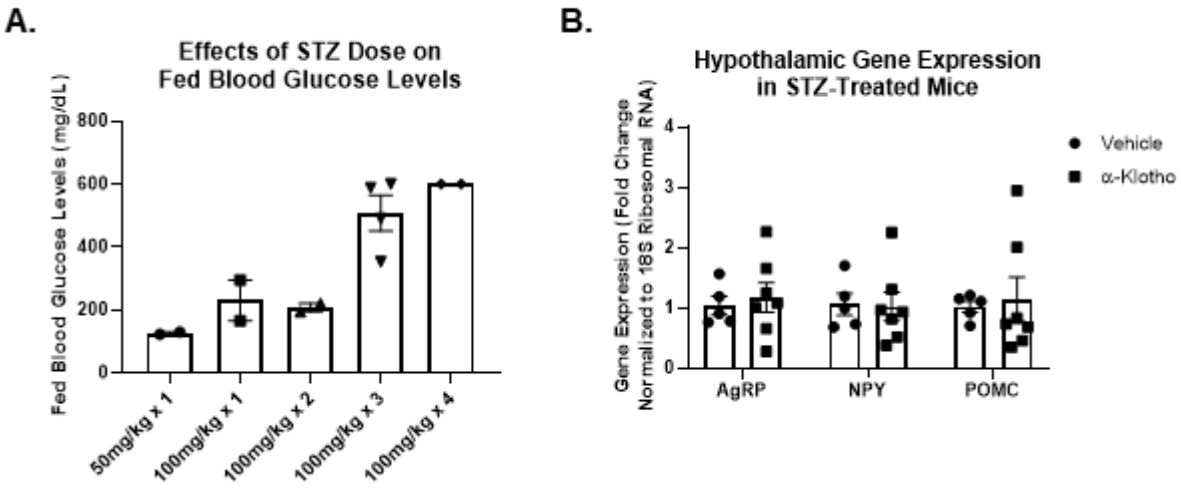

Supplemental Figure 2.3

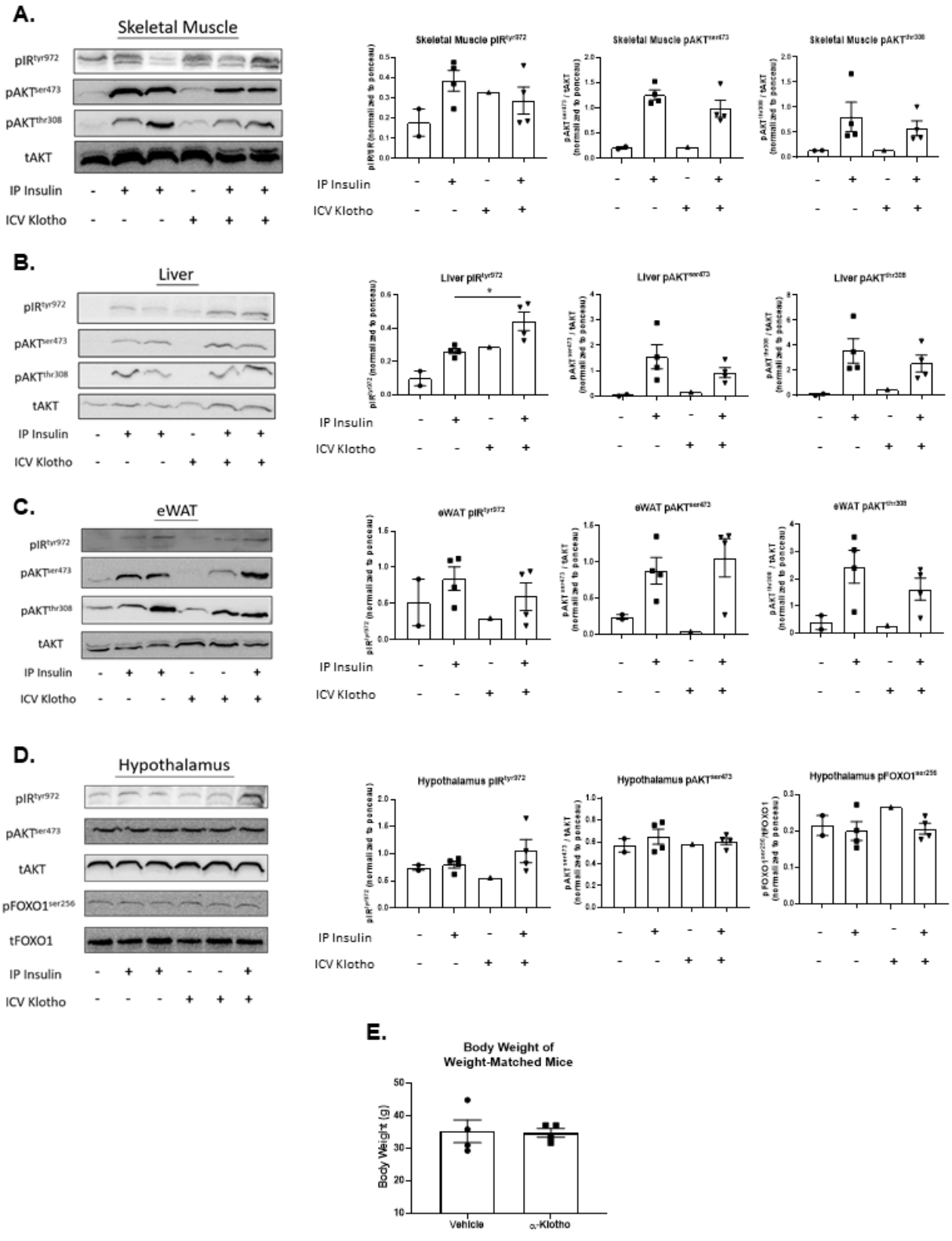

Supplemental Figure 2.4

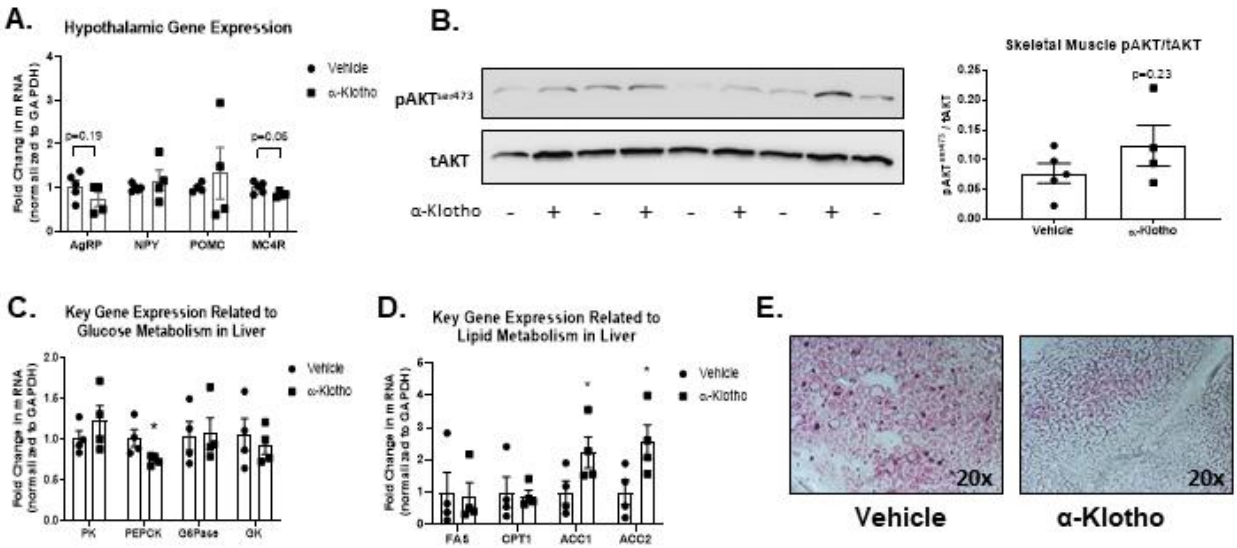

Supplemental Figure 2.5

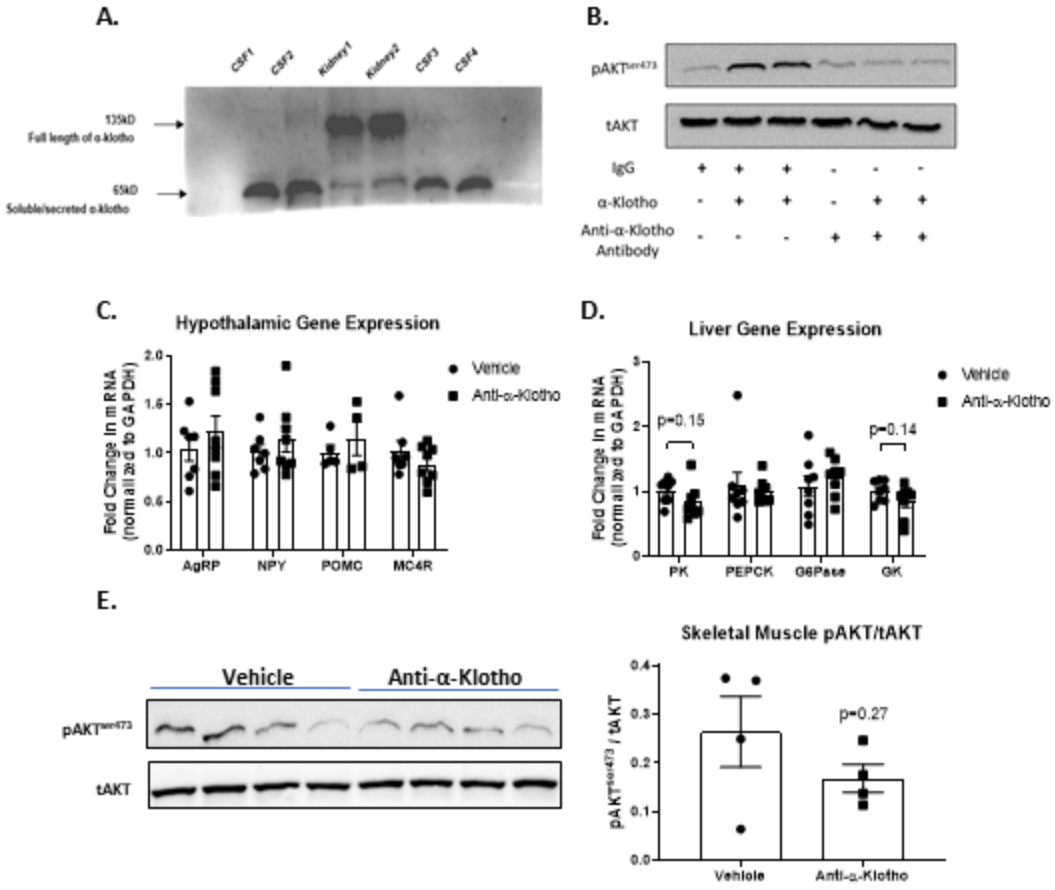

Supplemental Figure 2.6

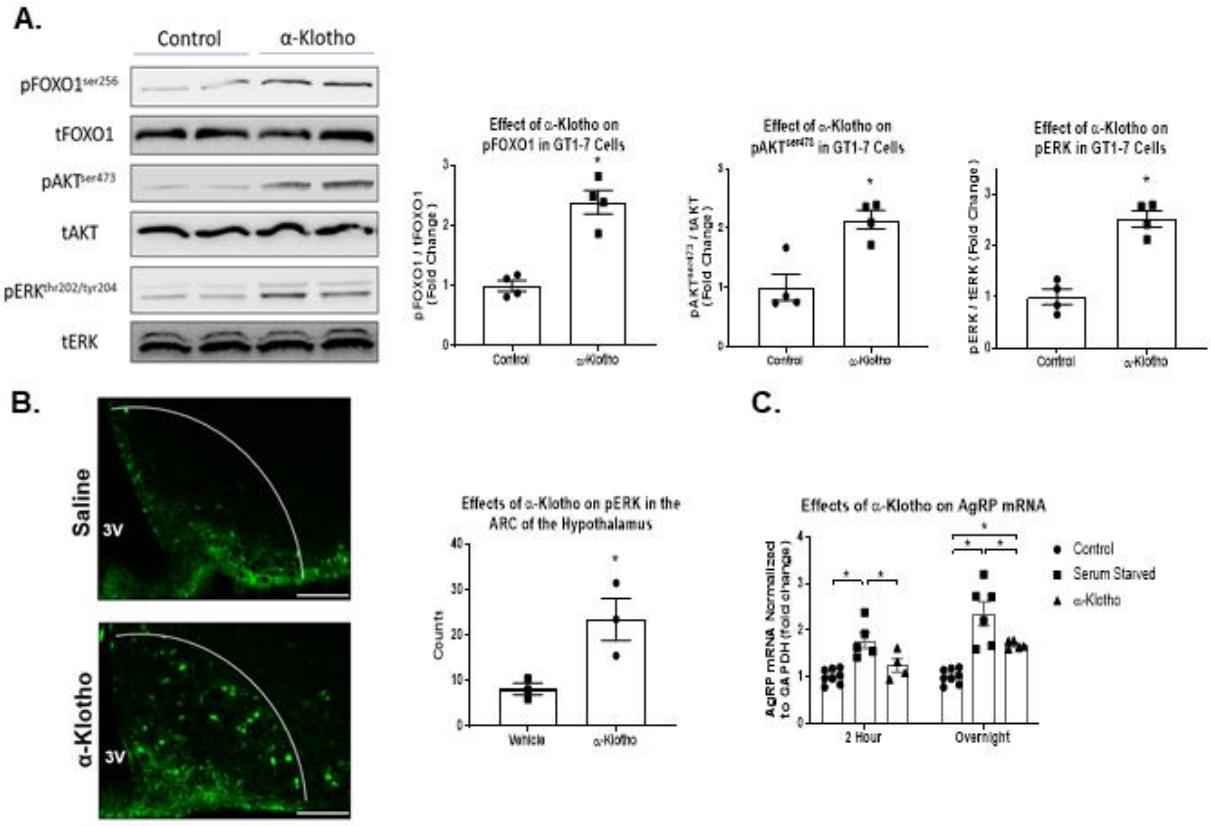

Supplemental Figure 2.7

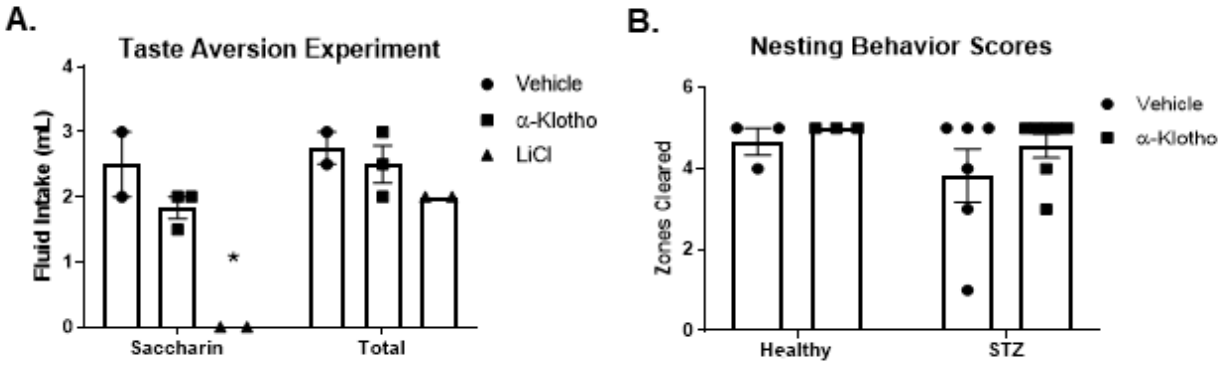

Supplemental Figure 2.8

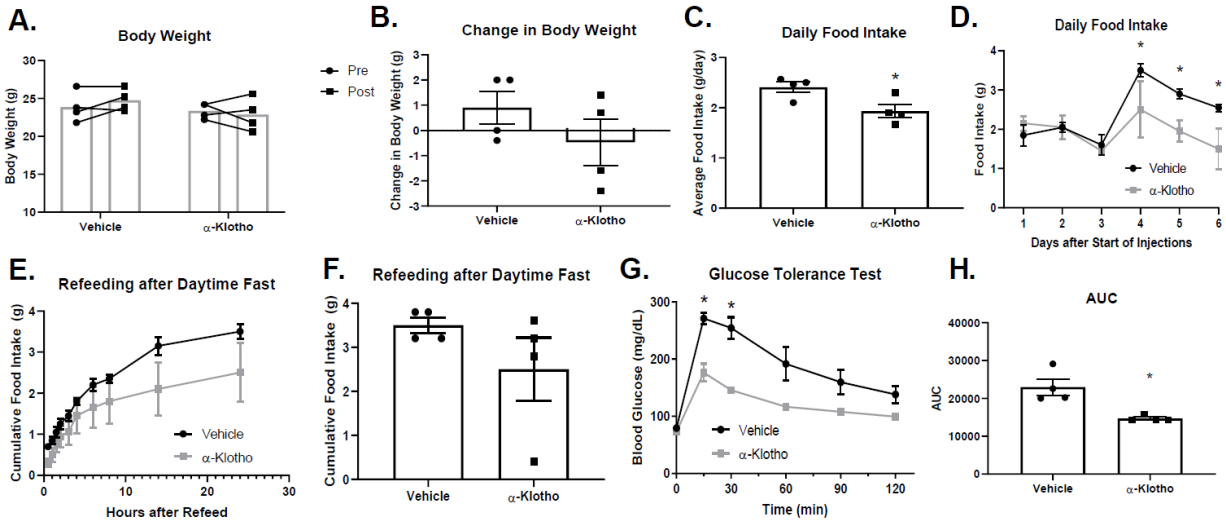

Supplemental Figure 2.9

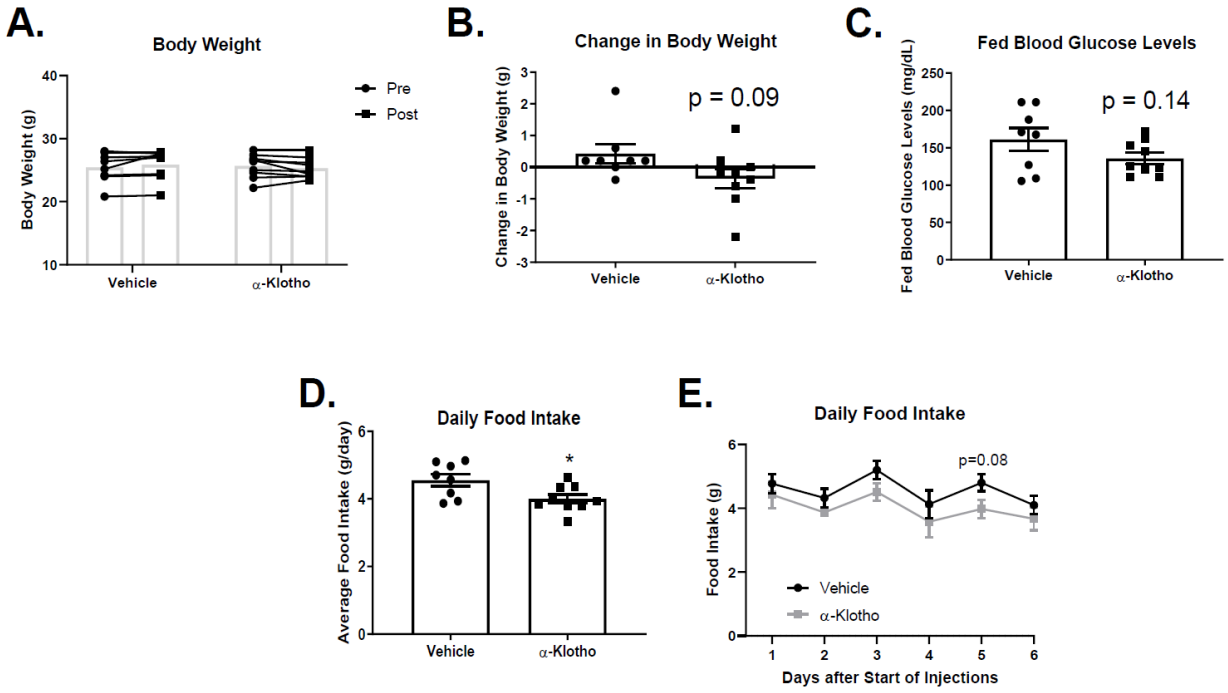

Supplemental Table 2.1

Gene	Forward primer	Reverse primer
GAPDH	AAATGGTGAAGGTCGGTGTG	TGAAGGGGTCGTTGATGG
ACC1	CGGCAGTACCTGCGAGTAGAG	GGGCGAATACACATTTGTCGTA
ACC2	GGGCCCTGGGAGACAAGA	GGGTAAGGTTGGGATTTGCA
FAS	TTCCAAGACGAAAATGATGC	AATTGTGGGATCAGGAGAGC
CPT1	TCTTGCAGTCGACTCACCTT	TCCACAGGACACATAGTCAGG
G6Pase	TTACCAAGACTCCCAGGACTG	GAGCTGTTGCTGTAGTAGTCG
GK	CCCTGAGTGGCTTACAGTTC	ACGGATGTGAGTGTTGAAGC
L-PK	CTTGCTCTACCGTGAGCCTC	ACCACAATCACCAGATCACC
PEPCK	TGGCTACGTC CCTAAGGAA	GGTCCTCCAGATACTTGTCGA
NPY	CCCAGCTCACATATTTATCTAGAG	TATGTGGACGGGGCAGAAGATCCAGG
AgRP	GCGGAGGTGCTAGATCCACA	AGGACTCGTGCAGCCTTACAC
POMC	CTCCGCTCTGCGACACTACA	ACCTCACCACGGAGAGCAAC
MC4R	GCG TTT CGA ATG GGT CGG AAA CCA	CCG CAA TGG AAA GCA GGC TGC AA

Chapter 3

Centrally Circulating α-Klotho Inversely Correlates with Human Obesity and Modulates Arcuate Cell Populations in Mice

ABSTRACT

OBJECTIVE: Our lab recently identified the centrally circulating α-klotho protein as a novel hypothalamic regulator of food intake and glucose metabolism in mice. The current study aimed to investigate novel molecular effectors of central α-klotho in the arcuate nucleus of the hypothalamus (ARC), while further deciphering its role regulating energy balance in both humans and mice.

METHODS: Cerebrospinal fluid (CSF) was collected from 22 adults undergoing lower limb orthopedic surgeries and correlations between body weight and α-klotho were determined using an α-klotho ELISA kit. To investigate the effects of α-klotho on energy expenditure (EE), 2-day intracerebroventricular (ICV) treatment was performed in diet-induced obesity (DIO) mice housed in metabolic cages. Immunohistochemical staining for cFOS and patch clamp electrophysiology were used to determine the effects of central α-klotho on proopiomelanocortin (POMC) and tyrosine hydroxylase (TH) neurons. Additional stains were performed to determine novel roles for central α-klotho to regulate non-neuronal cell populations in the ARC. Lastly, ICV pretreatment with fibroblast growth factor receptor (FGFR) or PI3kinase inhibitors was performed to determine the intracellular signaling involved in α-klotho-mediated regulation of ARC nuclei.

RESULTS: Obese/overweight human subjects had significantly lower CSF α-klotho concentrations compared to lean counterparts (1044±251 vs. 1616±218 pmol/L respectively). Additionally, 2 days ICV α-klotho treatment increased EE in DIO mice. α-Klotho had no effects

on TH neuron activity, but elicited varied responses in POMC neurons, with ~44% experiencing excitatory and ~56% inhibitory effects. Inhibitor experiments identified an α-klotho→FGFR→PI3kinase signaling mechanism in the regulation of ARC POMC and NPY/AgRP neurons. Acute ICV α-klotho treatment also increased phosphorylated ERK in ARC astrocytes via FGFR signaling.

CONCLUSION: Our human CSF data provides the first evidence that impaired central α-klotho bioavailability may be involved in the pathophysiology of obesity. Furthermore, results in mouse models identify ARC POMC neurons and astrocytes as novel molecular effectors of central α-klotho. Overall, the current study highlights prominent roles of α-klotho→FGFR→PI3kinase signaling in the homeostatic regulation of ARC neurons and whole-body energy balance.

T. Landry, P. Li, D. Shookster, Z. Jiang, H. Li, B.T. Laing, W. Bunner, T. Langton, Q. Tong, and H. Huang. *Molecular Metabolism*. 2021.

3.1. Introduction

3.1.1. Background- Recent evidence identifies the anti-aging protein α-klotho as a potent, yet complex, hormonal regulator of whole-body metabolism. α-Klotho can be secreted from the kidney [90] and act on peripheral tissues to regulate insulin sensitivity [91], promote insulin release [69,98], protect pancreatic β cells from oxidative damage [99], increase resting energy expenditure [97], and stimulate lipid oxidation [97]. Furthermore, blood α-klotho concentrations are reduced in patients with diabetes or obesity [102,143,145,167,168], while experimentally reversing these impairments has been shown to be therapeutic in various rodent models of metabolic disease [69,97–99,102].

Despite its prominent roles in peripheral metabolism, α-klotho can't cross the blood brain barrier due to its molecular weight [92,119], resulting in a separate, relatively unexplored, pool of α-klotho secreted from the choroid plexus into the cerebrospinal fluid (CSF) [90,130]. Our lab recently provided the first evidence that CSF α-klotho also regulates energy balance and glucose metabolism [218]. Intracerebroventricular (ICV) administration of α-klotho resulted in suppressed appetite, reduced body weight, improved insulin release, and reduced hepatic gluconeogenic gene expression in mouse models of Type I and II diabetes. We also observed that α-klotho is a novel negative regulator of neuropeptide Y/agouti-related peptide- (NPY/AgRP)-expressing neurons in the arcuate nucleus (ARC) of the hypothalamus, which are critically involved in inducing hunger [34], reducing energy expenditure [39], and regulating glucose metabolism [35,54]. Mechanistically, α-klotho acts as a scaffolding protein to promote FGFR activity and downstream PI3kinase signaling [151], a phenomenon that was found to be essential to central α-klotho-mediated regulation of energy balance and NPY/AgRP neurons [218].

The ARC contains many other cell types critical to metabolic regulation. Similar to NPY/AgRP neurons, ARC tyrosine hydroxylase-expressing (TH) neurons project to the paraventricular nucleus (PVN) to stimulate food intake [45]. Conversely, ARC proopiomelanocortin- (POMC)-expressing neurons induce satiety, increase energy expenditure, and reduce hepatic glucose output [14,19,219], in part via PI3kinase signaling [73]. Even non-neuronal ARC astrocytes and tanycytes are essential to nutrient sensing, hormonal transport, and neuronal health [220–222], roles recently found to be dependent on FGFR function [217,223].

2.1.2. Main objective/hypothesis- Considering the diverse ARC cell types, the current study aimed to identify novel molecular effectors of the α-klotho→FGFR→PI3kinase signaling axis in the ARC, hypothesizing that, in addition to NPY/AgRP neurons, central α-klotho regulates ARC POMC and TH neurons, as well as astrocytes, to increase energy expenditure and promote body weight homeostasis.

3.2. Methods

3.2.1. Human cerebrospinal fluid (CSF) collection- All human protocols were approved by the medical ethics committee of Beijing Friendship Hospital, Capital Medical University (Beijing, China). After informed consent was provided, CSF was collected from twenty-two adults (10 male, 12 female, 18-83 years old) undergoing lower limb orthopedic surgeries at the Beijing Friendship Hospital, Beijing, China. All patients were clear of CNS infections, renal diseases, severe cardiopulmonary diseases such as myocardial infarction or chronic obstructive pulmonary disease, and malignant tumors. Patients were chosen using systematic sampling in odd sequence on the same day each week. CSF was collected from the first, third, fifth, etc. surgery patients each day.

Briefly, 1.0 mL CSF was collected during administration of spinal block anesthesia. Patients laid on their sides with their backs at the edge of the operation bed, curled their shoulders and legs, and arched out their lower backs. The needle was placed past the dura mater into subarachnoid space and between lumbar vertebrae, usually between L3 and L4 or L4 and L5 to minimize risk of injury to the spinal cord. All specimens were immediately flash-frozen in liquid nitrogen before storage at -80℃. α-Klotho CSF concentrations were measured by ELISA using a human soluble α-klotho assay kit (27998, IBL).

3.2.2. Animals- C57BL/6, B6.Tg(NPY-hrGFP)1Lowl/J (NPY-GFP reporter), and Tg(Pomc1-cre)16Lowl/J (POMC-Cre) mice were cared for in accordance with the National Institutes of Health *Guide for the Care and Use of Laboratory Animals*, and experimental protocols were approved by Institutional Animal Care and Use Committees of East Carolina University or University of Texas Health Science Center as appropriate. Mice were housed at 20–22°C with a 12-h light-dark cycle.

3.2.3. High-fat diet-induced obesity- 5-6-week-old male C57BL/6 mice were given ad libitum access to a high-fat diet with a kilocalorie composition of 58%, 25%, and 17% of fat, carbohydrate, and protein, respectively, for 10 weeks (D12331; Research Diets, New Brunswick, NJ) before undergoing intracerebroventricular (ICV) cannulation.

3.2.4. Intracerebroventricular (ICV) cannulation and treatment- ICV procedures were performed as previously described [218]. Prior to the procedure, mice were given oral analgesic meloxicam and anesthetized with an isoflurane vaporizer. Mice were placed on a stereotaxic device, and a

midline incision was made on the head. A hole was drilled (1.0 mm lateral, −0.5 mm posterior, 2.5 mm deep to the bregma), and a cannula was placed into the lateral ventricle. Another hole was drilled, and a screw was placed approximately at the ipsilateral lambdoid structure to aid in supporting the cannula in the skull with 3M carboxylate dental cement. Mice recovered for 14 days before immunohistochemical experiments and 7 days before all other experiments.

ICV treatments included: 2.0 ug α-klotho (R&D Systems) [218], 10 minutes pretreatment with 25ug PD1703074 for FGFR inhibition (Fisher Scientific) [195], and/or 1 hour pretreatment with 10ng wortmannin for PI3kinase inhibition (Fisher Scientific) [68]. All ICV treatments, were administered via Hamilton syringe as 2.0 μL between 6:30 and 7:30 P.M. Validation of cannula placement was performed by post-mortem visualization of canula path in brain slices [218].

3.2.5. Energy expenditure and body composition- Energy expenditure was measured using the indirect calorimetry TSE PhenoMaster metabolic cages. Diet-induced obesity (DIO) mice were placed in these cages at 16-17-weeks old and allowed two days for acclimatization before beginning data analysis (Supplemental Figure 1). To normalize oxygen consumption and carbon dioxide production to lean body mass, body composition was determined by Echo MRI (Echo Medical Systems, Houston, MA, USA) immediately before placement in the metabolic cages.

3.2.6. Food intake and body weight measurements- Food intake and body weight were measured daily. Food intake was measured by weighing food (8–9 g) and subtracting from the total food. Bedding was inspected thoroughly for residual bits of food, which were included in measurements.

3.2.7.Quantitative PCR- To assess thermogenic gene expression, brown adipose tissue (BAT) and inguinal white adipose tissue (iWAT) was removed and flash frozen from euthanized mice after two days ICV treatment with α-klotho or vehicle. RNA was extracted by Trizol (Thermo Fisher Scientific, Waltham, MA). The expressions of specific mRNA were analyzed using quantitative real-time PCR (RT-qPCR) (Power SYBR Green PCR Master Mix; Applied Biosystems, Foster City, CA). Reactions were performed in triplicate for each sample, while 18S ribosomal RNA was used as a reference gene for normalization.

3.2.8. Immunohistochemistry- For immunofluorescent analysis, mice were intracardially perfused with PBS followed by 10% formalin before immunohistochemistry was performed as described previously [224]. Briefly, brains were sliced into 20-µm coronal sections using a freezing microtome (VT1000 S; Leica, Wetzlar, Germany) and incubated overnight in antibody to phosphorylated $ERK^{thr202/tyr204}$ (1:500; Cell Signaling Technology, Danvers, MA), cFOS (1:250; Santa Cruz Biotechnology, Santa Cruz, CA), POMC (1:3000; Phoenix Pharmaceuticals), glial fibrillary-acid protein (GFAP) (1:1000; Millipore), tyrosine hydroxylase (TH) (1:100000; Millipore), doublecortin (DCX) (1:800; Cell Signaling Technology), phosphorylated $STAT3^{ser754}$ (1:3000; Cell Signaling Technology) and/or Ki67 (1:500; Abcam), followed by incubation with Alexa-fluorophore secondary antibody for 1 h (Abcam). Stains were photographed using an optical microscope (DM6000; Leica), followed by blind analysis using ImageJ. At least three anatomically matched images per mouse were quantified.

3.2.9. Stereotaxic microinjections- To express green fluorescent protein (GFP) in POMC neurons, POMC-cre mice (7-8 weeks) were anesthetized with a mixture of ketamine (100 mg/kg) and xylazine (10 mg/kg) and placed in a stereotaxic frame. AAVs were delivered bilaterally to the ARC (200 nl/site at 30 nl/min) using the following coordinates (distances from bregma): 1.4 mm posterior, 1.6 mm lateral ± 0.2 mm, and 5.8 mm deep, with a 0.5 µl Hamilton syringe connected to a motorized stereotaxic injector (Quintessential Stereotaxic Injector; Stoelting). The injection needle was maintained in place for 5 min following injections to minimize virus spread up the needle track. The virus used was AAV-EF1α-Flex-GFP (> 1×10^{12} GC/ml, UNC Vector Core) and AAV (DJ8)-Flex-mCherry (> 1×10^{12} GC/ml, Optogenetics and Viral Vectors Core at Baylor College of Medicine). Mice recovered for 1-2 weeks before electrophysiological recordings.

3.2.10. Electrophysiological Recordings- Electrophysiological experiments were conducted in acutely prepared hypothalamic slices, as previously described [225,226]. Briefly, 8-10-week-old adult mice were deeply anesthetized with a mixture of ketamine/xylazine (intraperitoneally) and transcardially perfused with ice-cold cutting solution containing the following (in mM): 75 sucrose, 73 NaCl, 26 $NaHCO_3$, 2.5 KCl, 1.25 NaH_2PO_4, 15 glucose, 7 $MgCl_2$, and 0.5 $CaCl_2$, saturated with 95% O_2/5% CO_2. The brains were quickly removed and blocked, with the rostral face of the block glued to the specimen plate of the buffer tray then immersed in an ice-cold cutting solution. Coronal slices (280 µm) containing ARC were sectioned using a Leica VT1000S Vibratome and transferred to a holding chamber with artificial CSF (aCSF) containing the following (in mM): 123 NaCl, 26 $NaHCO_3$, 2.5 KCl, 1.25 NaH_2PO_4, 10 glucose, 1.3 $MgCl_2$, and 2.5 $CaCl_2$, and saturated with 95% O_2/5% CO_2 at 31–33°C for 30 min, then maintained at room temperature for at least 1 h to allow for recovery before any electrophysiological recordings.

Individual slices were transferred from the holding chamber to a recording chamber, where they were submerged and continuously perfused with oxygenated aCSF at ~2 ml/min. GFP-expressing POMC neurons in the ARC were first located under epifluorescence illumination, and whole-cell patch-clamp recordings were performed on 16 POMC neurons from 6 mice (3 male, 3 female) under infrared-differential interference contrast visualization at 30-32°C on a fixed-stage, upright microscope (model BX51WI, Olympus) equipped with a water-immersion 40× objective. Pipettes with a resistance of 3–5 MΩ were pulled from borosilicate glass (outer diameter, 1.5 mm; inner diameter, 1.1 mm; Sutter Instruments) using a horizontal puller (P-97, Sutter) and filled with an internal patch solution containing the following (in mM): 142 K-gluconate, 10 HEPES, 1 EGTA, 2.5 $MgCl_2$, 4 Mg-ATP, 0.3 Na-GTP, and 10 Na_2-phosphocreatine, adjusted to pH 7.25–7.35, osmolality 295–305 with KOH. After "breaking into" cells, at least 5 minutes was given for baseline to be established, before obtaining baseline measurements for another 5-9 minutes. α-Klotho was then administered at 3.65mM in aCSF. The liquid junction potential was not corrected, and series resistance (Rs) was bridge balanced.

3.2.11. Statistical analysis- Pearson's correlation coefficients were used to determine associations between CSF α-klotho concentrations and other variables. Unpaired *t* tests or one-way ANOVA with Tukey's correction for multiple comparisons were used to determine differences between or among groups, respectively, in CSF α-klotho, oxygen consumption, carbon dioxide production, locomotor activity, gene expression, food intake, body weight, or proteins of interest detected by immunofluorescence. To compare pre-post within-group changes over the course of 2-day experiments, paired *t* tests were performed. Unpaired or paired *t* tests were used for between or within-neuron patch clamp electrophysiology experiments, respectively. All analyses were

performed using GraphPad Prism statistics software, and $p<0.05$ was considered statistically significant.

3.3. Results

3.3.1. Human CSF α-klotho concentrations are reduced in overweight and obese adults

CSF was collected from 22 adults (10 male, 12 female) with an average age and BMI of 52.3±17.1 and 25.7±3.6, respectively (Supplemental Table 1). CSF α-klotho concentrations exhibited a strong inverse correlation with body weight and BMI (R=-0.6823 and -0.7822 respectively) (Fig. 1A-B). There were no correlations between CSF α-klotho concentrations and fasting blood glucose, cholesterol, or triglycerides (Fig. 1D-F). Subjects were then stratified into lean (BMI<25) and overweight/obese (BMI>25) categories (mean BMI's were 22.8±1.7 and 28.6±2.4, respectively). Although there were no significant differences in age, height, fasting blood glucose, blood triglycerides, total cholesterol, or LDL levels between the groups (Supplemental Table 1), overweight/obese subjects had significantly lower CSF α-klotho concentrations and serum HDL levels compared to lean counterparts (1044±251 vs. 1616±218 pmol/L and 1.2±0.2 vs. 1.0±0.2 mmol/L respectively) (Fig. 1C and Supplemental Table 1). To our knowledge, this is the first data to illustrate a strong negative correlation between CSF α-klotho and body weight in human subjects, suggesting the potential involvement of central α-klotho concentrations in the development of obesity.

3.3.2. Two days ICV α-klotho treatment increases energy expenditure in DIO mice

To further investigate the role of central α-klotho in energy balance regulation, two days ICV α-klotho treatment was performed in male DIO mice. Consistent with previous results, two days ICV

α-klotho treatment significantly decreased daily food intake (20.3%) and resulted in modest reductions in body weight (1.5%) compared to vehicle-treated controls (Supplemental Fig. 2). ICV α-klotho treatment also significantly increased average daily oxygen consumption (10.9%) and carbon dioxide production (11.2%), with no effects on locomotor activity (Fig. 2A-F). These data suggest a novel ability of central α-klotho to improve energy balance by increasing daily energy expenditure.

UCP1 gene expression also strongly trended to be elevated in BAT and iWAT of α-klotho-treated mice (1.4-fold; p=0.07 and 6.4-fold; p=0.11, respectively), suggesting potentially increased thermogenesis and browning of white adipose tissue (Fig. 2G-H). There were also trends toward increased NRF1 gene expression in the BAT of α-klotho-treated mice (1.3-fold; p=0.09), while there were no differences in PRDM16, CIDEA, PGC1α, PPARγ, or NRF1 gene expression in either BAT or iWAT.

3.3.3. Central α-klotho has no obvious effects on TH neuron activity in fasted mice

Previous reports identify direct, inhibitory action of central α-klotho on ARC NPY/AgRP neurons [218]; thus, we aimed to investigate the possibility of additional neuronal targets of central α-klotho in the hypothalamus. For example, TH neurons elicit orexigenic effects in the ARC and regulate thermogenesis in the PVN [37,45]. However, immunofluorescent staining revealed acute ICV α-klotho treatment had no obvious effects on cFOS colocalization with TH neurons in the hypothalami of fasted male or female mice (Fig. 3).

3.3.4. Central α-klotho regulates ARC POMC neuron activity in fasted mice

POMC neurons are another ARC neuron population involved in reducing hunger and increasing energy expenditure [14,19,219]. We performed patch clamp electrophysiology experiments and 7 out of 16 POMC neurons analyzed exhibited increased firing rate and membrane potential when treated with α-klotho (0.47±0.13 vs. 1.40±0.28 Hz. and -50.52±1.02 vs. -47.57±1.17 mV, respectively) (Fig. 4A-C). Interestingly, all POMC neurons recorded responded to α-klotho, with 9 out of 16 POMC neurons exhibiting decreased firing rate and membrane potential (0.30±0.09 vs. 0.08±0.06 Hz and -47.33±0.73 vs. -52.10±1.76 mV, respectively) (Supplemental Fig. 3A-C). While these data identify POMC neurons as novel neuronal effectors of central α-klotho function, they also highlight the heterogeneity of the POMC-expressing neuron population [227]. For example, POMC neurons stimulated by α-klotho had significantly lower baseline membrane potentials compared to those antagonized by α-klotho, while there were no differences in baseline firing rate (Supplemental Fig. 3D-E).

To further investigate the complex effects of central α-klotho on ARC POMC neuron activity, we performed immunofluorescent staining for cFOS. While acute ICV α-klotho treatment had no effects on ARC POMC neuron activity in fed mice (Supplemental Fig. 4), cFOS colocalization with ARC POMC neurons was significantly elevated in response to acute ICV α-klotho treatment in both fasted male (1.9-fold) and female (1.7-fold) mice (Fig. 4D-J). These data highlight potent excitatory effects of α-klotho on ARC POMC neurons in the fasted status, despite the heterogenous response of POMC neurons observed in electrophysiology experiments.

3.3.5. Central α-klotho increases ARC POMC neuron activity, at least in part, via FGFR's

Previous studies demonstrate α-klotho's role as a scaffolding protein to facilitate FGF23-FGFR binding and downstream signaling, a phenomenon that was found to be critical to α-klotho-

mediated NPY/AgRP neuron inhibition [151,205,218]. To investigate the importance of FGFR's to α-klotho-mediated POMC activation, ICV pretreatment with the FGFR inhibitor PD173074 was performed. When FGFR activity was inhibited, α-klotho no longer significantly increased POMC neuron activity (1.4-fold increase under FGFR blockade, $p=0.13$; vs. 2.1-fold increase with vehicle-treated controls, $p<0.05$) (Fig. 5). The blunted effects of α-klotho in response to FGFR inhibition may indicate central α-klotho regulates POMC neurons, at least in part, via FGFR activity (Fig. 5).

3.3.6. α-Klotho/PI3kinase signaling regulates ARC POMC and NPY/AgRP neuron activity

PI3kinase is a prominent signaling mechanism in the regulation of energy balance, ARC neuron activity, and α-klotho-mediated downregulation of AgRP gene expression [73,218]. When central PI3kinase signaling was impaired using ICV wortmannin treatment, α-klotho no longer significantly increased POMC neuron activity compared to PI3kinase inhibition alone (Fig. 6). Past experiments from our lab also indicate α-klotho downregulates AgRP gene expression via PI3kinase signaling [218]. Consistent with previous reports, in the current study, acute ICV α-klotho treatment significantly reduced NPY/AgRP neuron activity (~46%) (Fig. 7). Furthermore, PI3kinase inhibition attenuated this α-klotho-mediated suppression of NPY/AgRP neuron activity (Fig. 7). Overall, these data suggest PI3kinase signaling is critical to α-klotho-mediated regulation of both NPY/AgRP and POMC neurons.

3.3.7. ICV α-Klotho treatment increases phosphorylated ERK$^{thr202/tyr204}$- in ARC astrocytes

We next aimed to determine if central α-klotho was involved in the regulation of ARC astrocytes, cells involved in nutrient sensing, hormonal transport, and neuronal health [220]. ERK signaling

is a key regulatory mechanism in astrocyte function, and has also been identified as a downstream signaling mechanism of α-klotho in the ARC [218,221,222,228]. There were distinct differences in the localization of phosphorylated $ERK^{thr202/tyr204}$ in the ARC between the two groups. α-Klotho-treated mice exhibited 1.4-fold higher $pERK^{thr202/tyr204}$ in cells expressing the astrocytic marker GFAP (Fig. 8), with qualitatively higher $pERK^{thr202/tyr204}$ concentration in the tanycytic region bordering the third ventricle. Mechanistically, pretreatment with the FGFR inhibitor PD173074 completely abolished this phenomenon (Fig. 8).

Overall, these data may indicate a novel role for central α-klotho/FGFR signaling to regulate astrocyte function in the ARC, suggesting involvement in supporting other nutrient-sensing and hormonal functions. For example, leptin sensitivity and transport is closely connected to astrocyte function [221,222]. Supporting the hypothesis that α-klotho facilitates hormonal transport and sensitivity, acute ICV α-klotho treatment in fasted mice significantly increased phosphorylated STAT3 by 2.1-fold in NPY/AgRP neurons, which is an inhibitory signaling mechanism in these neurons and a critical downstream mediator of leptin (Supplemental Fig. 5).

Furthermore, longer duration (12-days) α-klotho treatment increased Ki67 expression 3.0-fold in the ARC (Supplemental Fig. 6), which is an indication of increased proliferating cells. This increase in active progenitor cells is likely non-neuronal as demonstrated by no effects of long-term α-klotho treatment on number of total POMC, NPY/AgRP, and DCX- (a marker of neurogenesis) expressing cells in the ARC (Supplemental Fig. 7). However, the anatomical distribution of Ki67 expression in the ARC suggests the proliferating cells may be astrocytes or tanycytes, which would indicate α-klotho not only regulates the function of mature astrocytes, but may also be involved in the generation of new astrocytes.

3.4. Discussion

A recent study from our lab provided promising evidence that central α-klotho may be a critical regulator of hypothalamic neurons and metabolism [218]. Aiming to more comprehensively decipher central α-klotho's metabolic role, the current study identified diverse novel functions of central α-klotho in the regulation of energy balance and ARC cell populations. Our data indicates central α-klotho increases energy expenditure, modulates NPY/AgRP and POMC neuron activity via FGFR→PI3kinase signaling, and regulates astrocytes via FGFR→ERK signaling. Furthermore, to our knowledge, we provide the first evidence that CSF α-klotho concentrations and body weight exhibit a strong inverse correlation in humans, potentially implicating central α-klotho in the pathology of obesity.

Previous reports indicate blood α-klotho concentrations are reduced in humans with Type 2 Diabetes [143,145]. However, there is no correlation between peripheral and central α-klotho concentrations, and regulation of circulating CSF α-klotho levels is poorly understood [147]. The few studies examining CSF α-klotho concentrations in humans and rodents have determined no diurnal variations [148], decreased levels in females [147,148], an inverse correlation with age [148], and a positive correlation with FGF23 [147]. Additionally, human CSF α-klotho concentrations are reduced in some neurological disorders such as Alzheimer's Disease [148] and Multiple Sclerosis [149]. Interestingly, we observed CSF α-klotho levels to exhibit a strong, inverse correlation with body mass and BMI. These data may suggest the involvement of central α-klotho in the pathology of obesity and could possibly identify CSF α-klotho levels as a novel preclinical marker in body weight disorders. Considering previous data showing ICV α-klotho treatment decreases hepatic lipid accumulation and central α-klotho inhibition rapidly impairs glucose clearance [218], we also hypothesized CSF α-klotho may inversely correlate with blood

glucose, TG's, or cholesterol. Surprisingly, no such relationships were observed, nor were there significant differences in these variables between lean and overweight/obese subjects. Notably, blood glucose, TG's, and cholesterol often exhibit a weak relationship with BMI [229–231], and a limitation of the current study is a small sample size. Future studies utilizing a larger sample size may discover additional correlations between CSF α-klotho concentrations and blood glucose or lipids.

Consistent with previous reports, ICV α-klotho treatment suppressed food intake and resulted in modest body weight reductions in DIO mice [218]. Indirect calorimetry also determined ICV α-klotho treatment increases resting energy expenditure, independent of locomotor activity. Gene expression analysis revealed that increased thermogenesis in BAT and browning of iWAT may be the mechanism underlying increased energy expenditure. While the mechanism for α-klotho-mediated increases in energy expenditure remains unclear, these data highlight a potent role for central α-klotho to improve energy balance by regulating both caloric consumption and utilization. The observed ICV α-klotho phenotype may be a result of its diverse functions regulating the intricate neurocircuitry in ARC cell populations. For example, α-klotho is an antagonist of ARC NPY/AgRP neurons [218], which, when activated, stimulate food intake, increase circulating glucose levels, decrease energy expenditure, and result in weight gain [34,35,39,54]. Here we identify α-klotho as a novel modulator of ARC POMC neurons, which have opposite metabolic effects compared to NPY/AgRP neurons [12,14]. Interestingly, α-klotho elicited varied effects on POMC neurons during electrophysiological experiments, with ~44% experiencing excitatory and ~56% inhibitory effects. These findings highlight the heterogeneity of the POMC neuron population, with ~72% being "canonical" expressing high levels of POMC and very low levels of AgRP, and ~28% expressing low levels of POMC and high levels of AgRP [26]. α-Klotho

decreases AgRP gene expression and inhibits AgRP-expressing neuron activity [218], which may suggest α-klotho inhibits the POMC neurons expressing high levels of AgRP. Additionally, POMC neurons have variable receptor and neurotransmitter expression, which likely also alters their response to α-klotho [26,27].

It is also possible α-klotho regulates POMC neurons indirectly via presynaptic inputs. For example, α-klotho's previously documented direct inhibitory role in NPY/AgRP neurons [218] may indirectly stimulate POMC activity via relieved NPY/AgRP-mediated GABAergic inputs. Interestingly, NPY/AgRP→POMC connectivity is complex, highlighted by differences in the effects of spontaneous vs. stimulated NPY/AgRP neuron activity. POMC neurons exhibit no change in inhibitory post-synaptic currents (IPSC's) when NPY/AgRP neuron activity or neurotransmitter release is disrupted [28,43]; however, optogenetic stimulation of NPY/AgRP neurons consistently inhibits POMC neurons via direct GABAergic inputs [28,42]. Notably, the current study determined α-klotho regulates NPY/AgRP and POMC neurons via FGFR's, which are expressed in both populations [193]. As a result, it is likely α-klotho can elicit direct, postsynaptic regulation of both these neurons via its role as a scaffolding protein in FGFR's.

Orexigenic ARC TH neurons are also intricately involved in NPY/AgRP and POMC neurocircuitry. For example, TH and NPY/AgRP neurons exhibit a bidirectional synaptic mechanism during which TH neurons stimulate food intake via direct excitatory dopamine action on NPY/AgRP neurons, and NPY/AgRP neurons regulate thermogenesis via Y1 receptors on TH neurons [37,41,45]. Furthermore, both dopamine and GABA released from TH neurons exhibit direct inhibitory action on POMC neurons. Similar to POMC neurons, TH neurons are also a heterogenous neuron population. TH is the rate-limiting enzyme in dopamine and catecholamine synthesis [44]; both of which have varied effects on metabolism. For example, dopamine

stimulates food intake [41] and catecholamines induce satiety [232,233]. In the current study ICV α-klotho had no significant effects on ARC or PVN TH neuron activity, suggesting TH neurons may not be involved in α-klotho's hypothalamic function. However, one α-klotho-treated mouse appeared to be a statistical outlier (greater than two standard deviations different from the mean). Removal of this animal reveals trends toward α-klotho-mediated TH neuron suppression in males only, highlighting the need for further research into this phenomenon. Overall, while the current study does not identify a specific role of α-klotho to regulate hypothalamic TH neurons, future studies using electrophysiology on single TH neurons would help clarify these complicated findings among different TH subpopulations.

We also aimed to determine if α-klotho had additional functions in the ARC independent of neuronal activity. In hippocampal cells, α-klotho has been described as a regulator of neurogenesis and astrocyte metabolism [228,234]. While there were no effects of α-klotho on ARC neurogenesis in DIO mice, we did observe an ability of α-klotho to regulate astrocyte function. ARC astrocytes are critically involved in hormonal transport, nutrient sensing, and neuronal maintenance [221], and α-klotho treatment increased phosphorylated ERK specifically in this cell type. ERK signaling in astrocytes is essential to leptin transport through the blood brain barrier [222], suggesting a novel role for central α-klotho to regulate hormonal transport. This hypothesis was supported by increased phosphorylated STAT3, a key downstream mediator of leptin, in NPY/AgRP neurons in response to α-klotho treatment. Considering the diverse functions of central α-klotho in the ARC, deciphering the molecular mechanisms involved is essential to understanding the complex questions surrounding homeostatic and disordered regulation of metabolism.

α-Klotho has a well-documented role as a scaffolding protein in the FGF23→FGFR complex [151], and experimental FGFR activation has recently been shown to elicit therapeutic effects in

metabolic disease models [193,194,198]. We determined α-klotho regulates astrocytes via an FGFR→ERK mechanism, similar to the mechanism underlying sustained diabetes remission in response to acute FGF1 microinjection [217]. Interestingly, α-klotho only trended to increase POMC neuron activity when FGFR activity was inhibited. This suggests α-klotho may regulate POMC neurons via FGFR's, but concurrent receptors are likely involved. Notably, the specific receptor of α-klotho is currently not known, but one potential mechanism could be through transient receptor potential vanilloid-like (TRPV) channels. TRPV channels increase POMC neuron activity to reduce food intake [20], and α-klotho has a well-documented role to hydrolyze these receptor like-channels in renal tubules and pancreatic β cells to increase their membrane localization [69,98,158].

PI3Kinase is another potent regulator of ARC neuron populations and a downstream effector of α-klotho [73,218]. While it has previously been shown that PI3kinase is essential to α-klotho-mediated AgRP mRNA downregulation, it was unclear whether PI3kinase was equally important to α-klotho-mediated NPY/AgRP neuron inhibition [218]. The current study showed PI3kinase inhibition completely abolished α-klotho-mediated NPY/AgRP neuron inhibition and POMC activation. These data indicate a prominent α-klotho→FGFR→PI3kinase signaling axis involved in the regulation of ARC neuron populations.

To summarize, this study identified diverse novel functions of α-klotho in the ARC via various molecular mechanisms. Experiments revealed α-klotho regulates astrocytes via FGFR→ERK signaling, as well as NPY/AgRP neurons and POMC neurons via FGFR→PI3kinase signaling. Furthermore, CSF α-klotho's prominent role in energy balance was demonstrated by strong inverse correlations with body weight and an ability to increase energy expenditure. Further investigation

into these novel molecular mechanisms could be integral to deciphering the complex physiology underlying homeostatic and disordered regulation of metabolism.

Chapter 3 Figures

Figure Legend:

Figure 3.1. Cerebrospinal fluid α-klotho concentrations are reduced in overweight and obese adults. CSF α-klotho concentrations are inversely correlated with (A) Body weight and (B) BMI (n=22). (C) Comparison of CSF α-klotho concentrations when subjects are stratified into lean vs. overweight/obese categories based on BMI. (n=11/group). CSF α-klotho concentrations are not correlated with (D) Fasting Blood Glucose, (E) Triglycerides, or (F) Cholesterol. ● represents lean; □ represents overweight or obese. Data represented as mean ± SEM. * indicates $p<0.05$ vs. lean subjects.

Figure 3.2. Two days ICV α-klotho treatment increases energy expenditure in DIO mice. (A-B) Oxygen consumption, (C-D) Carbon dioxide production, and (E-F) Locomotor activity in 16- to 17-week-old male DIO mice after 2 days ICV α-klotho (2.0ug) or vehicle (2.0uL) injections (n=7-8/group). (G) BAT gene expression and (H) iWAT gene expression (n=7-9/group). Data represented as mean ± SEM. * indicates $p<0.05$ vs. vehicle controls.

Figure 3.3. Acute ICV α-klotho treatment has no effects on TH-expressing neuron activity in the ARC or PVN. Representative images of cFOS (green) colocalized with TH-expressing neurons (red) in the (A) ARC and (B) PVN of mice acutely treated with ICV vehicle (2.0uL) or α-klotho (2.0ug) before an overnight fast. (C) Total TH-expressing neurons, (D) cFOS colocalization, and (E) proportion of active TH-expressing neurons in male mice (n=6-7/group). (F) Total TH-expressing neurons, (G) cFOS colocalization, and (H) proportion of active TH-expressing neurons in female mice (n=5-7/group). 3V = Third ventricle; Scale bar = 50um. Data represented as mean ± SEM. * indicates $p<0.05$ vs. vehicle controls.

Figure 3.4. Acute ICV α-klotho treatment increases ARC POMC neuron activity in fasted mice. (A) Representative whole cell patch clamp recording, (B) action potential frequency, and (C) membrane potential of a POMC neuron stimulated by α-klotho treatment (n=7 neurons). (D) Representative images of cFOS (green) colocalized with POMC (red) in the ARC of healthy, male mice acutely treated with ICV α-klotho (2.0ug) or vehicle (2.0uL) before an overnight fast. (E) Total POMC neurons, (F) cFOS colocalization, (G) and proportion of active POMC neurons in male mice (n=6-7/group). (H) Total POMC neurons, (I) cFOS colocalization, and (J) proportion of active POMC neurons in female mice (n=6/group). 3V = Third ventricle; Scale bar = 50um. Data represented as mean ± SEM. * indicates $p<0.05$ vs. vehicle controls.

Figure 3.5. Central α-klotho increases ARC POMC neuron activity, at least in part, via FGFR's. (A) Representative images of cFOS (green) colocalized with POMC (red) in the ARC of healthy, male mice acutely treated with vehicle (2.0uL), α-klotho (2.0ug), FGFR inhibitor alone (25ug), or FGFR inhibitor 10 minutes before α-klotho before an overnight fast. (B) Total POMC neurons, (C) cFOS colocalization, and (D) proportion of active POMC neurons (n=3-5/group). 3V = Third ventricle; Scale bar = 50um. Data represented as mean ± SEM. n.s = not significant; * indicates $p<0.05$.

Figure 3.6. PI3kinase inhibition blunts α-klotho-mediated ARC POMC neuron activation. (A) Representative images of cFOS (green) colocalized with POMC (red) in the ARC of healthy, male mice acutely treated with vehicle (2.0uL), α-klotho (2.0ug), wortmannin alone (10ng), or wortmannin one hour before α-klotho before an overnight fast. (B) Total POMC neurons, (C)

cFOS colocalization, and (D) proportion of active POMC neurons (n=4-5/group). 3V = Third ventricle; Scale bar = 50um. Data represented as mean ± SEM. n.s = not significant; * indicates $p<0.05$.

Figure 3.7. PI3kinase inhibition abolishes α-klotho-mediated ARC NPY/AgRP neuron inhibition. (A) Representative images of cFOS (red) colocalized with NPY/AgRP (green) in the ARC of healthy, male mice acutely treated with vehicle (2.0uL), α-klotho (2.0ug), wortmannin alone (10ng), or wortmannin one hour before α-klotho before an overnight fast. (B) Total NPY/AgRP neurons, (C) cFOS colocalization, and (D) proportion of active NPY/AgRP neurons (n=3-4/group). 3V = Third ventricle; Scale bar = 50um. Data represented as mean ± SEM. n.s = not significant; * indicates $p<0.05$.

Figure 3.8. Acute ICV α-klotho treatment stimulates phosphorylated ERK$^{thr202/tyr204}$ in ARC astrocytes. (A) Representative images of pERK$^{thr202/tyr204}$ (green) colocalized with GFAP (red) in the ARC of healthy, male mice acutely treated with vehicle (2.0uL), ICV α-klotho (2.0ug), FGFR inhibitor alone (25ug), or FGFR inhibitor 10 minutes before α-klotho (2.0ug) before an overnight fast. (B) pERK$^{thr202/tyr204}$ colocalized with GFAP. 3V = Third ventricle; Scale bar = 50um. Data represented as mean ± SEM. n.s = not significant; * indicates $p<0.05$.

Supplemental Figure Legend:

Supplemental Table 3.1. Human Subject Characteristics. Data Presented as mean ± SD. M = male; F = female; * = significantly different than lean.

Supplemental Table 3.2. Primer sequences used during qPCR analysis.

Supplemental Figure 3.1. Experimental timeline of indirect calorimetry experiments.

Supplemental Figure 3.2. Two days ICV α-klotho treatment decreases food intake and reduces body weight in DIO mice. (A) Average daily food intake, (B) Body weight, and (C) Changes in body weight in 16- to 17-week-old male DIO mice after 2 days ICV α-klotho (2.0ug) or vehicle (2.0uL) injections (n=14/group). Data represented as mean ± SEM. * indicates $p<0.05$ vs. vehicle controls.

Supplemental Figure 3.3. POMC-expressing neurons exhibit a heterogenous response to α-klotho treatment. (A) Representative whole cell patch clamp recording, (B) action potential frequency, and (C) membrane potential of POMC neurons inhibited by α-klotho treatment (n=9 neurons). Differences in baseline (D) action potential frequency and membrane (E) potential between POMC neurons activated and inhibited by α-klotho treatment. Data represented as mean ± SEM. * indicates $p<0.05$.

Supplemental Figure 3.4. ICV α-klotho treatment has no effects on POMC neuron activity in fed mice. (A) Representative images of cFOS (green) colocalized with POMC (red) in the ARC of healthy, fed, male mice acutely treated with ICV α-klotho (2.0ug) or vehicle (2.0uL) the night before euthanasia. (B) Total POMC neurons, (C) cFOS colocalization, and (D) percent of active POMC neurons (n=4/group). 3V = Third ventricle; Scale bar = 50um. Data represented as mean ± SEM. * indicates $p<0.05$ vs. vehicle controls.

Supplemental Figure 5.5. Acute ICV α-klotho treatment increases pSTAT3^{ser753} in NPY-expressing neurons. (A) Representative images of pSTAT3^{ser754} (red) colocalized with NPY-expressing neurons (green) in the ARC of healthy, male mice acutely treated with ICV α-klotho (2.0ug) or vehicle (2.0uL) before an overnight fast. (B) Total NPY neurons, (C) pSTAT3^{ser754} colocalized with NPY-expressing neurons, and (D) percent of NPY neurons with pSTAT3^{ser754} colocalization. 3V = Third ventricle; Scale bar = 50um. Data represented as mean ± SEM. * indicates $p<0.05$ vs. vehicle controls.

Supplemental Figure 3.6. Twelve days ICV α-klotho treatment increases Ki67 expression in the ARC of DIO mice. (A) Representative image of Ki-67 in the ARC of 16- to 17-week-old male DIO mice after 12 days ICV α-klotho (2.0ug) or vehicle (2.0uL) injections (n=5-6/group). (B) Total Ki67. 3V = Third ventricle; Scale bar = 50um. Data represented as mean ± SEM. * indicates $p<0.05$ vs. vehicle controls.

Supplemental Figure 3.7. Twelve days ICV α-klotho treatment has no effects on ARC neurogenesis in DIO mice. (A) Representative images of POMC, NPY, and DCX in ARC of 16- to 17-week-old male DIO mice after 12 days ICV α-klotho (2.0ug) or vehicle (2.0uL) injections (n=3-6/group). Total (B) POMC, (C) NPY/AgRP, and (D) DCX-expressing cells. 3V = Third ventricle; Scale bar = 50um. Data represented as mean ± SEM. * indicates $p<0.05$ vs. vehicle controls.

Figure 3.1

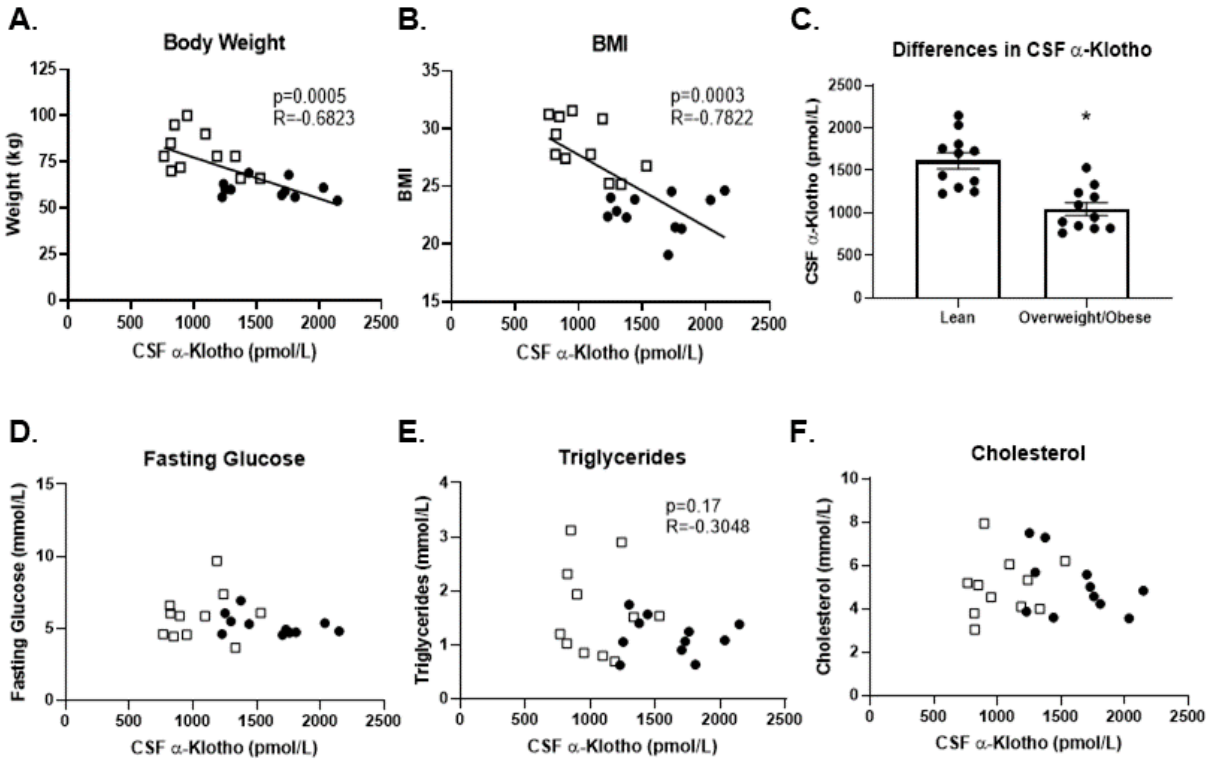
A.
Body Weight
p=0.0005
R=-0.6823
Weight (kg)
CSF α-Klotho (pmol/L)
B.
BMI
p=0.0003
R=-0.7822
BMI
CSF α-Klotho (pmol/L)
C.
Differences in CSF α-Klotho
CSF α-Klotho (pmol/L)
*
Lean
Overweight/Obese
D.
Fasting Glucose
Fasting Glucose (mmol/L)
CSF α-Klotho (pmol/L)
E.
Triglycerides
p=0.17
R=-0.3048
Triglycerides (mmol/L)
CSF α-Klotho (pmol/L)
F.
Cholesterol
Cholesterol (mmol/L)
CSF α-Klotho (pmol/L)

Figure 3.2

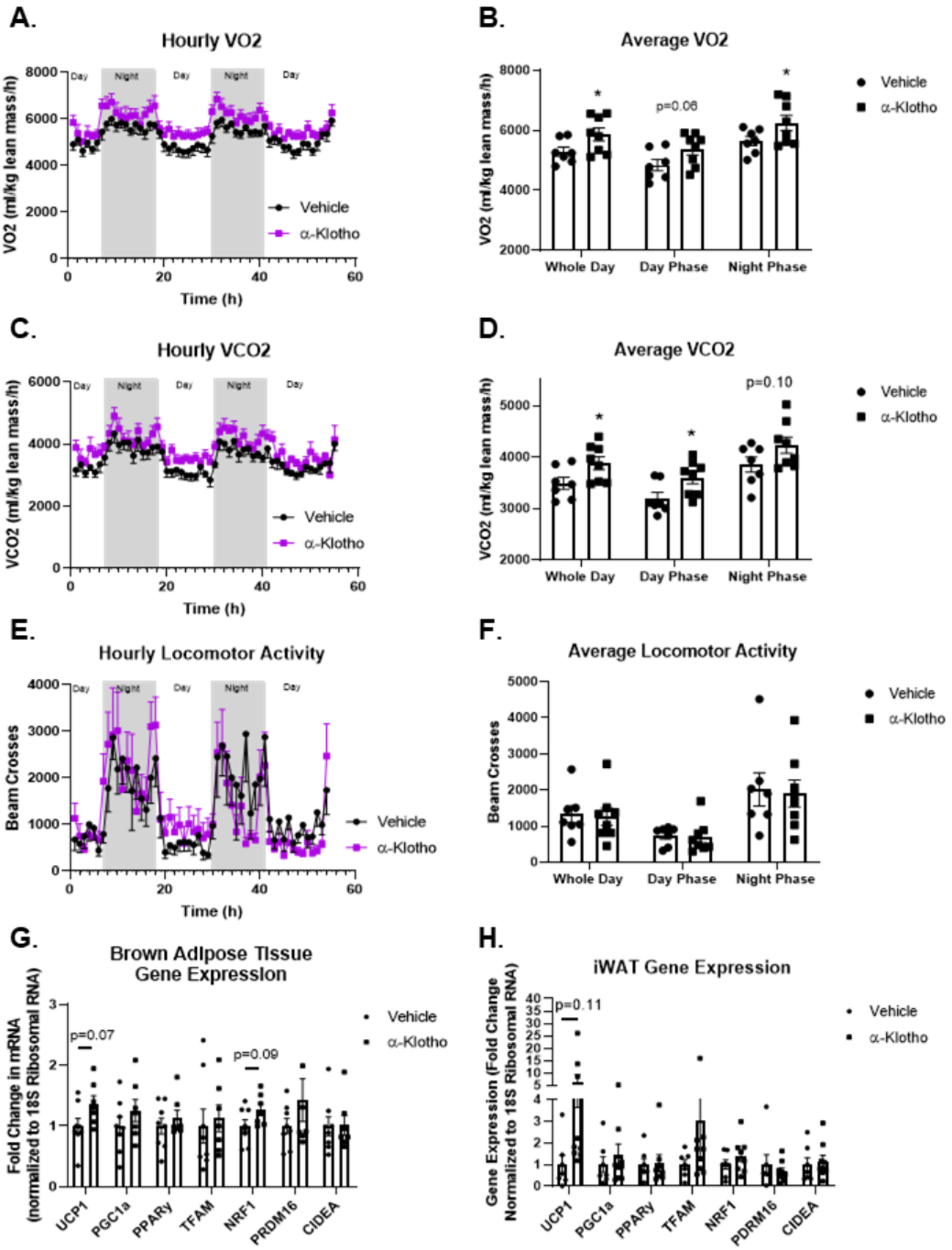
A.
Hourly VO2
VO2 (ml/kg lean mass/h)
Day
Night
Day
Night
Day
Vehicle
α-Klotho
Time (h)
B.
Average VO2
VO2 (ml/kg lean mass/h)
p=0.06
Whole Day
Day Phase
Night Phase
Vehicle
α-Klotho
C.
Hourly VCO2
VCO2 (ml/kg lean mass/h)
Time (h)
D.
Average VCO2
VCO2 (ml/kg lean mass/h)
p=0.10
E.
Hourly Locomotor Activity
Beam Crosses
F.
Average Locomotor Activity
G.
Brown Adipose Tissue
Gene Expression
Fold Change in mRNA
(normalized to 18S Ribosomal RNA)
p=0.07
p=0.09
UCP1
PGC1a
PPARγ
TFAM
NRF1
PRDM16
CIDEA
H.
iWAT Gene Expression
Gene Expression (Fold Change
Normalized to 18S Ribosomal RNA)
p=0.11

Figure 3.3

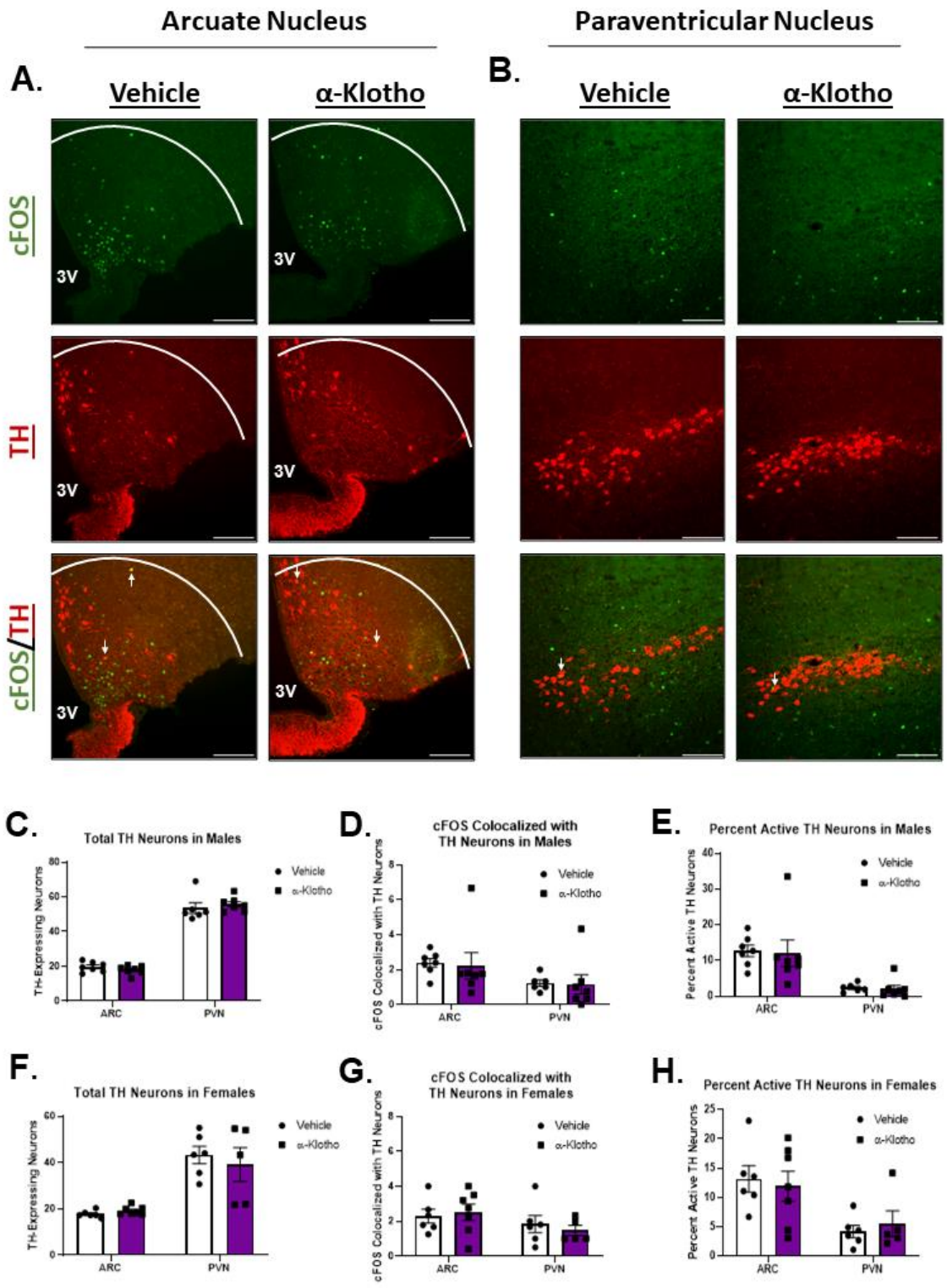
Arcuate Nucleus
Paraventricular Nucleus
A.
B.
Vehicle
α-Klotho
cFOS
TH
cFOS/TH
3V
C.
Total TH Neurons in Males
TH-Expressing Neurons
ARC
PVN
Vehicle
α-Klotho
D.
cFOS Colocalized with TH Neurons in Males
cFOS Colocalized with TH Neurons
E.
Percent Active TH Neurons in Males
Percent Active TH Neurons
F.
Total TH Neurons in Females
G.
cFOS Colocalized with TH Neurons in Females
H.
Percent Active TH Neurons in Females

Figure 3.4

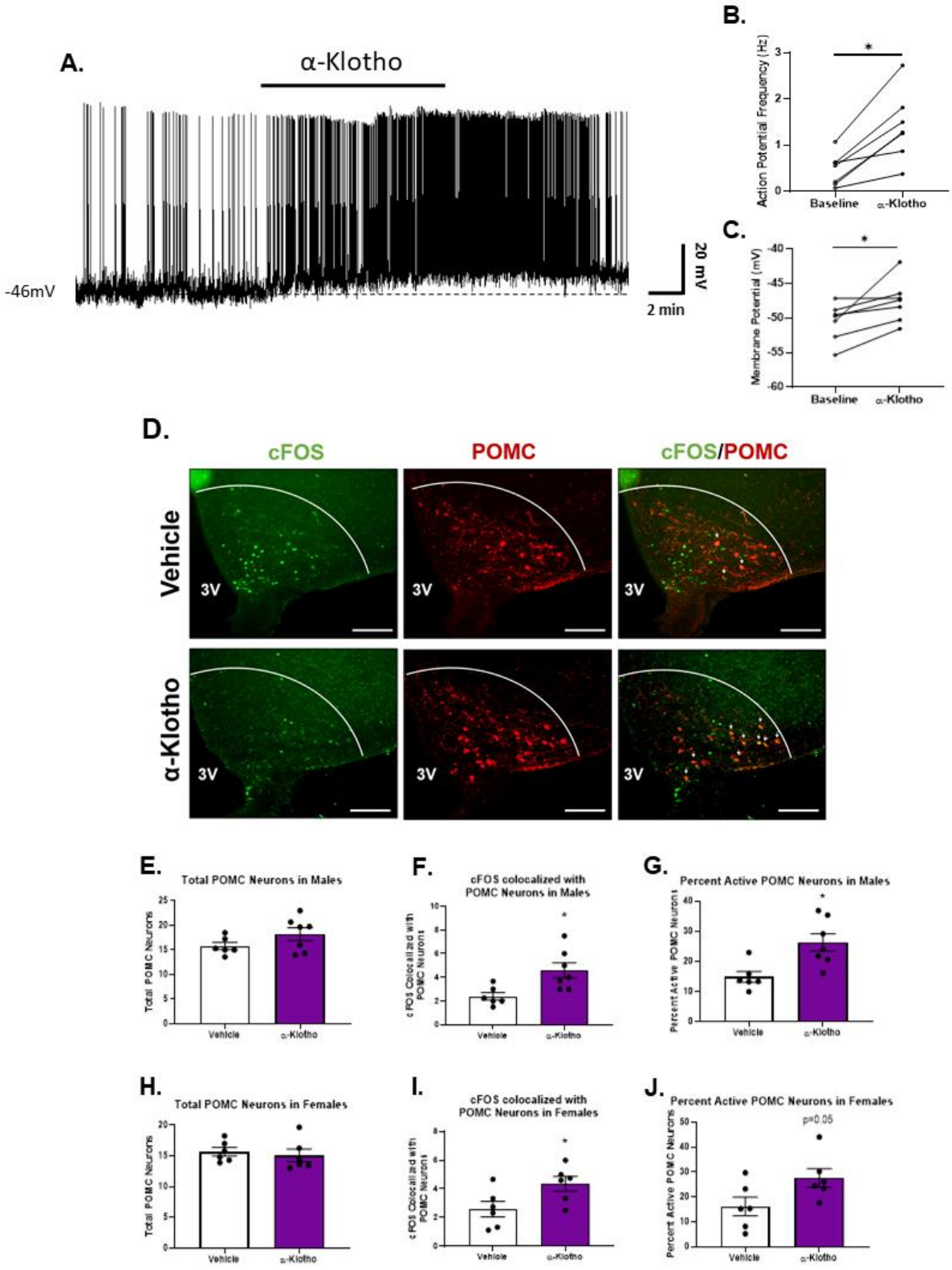
A.
α-Klotho
-46mV
20 mV
2 min
B.
Action Potential Frequency (Hz)
Baseline
α-Klotho
C.
Membrane Potential (mV)
Baseline
α-Klotho
D.
cFOS
POMC
cFOS/POMC
Vehicle
α-Klotho
3V
E.
Total POMC Neurons in Males
Total POMC Neurons
Vehicle
α-Klotho
F.
cFOS colocalized with POMC Neurons in Males
cFOS Colocalized with POMC Neurons
G.
Percent Active POMC Neurons in Males
Percent Active POMC Neurons
H.
Total POMC Neurons in Females
I.
cFOS colocalized with POMC Neurons in Females
J.
Percent Active POMC Neurons in Females
p=0.05

Figure 3.5

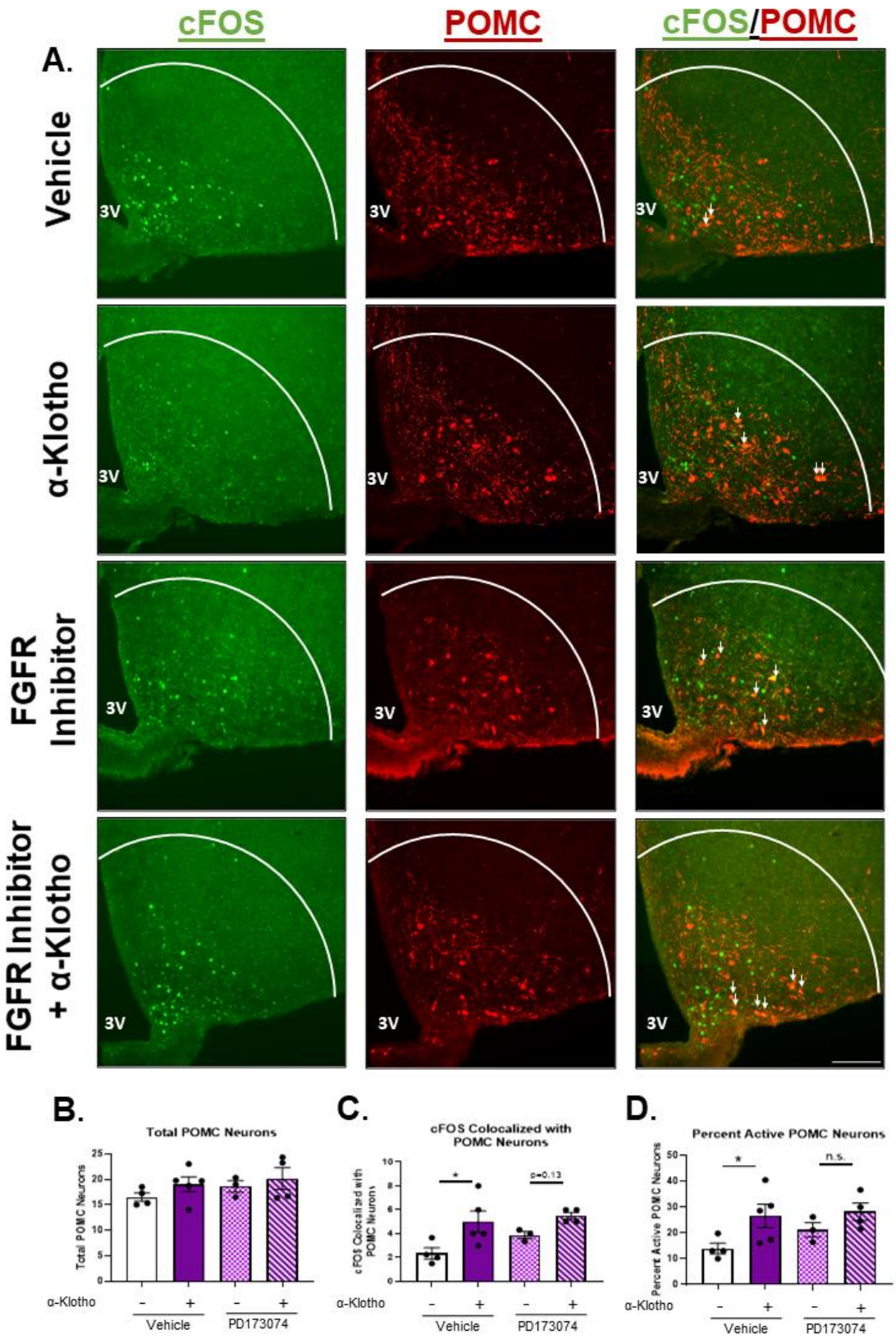
cFOS
POMC
cFOS/POMC
A.
Vehicle
α-Klotho
FGFR Inhibitor
FGFR Inhibitor + α-Klotho
3V
B.
Total POMC Neurons
Total POMC Neurons
α-Klotho
Vehicle
PD173074
C.
cFOS Colocalized with POMC Neurons
cFOS Colocalized with POMC Neurons
*
p=0.13
D.
Percent Active POMC Neurons
Percent Active POMC Neurons
*
n.s.

Figure 3.6

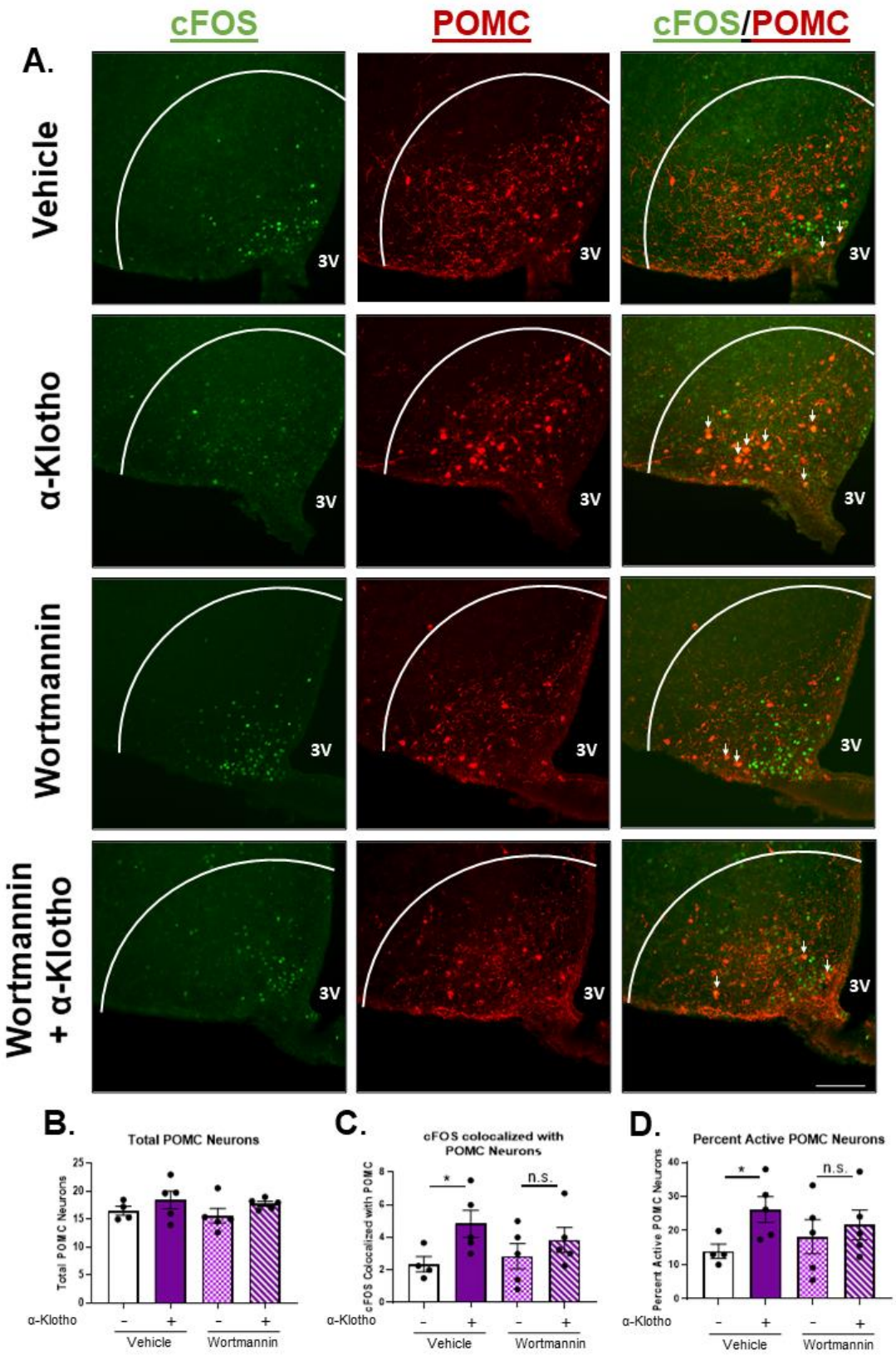
cFOS
POMC
cFOS/POMC
A.
Vehicle
α-Klotho
Wortmannin
Wortmannin + α-Klotho
3V
B.
Total POMC Neurons
Total POMC Neurons
α-Klotho
Vehicle
Wortmannin
C.
cFOS colocalized with POMC Neurons
cFOS Colocalized with POMC
*
n.s.
D.
Percent Active POMC Neurons
Percent Active POMC Neurons

Figure 3.7

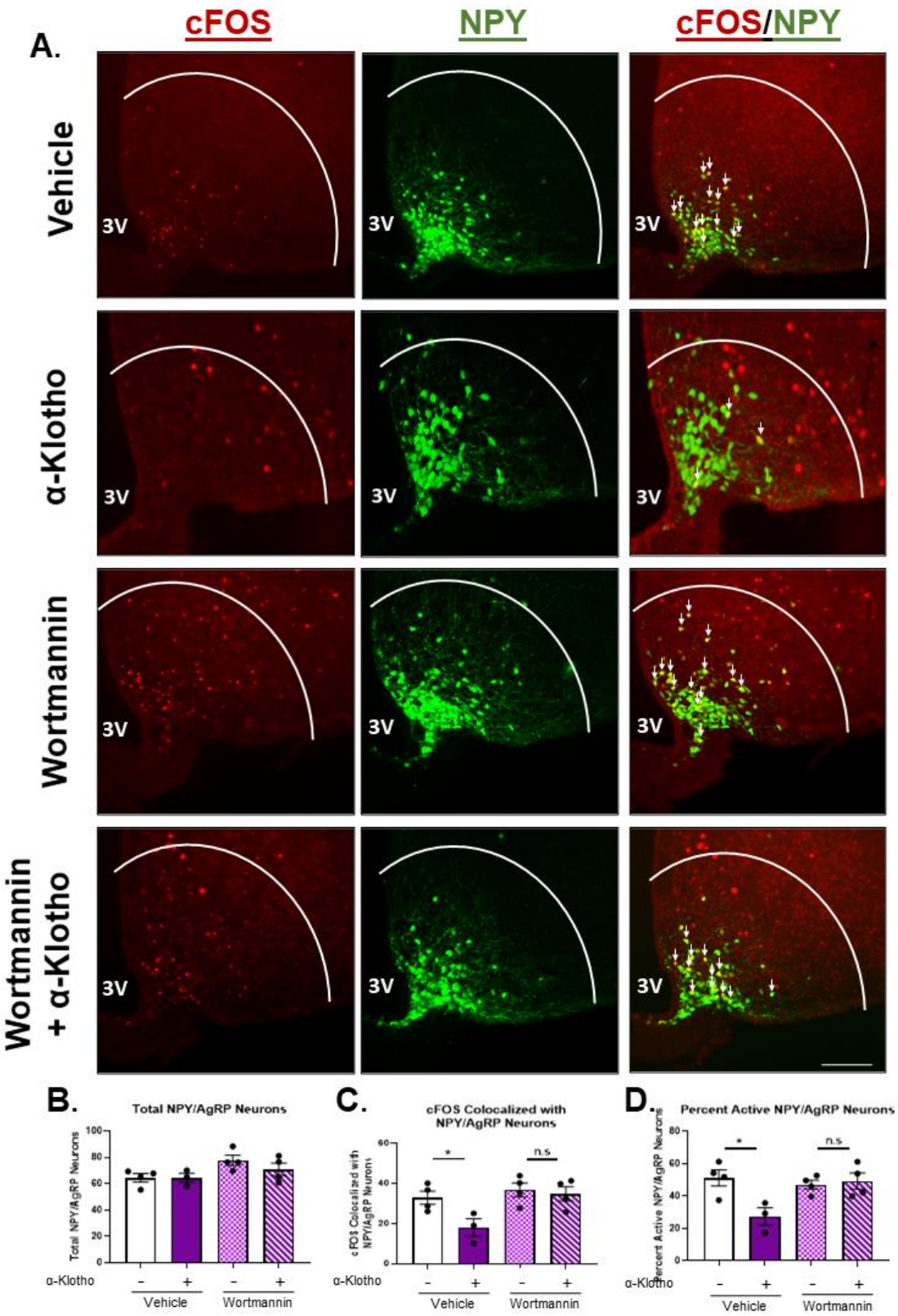
A.
cFOS
NPY
cFOS/NPY
Vehicle
α-Klotho
Wortmannin
Wortmannin + α-Klotho
3V
B.
Total NPY/AgRP Neurons
Total NPY/AgRP Neurons
α-Klotho
Vehicle
Wortmannin
C.
cFOS Colocalized with NPY/AgRP Neurons
cFOS Colocalized with NPY/AgRP Neurons
*
n.s
D.
Percent Active NPY/AgRP Neurons
Percent Active NPY/AgRP Neurons

Figure 3.8

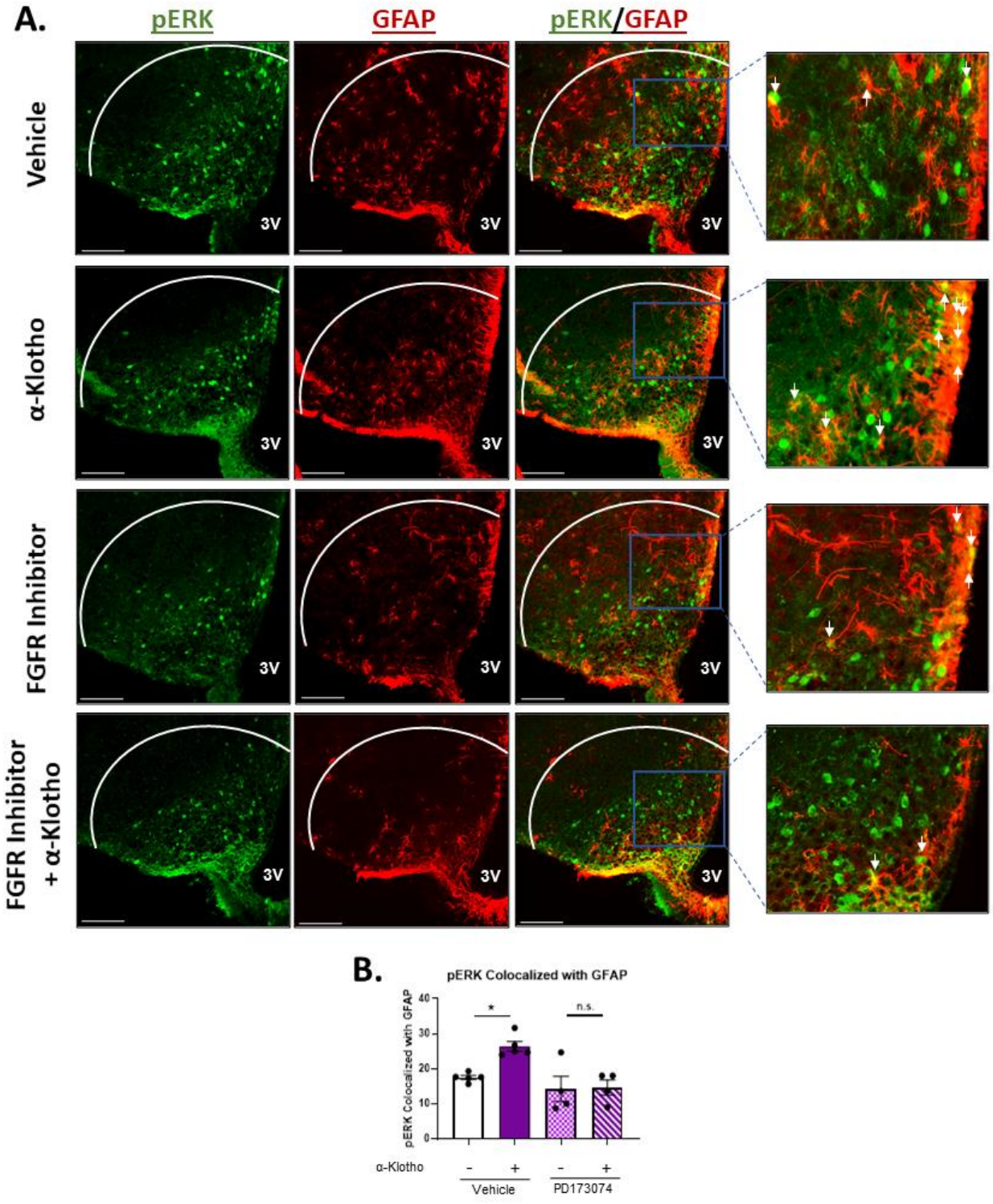
A.
pERK
GFAP
pERK/GFAP
Vehicle
α-Klotho
FGFR Inhibitor
FGFR Inhibitor + α-Klotho
3V
B.
pERK Colocalized with GFAP
pERK Colocalized with GFAP
40
30
20
10
0
*
n.s.
α-Klotho
-
+
-
+
Vehicle
PD173074

Supplemental Table 1

	Lean (n=11)	Overweight/Obese (n=11)
Sex	M: 5 F: 6	M: 5 F: 6
Age (yrs.)	57.0 ± 12.3	47.5 ± 20.3
Weight (kg.)	60.5 ± 5.1	79.5 ± 11.9*
Height (m.)	1.63 ± 0.09	1.67 ± 0.1
BMI	22.8 ± 1.7	28.6 ± 2.4*
Fasting Glucose (mmol/L)	5.2 ± 0.7	5.9 ± 1.8
Triglycerides (mmol/L)	1.15 ± 0.36	1.62 ± 0.85
Total Cholesterol (mmol/L)	5.06 ± 1.35	5.02 ± 1.36
HDL (mmol/L)	1.19 ± 0.17	1.00 ± 0.24*
LDL (mmol/L)	3.02 ± 1.0	3.07 ± 0.93

Supplemental Table 2

Gene	Forward primer	Reverse primer
PPAR γ	GGTGAACCACTGATATTCAGGA	AATGGCATCTCTGTGTCAACC
PGC1 α	CCCTGCCATTGTTAAGACC	TGCTGCTGTTCCTGTTTTC
UCP1	ACTGCCACACCTCCAGTCATT	CTTTGCCTCACTCAGGATTGG
TFAM	CAAGTCAGCTGATGGGTATGG	TTTCCCTGAGCCGAATCATCC
NRF1	CAGCACCTTTGGAGAATGTG	CCTGGGTCATTTTGTCCACA
PRDM16	CAGCACGGTGAAGCCATTC	GCGTGCATCCGCTTGTG
CIDEA	TGCTCTTCTGTATCGCCCAGT	GCCGTGTTAAGGAATCTGCTG
18S	GTAACCCGTTGAACCCCATT	CCATCCAATCGGTAGTAGCG

Supplemental Figure 1

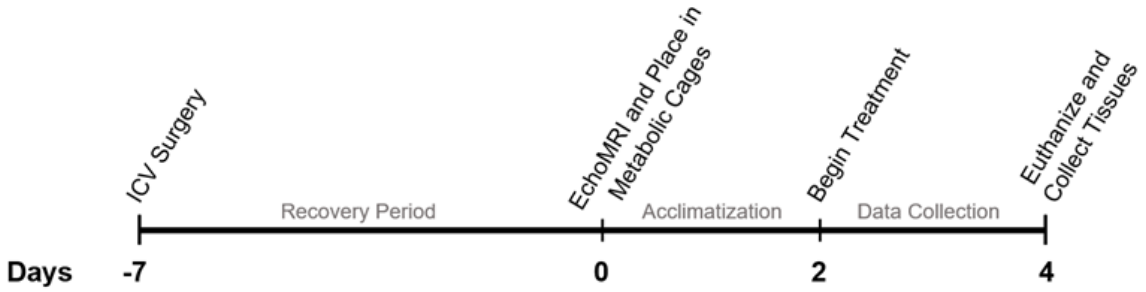

Supplemental Figure 2

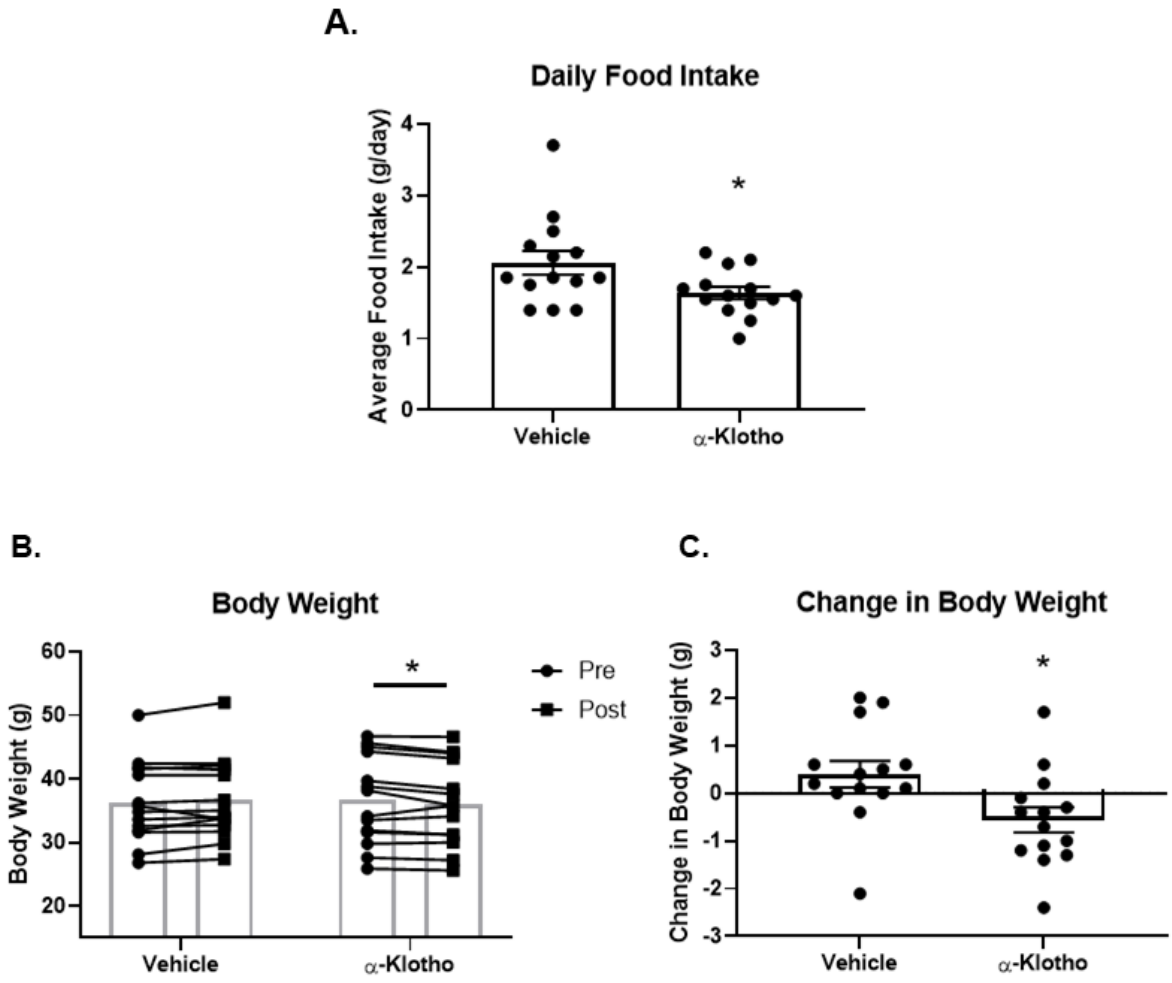

Supplemental Figure 3

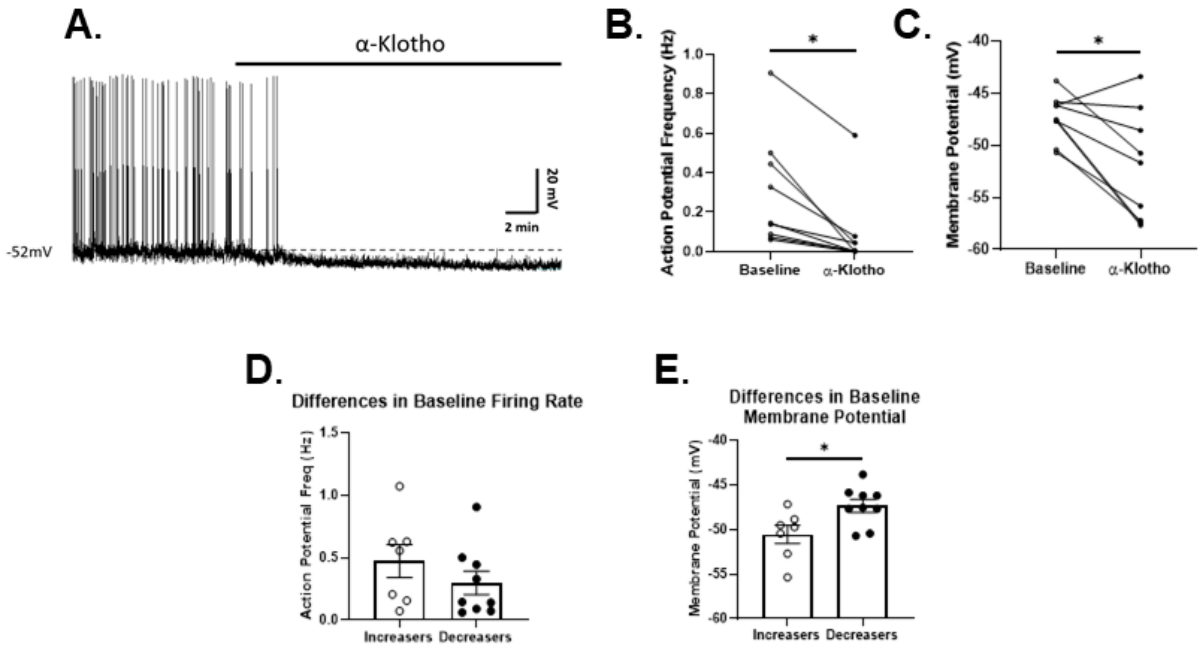

Supplemental Figure 4

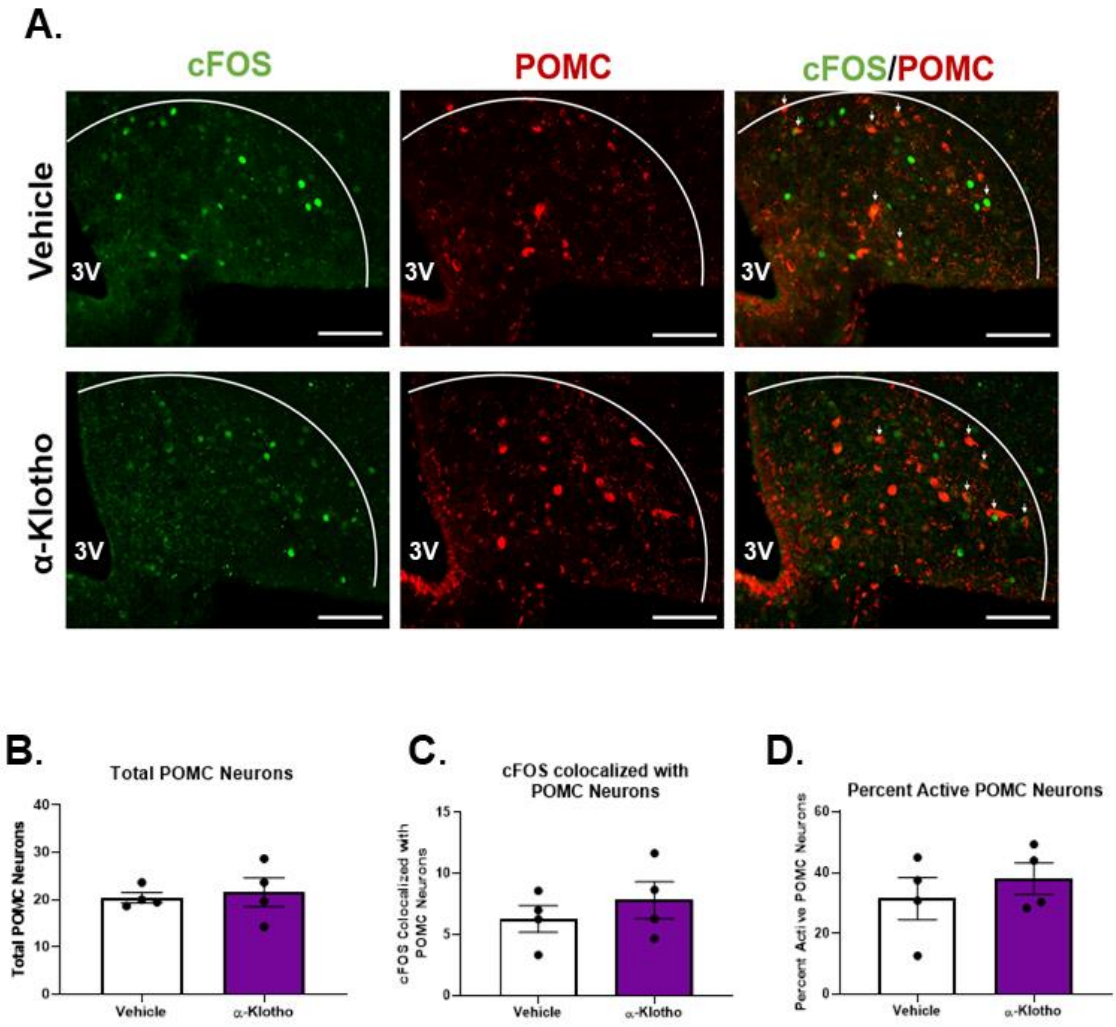

Supplemental Figure 5

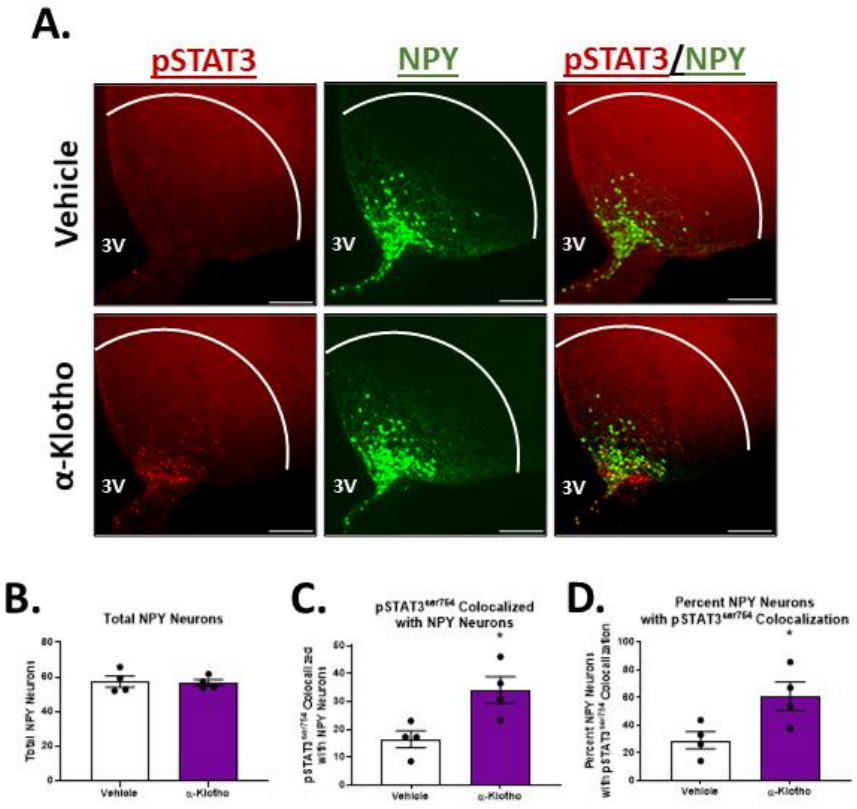

Supplemental Figure 6

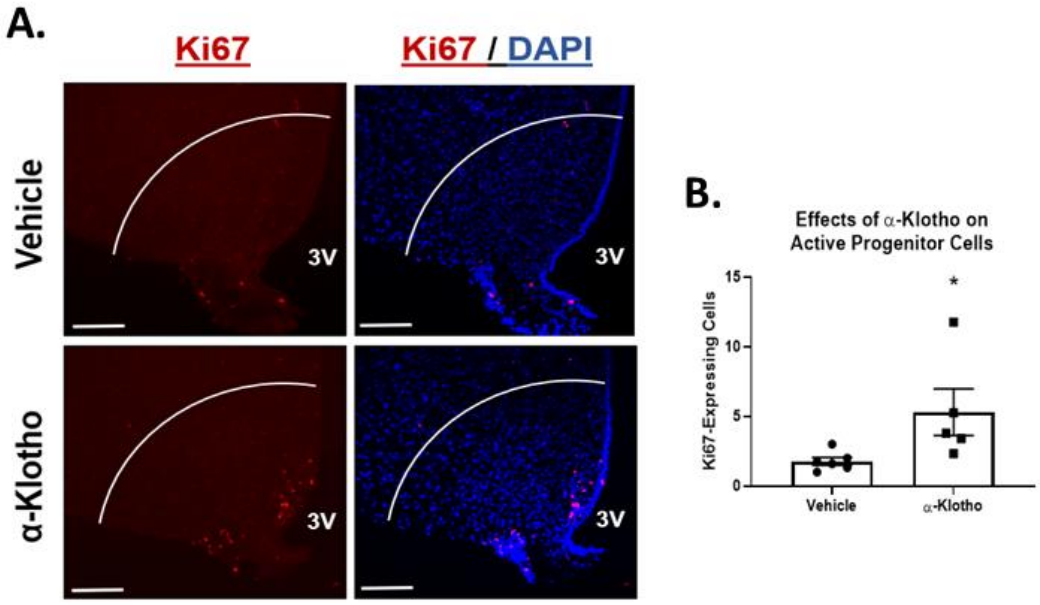

Supplemental Figure 7

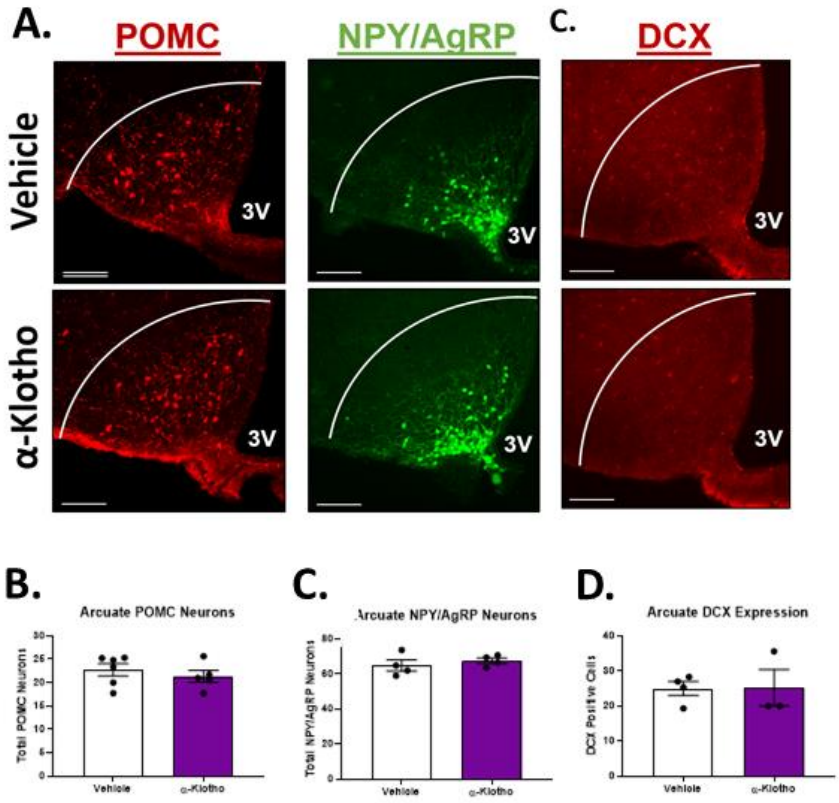

Chapter 4

Conclusions

4.1. Summary of central α-klotho and metabolism-

Despite minimal research into its functions in the CNS, central α-klotho has a clear prominent role in metabolic regulation. Central α-klotho elicits promising therapeutic potential in metabolic disease states by decreasing food intake, increasing energy expenditure, improving insulin secretion, and reducing hepatic gluconeogenic gene expression. Furthermore, reduced CSF α-klotho concentrations are observed in overweight populations, suggesting impaired α-klotho function may be involved in the pathophysiology of metabolic disease and potentially identifying CSF α-klotho as a preclinical marker of these disorders. Mechanistically, α-klotho→FGFR→PI3kinase signaling suppresses ARC NPY/AgRP and stimulates POMC neuron activity, which is likely essential to central α-klotho's effects on peripheral metabolism. Central α-klotho also alters intracellular signaling in ARC astrocytes via α-klotho→FGFR→ERK signaling, strongly implicating the α-klotho→FGFR signaling axis in homeostatic CNS regulation of metabolism.

4.2.Future directions: α-klotho and FGFR's-

Similar to peripheral tissues, central FGFR's have recently been popular subjects of metabolism research in the brain. ICV FGF19 and FGF21 elicit similar therapeutic effects to ICV α-klotho via FGFR's, including decreased food intake, reduced weight, improved glucose clearance, inhibited NPY/AgRP neuron activity, and suppressed hepatic gluconeogenic gene expression [193–197]. In fact, brain-specific β-klotho knockout even abolishes many of the weight-reducing and glucose-lowering effects of peripheral FGF19/21 administration

[179,197,203]. Since β-klotho's role is to stabilize FGF19/21 interaction with FGFR's [180–182], this strongly indicates that brain FGFR's are the primary mediators of peripheral and central FGF19/21 metabolic function. This dissertation demonstrated FGFR's to be equally important to many of the metabolic effects of central α-klotho, identifying FGFR's as promising targets of both future research and pharmacological intervention in cases of metabolic disease.

Despite the encouraging evidence observing FGFR activation to elicit therapeutic effects in metabolic disease models, studies investigating FGFR involvement in the pathology of diabetes and obesity produce equivocal results depending on animal model and experimental approach. ICV treatment with the popular FGFR inhibitor PD173074 impairs glucose clearance in healthy rats, but is described as stress-related [198,199], and ICV PD173074 in DIO mice elicits no phenotype [193,200]. Furthermore, antibody-mediated inhibition of FGFR1 in rodents and monkeys increases energy expenditure, decreases food intake, and reduces body weight, while genetic deletion of FGFR1 in NPY/AgRP neurons also results in no metabolic phenotype [71,201,202]. Future studies should investigate the specific roles of FGFR's, their isoforms, and their neuronal effectors in central regulation of metabolism by performing selective deletion of FGFR isoforms in specific neurons of mature mice using the inducible Cre-LoxP system or Crispr-Cas9.

4.3. Future directions: Alternative mechanisms of central α-klotho-

In this dissertation a novel brain α-klotho/FGFR/PI3kinase signaling axis was identified in the regulation of ARC neurons and whole body metabolism; however, there are likely other molecular mechanisms involved in the vital functions of central α-klotho. For example, at this time, the important of α-klotho-induced phosphorylated ERK in the hypothalamus is not known.

ERK signaling negatively regulates NPY/AgRP neurons, possibly via kruppel-like factor 4, and is involved in hypothalamic FGF1- and FGF19-mediated glucose lowering [193,216,217]. α-Klotho's ability to hydrolyze and increase activity of TRP channels may also be important to CNS regulation of metabolism. TRP channels are important to stimulating POMC neuron depolarization and subsequent increases in thermogenesis and reductions in food intake [20,235]. Lastly, α-klotho may have direct effects on metabolism via trx interacting protein (TXNIP) [94]. TXNIP, which has been shown to be inhibited by α-klotho and trx, has been identified as a mediator of overactive NPY/AgRP neuron pathologies, including hyperphagia, adiposity, reduced energy expenditure, and leptin resistance [106,236,237]. Overall, these documented physiological effectors of α-Klotho in peripheral tissues provide additional signaling pathway that may be promising foci of future investigations into central α-klotho's metabolic functions.

4.4. Closing Remarks-

In summary, investigation into central α-klotho-mediated regulation of energy balance and glucose metabolism is a very new topic of research. Only α-klotho's function in the ARC has been investigated and additional roles in other regions of the brain are likely. Moreover, while the evidence implicating α-klotho as a therapeutic target and preclinical marker of metabolic disease is encouraging, many additional experiments are needed to determine dose-response and effects of long term α-klotho administration. Doses used in ICV treatment studies are supraphysiological and, similar to leptin and insulin, developed resistances to α-klotho are possible. Development of new tools to specifically manipulate centrally circulating α-klotho levels within physiological ranges would be extremely valuable to thoroughly elucidating this critical protein's diverse and complex metabolic functions.

Chapter 4 Figures

Figure Legend:

Figure 4.1. Graphical Abstract. α-Klotho circulating in the CSF suppresses NPY/AgRP neuron activity and increases POMC neuron activity via FGFR→PI3kinase signaling, regulates astrocytes via FGFR→ERK signaling, and has no effects on TH neuron activity. These roles of α-klotho in the arcuate nucleus are likely involved in α-klotho-mediated suppression of appetite, increases in energy expenditure, and improvements in glucose clearance.

Figure 4.1.

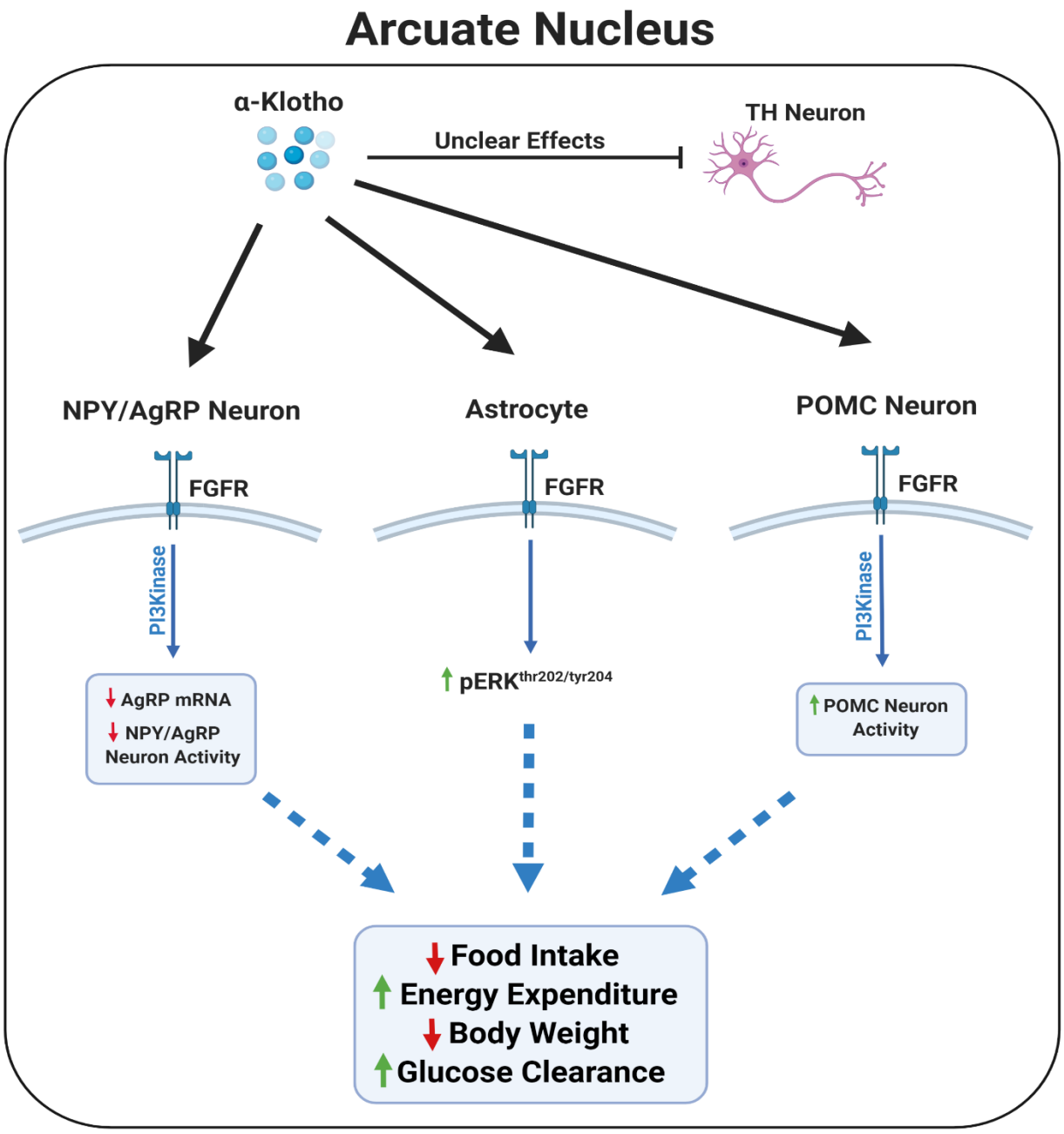
Arcuate Nucleus
α-Klotho
Unclear Effects
TH Neuron
NPY/AgRP Neuron
Astrocyte
POMC Neuron
FGFR
FGFR
FGFR
PI3Kinase
PI3Kinase
AgRP mRNA
NPY/AgRP Neuron Activity
pERKthr202/tyr204
POMC Neuron Activity
Food Intake
Energy Expenditure
Body Weight
Glucose Clearance

References:

[1] M.D. Jensen, D.H. Ryan, C.M. Apovian, J.D. Ard, A.G. Comuzzie, K.A. Donato, F.B. Hu, V.S. Hubbard, J.M. Jakicic, R.F. Kushner, C.M. Loria, B.E. Millen, C.A. Nonas, F.X. Pi-Sunyer, J. Stevens, V.J. Stevens, T.A. Wadden, B.M. Wolfe, S.Z. Yanovski, 2013 AHA/ACC/TOS Guideline for the Management of Overweight and Obesity in Adults, J. Am. Coll. Cardiol. 63 (2014) 2985–3023. doi:10.1016/j.jacc.2013.11.004.

[2] K. Rahmouni, M.L.G. Correia, W.G. Haynes, A.L. Mark, Obesity-associated hypertension: New insights into mechanisms, Hypertension. 45 (2005) 9–14. doi:10.1161/01.HYP.0000151325.83008.b4.

[3] G. De Pergola, F. Silvestris, Obesity as a major risk factor for cancer, J. Obes. 2013 (2013). doi:10.1155/2013/291546.

[4] M.M. Mielke, P.P. Zandi, H. Shao, M. Waern, S. Östling, X. Guo, C. Björkelund, L. Lissner, I. Skoog, D.R. Gustafson, The 32-year relationship between cholesterol and dementia from midlife to late life, Neurology. 75 (2010) 1888–1895. doi:10.1212/WNL.0b013e3181feb2bf.

[5] F.S. Luppino, A.K.B. Van Reedt Dortland, K.J. Wardenaar, P.F. Bouvy, E.J. Giltay, F.G. Zitman, B.W.J.H. Penninx, Symptom dimensions of depression and anxiety and the metabolic syndrome, Psychosom. Med. 73 (2011) 257–264. doi:10.1097/PSY.0b013e31820a59c0.

[6] T. MYLES, Obesity as an independent risk factor for infectious morbidity in patients who undergo cesarean delivery, Obstet. Gynecol. 100 (2002) 959–964. doi:10.1016/s0029-7844(02)02323-2.

[7] S. Naveau, V. Giraud, E. Borotto, A. Aubert, F. Capron, J.C. Chaput, Excess weight risk factor for alcoholic liver disease, Hepatology. 25 (1997) 108–111. doi:10.1002/hep.510250120.

[8] B. Stengel, M.E. Tarver-Carr, N.R. Powe, M.S. Eberhardt, F.L. Brancati, Lifestyle factors, obesity and the risk of chronic kidney disease, Epidemiology. 14 (2003) 479–487. doi:10.1097/01.EDE.0000071413.55296.c4.

[9] A.D. American Diabetes Association, Economic Costs of Diabetes in the U.S. in 2017., Diabetes Care. 41 (2018) 917–928. doi:10.2337/dci18-0007.

[10] C. Blouet, S.-M. Liu, Y.-H. Jo, S. Chua, G.J. Schwartz, TXNIP in Agrp Neurons Regulates Adiposity, Energy Expenditure, and Central Leptin Sensitivity, J. Neurosci. 32 (2012) 9870–9877.

[11] M. Claret, M.A. Smith, R.L. Batterham, C. Selman, A.I. Choudhury, L.G.D. Fryer, M. Clements, H. Al-Qassab, H. Heffron, A.W. Xu, J.R. Speakman, G.S. Barsh, B. Viollet, S. Vaulont, M.L.J. Ashford, D. Carling, D.J. Withers, AMPK is essential for energy homeostasis regulation and glucose sensing by POMC and AgRP neurons., J. Clin. Invest. 117 (2007) 2325–36. doi:10.1172/JCI31516.

[12] L. Huo, K. Gamber, S. Greeley, J. Silva, N. Huntoon, X.H. Leng, C. Bjørbæk, Leptin-Dependent Control of Glucose Balance and Locomotor Activity by POMC Neurons, Cell Metab. 9 (2009) 537–547. doi:10.1016/j.cmet.2009.05.003.

[13] D. Huszar, C.A. Lynch, V. Fairchild-Huntress, J.H. Dunmore, Q. Fang, L.R. Berkemeier, W. Gu, R.A. Kesterson, B.A. Boston, R.D. Cone, F.J. Smith, L.A. Campfield, P. Burn, F. Lee, Targeted disruption of the melanocortin-4 receptor results in obesity in mice., Cell. 88 (1997) 131–41.

[14] C. Zhan, J. Zhou, Q. Feng, J. -e. Zhang, S. Lin, J. Bao, P. Wu, M. Luo, Acute and Long-Term Suppression of Feeding Behavior by POMC Neurons in the Brainstem and Hypothalamus, Respectively, J. Neurosci. 33 (2013) 3624–3632. doi:10.1523/JNEUROSCI.2742-12.2013.
[15] J.K. Elmquist, C.F. Elias, C.B. Saper, From Lesions to Leptin: Review Hypothalamic Control of Food Intake and Body Weight, Neuron. 22 (1999) 221–232.
[16] E. Prodi, S. Obici, Minireview: The Brain as a Molecular Target for Diabetic Therapy, Endocrinology. 147 (2006) 2664–2669. doi:10.1210/en.2006-0143.
[17] M.L. Andermann, B.B. Lowell, Toward a Wiring Diagram Understanding of Appetite Control., Neuron. 95 (2017) 757–778. doi:10.1016/j.neuron.2017.06.014.
[18] G.J. Morton, D.E. Cummings, D.G. Baskin, G.S. Barsh, M.W. Schwartz, Central nervous system control of food intake and body weight, Nature. 443 (2006) 289–295. doi:10.1038/nature05026.
[19] L. Varela, T.L. Horvath, Leptin and insulin pathways in POMC and AgRP neurons that modulate energy balance and glucose homeostasis., EMBO Rep. 13 (2012) 1079–86. doi:10.1038/embor.2012.174.
[20] J.H. Jeong, D.K. Lee, S.M. Liu, S.C. Chua, G.J. Schwartz, Y.H. Jo, Activation of temperature-sensitive TRPV1-like receptors in ARC POMC neurons reduces food intake, PLoS Biol. 16 (2018). doi:10.1371/journal.pbio.2004399.
[21] A.C. Shin, N. Filatova, C. Lindtner, T. Chi, S. Degann, D. Oberlin, C. Buettner, Insulin receptor signaling in POMC, but not AgRP, neurons controls adipose tissue insulin action, Diabetes. 66 (2017) 1560–1571. doi:10.2337/db16-1238.
[22] K.C. da C. Rodrigues, R.M. Pereira, T.D.P. de Campos, R.F. de Moura, A.S.R. da Silva, D.E. Cintra, E.R. Ropelle, J.R. Pauli, M.B. de Araújo, L.P. de Moura, The Role of Physical Exercise to Improve the Browning of White Adipose Tissue via POMC Neurons, Front. Cell. Neurosci. 12 (2018) 88. doi:10.3389/fncel.2018.00088.
[23] A.W. Xu, L. Ste-Marie, C.B. Kaelin, G.S. Barsh, Inactivation of signal transducer and activator of transcription 3 in proopiomelanocortin (Pomc) neurons causes decreased Pomc expression, mild obesity, and defects in compensatory refeeding, Endocrinology. 148 (2007) 72–80. doi:10.1210/en.2006-1119.
[24] M.M. Ollmann, B.D. Wilson, Y.-K. Yang, J.A. Kerns, Y. Chen, I. Gantz, G.S. Barsh, Antagonism of Central Melanocortin Receptors in Vitro and in Vivo by Agouti-Related Protein, (n.d.).
[25] G.S.H. Yeo, I.S. Farooqi, S. Aminian, D.J. Halsall, R.G. Stanhope, S. O'Rahilly, A frameshift mutation in MC4R associated with dominantly inherited human obesity, Nat. Genet. 20 (1998) 111–112. doi:10.1038/2404.
[26] B.Y.H. Lam, I. Cimino, J. Polex-Wolf, S. Nicole Kohnke, D. Rimmington, V. Iyemere, N. Heeley, C. Cossetti, R. Schulte, L.R. Saraiva, D.W. Logan, C. Blouet, S. O'Rahilly, A.P. Coll, G.S.H. Yeo, Heterogeneity of hypothalamic pro-opiomelanocortin-expressing neurons revealed by single-cell RNA sequencing, Mol. Metab. 6 (2017) 383–392. doi:10.1016/j.molmet.2017.02.007.
[27] S.T. Hentges, V. Otero-Corchon, R.L. Pennock, C.M. King, M.J. Low, Proopiomelanocortin expression in both GABA and glutamate neurons, J. Neurosci. 29 (2009) 13684–13690. doi:10.1523/JNEUROSCI.3770-09.2009.
[28] A.R. Rau, S.T. Hentges, The relevance of AgRP neuron-derived GABA inputs to POMC neurons differs for spontaneous and evoked release, J. Neurosci. 37 (2017) 7362–7372.

doi:10.1523/JNEUROSCI.0647-17.2017.
[29] A.J. Newton, S. Hess, L. Paeger, M.C. Vogt, J. Fleming Lascano, E.A. Nillni, J.C. Brüning, P. Kloppenburg, A.W. Xu, AgRP Innervation onto POMC Neurons Increases with Age and Is Accelerated with Chronic High-Fat Feeding in Male Mice, Endocrinology. 154 (2013) 172–183. doi:10.1210/en.2012-1643.
[30] N. Zarjevski, I. Cusin, R. Vettor, F. Rohner-Jeanrenaud, B. Jeanrenaud, Intracerebroventricular administration of neuropeptide Y to normal rats has divergent effects on glucose utilization by adipose tissue and skeletal muscle, Diabetes. 43 (1994) 764–769. doi:10.2337/diab.43.6.764.
[31] S.Y. Qu, Y.K. Yang, J.Y. Li, Q. Zeng, I. Gantz, Agouti-related protein is a mediator of diabetic hyperphagia., Regul. Pept. 98 (2001) 69–75.
[32] H. Huang, S.H. Lee, C. Ye, I.S. Lima, B.-C. Oh, B.B. Lowell, J.M. Zabolotny, Y.-B. Kim, ROCK1 in AgRP Neurons Regulates Energy Expenditure and Locomotor Activity in Male Mice, Endocrinology. 154 (2013) 3660–3670. doi:10.1210/en.2013-1343.
[33] M. Vicent, C. Mook, M. Carter, S. Swoap, Optogenetic Activation of AgRP Neurons Lengthens and Deepens Daily Torpor in the Mouse, FASEB J. 31 (2017). doi:10.1209/0295-5075/88/18002.
[34] K. Nakajima, Z. Cui, C. Li, J. Meister, Y. Cui, O. Fu, A.S. Smith, S. Jain, B.B. Lowell, M.J. Krashes, J. Wess, Gs-coupled GPCR signalling in AgRP neurons triggers sustained increase in food intake, Nat. Commun. 7 (2016) 10268. doi:10.1038/ncomms10268.
[35] M.J. Krashes, B.P. Shah, J.C. Madara, D.P. Olson, D.E. Strochlic, A.S. Garfield, L. Vong, H. Pei, M. Watabe-Uchida, N. Uchida, S.D. Liberles, B.B. Lowell, An excitatory paraventricular nucleus to AgRP neuron circuit that drives hunger, Nature. 507 (2014) 238–242. doi:10.1038/nature12956.
[36] M.J. Krashes, S. Koda, C. Ye, S.C. Rogan, A.C. Adams, D.S. Cusher, E. Maratos-Flier, B.L. Roth, B.B. Lowell, Rapid, reversible activation of AgRP neurons drives feeding behavior in mice., J. Clin. Invest. 121 (2011) 1424–8. doi:10.1172/JCI46229.
[37] Y.C. Shi, J. Lau, Z. Lin, H. Zhang, L. Zhai, G. Sperk, R. Heilbronn, M. Mietzsch, S. Weger, X.F. Huang, R.F. Enriquez, P.A. Baldock, L. Zhang, A. Sainsbury, H. Herzog, S. Lin, Arcuate NPY controls sympathetic output and BAT function via a relay of tyrosine hydroxylase neurons in the PVN, Cell Metab. 17 (2013) 236–248. doi:10.1016/j.cmet.2013.01.006.
[38] S.M. Steculorum, J. Ruud, I. Karakasilioti, H. Backes, L. Engström Ruud, K. Timper, M.E. Hess, E. Tsaousidou, J. Mauer, M.C. Vogt, L. Paeger, S. Bremser, A.C. Klein, D.A. Morgan, P. Frommolt, P.T. Brinkkötter, P. Hammerschmidt, T. Benzing, K. Rahmouni, F.T. Wunderlich, P. Kloppenburg, J.C. Brüning, AgRP Neurons Control Systemic Insulin Sensitivity via Myostatin Expression in Brown Adipose Tissue, Cell. 165 (2016) 125–138. doi:10.1016/j.cell.2016.02.044.
[39] A.C. Könner, R. Janoschek, L. Plum, S.D. Jordan, E. Rother, X. Ma, C. Xu, P. Enriori, B. Hampel, G.S. Barsh, C.R. Kahn, M.A. Cowley, F.M. Ashcroft, J.C. Brüning, Insulin Action in AgRP-Expressing Neurons Is Required for Suppression of Hepatic Glucose Production, Cell Metab. 5 (2007) 438–449. doi:10.1016/j.cmet.2007.05.004.
[40] C.J. Small, Y.L. Liu, S.A. Stanley, I.P. Connoley, A. Kennedy, M.J. Stock, S.R. Bloom, Chronic CNS administration of Agouti-related protein (Agrp) reduces energy expenditure, Int. J. Obes. 27 (2003) 530–533. doi:10.1038/sj.ijo.0802253.
[41] M.S. Szczypka, R.J. Mandel, B.A. Donahue, R.O. Snyder, S.E. Leff, R.D. Palmiter, Viral

gene delivery selectively restores feeding and prevents lethality of dopamine-deficient mice, Neuron. 22 (1999) 167–178. doi:10.1016/S0896-6273(00)80688-1.
[42] D. Atasoy, J. Nicholas Betley, H.H. Su, S.M. Sternson, Deconstruction of a neural circuit for hunger, Nature. 488 (2012) 172–177. doi:10.1038/nature11270.
[43] Q. Tong, C.-P. Ye, J.E. Jones, J.K. Elmquist, B.B. Lowell, Synaptic release of GABA by AgRP neurons is required for normal regulation of energy balance, Nat. Neurosci. 11 (2008) 998–1000. doi:10.1038/nn.2167.
[44] S.C. Daubner, T. Le, S. Wang, Tyrosine hydroxylase and regulation of dopamine synthesis, Arch. Biochem. Biophys. 508 (2011) 1–12. doi:10.1016/j.abb.2010.12.017.
[45] X. Zhang, A.N. Van Den Pol, Hypothalamic arcuate nucleus tyrosine hydroxylase neurons play orexigenic role in energy homeostasis, Nat. Neurosci. 19 (2016) 1341–1347. doi:10.1038/nn.4372.
[46] L.J. Skov, C. Ratner, N.W. Hansen, J.J. Thompson, K.L. Egerod, H. Burm, L.S. Dalbøge, M.A. Hedegaard, C. Brakebusch, T.H. Pers, J. Perrier, B. Holst, RhoA in tyrosine hydroxylase neurones regulates food intake and body weight via altered sensitivity to peripheral hormones, J. Neuroendocrinol. 31 (2019). doi:10.1111/jne.12761.
[47] D. Burdakov, S.M. Luckman, A. Verkhratsky, Glucose-sensing neurons of the hypothalamus, in: Philos. Trans. R. Soc. B Biol. Sci., Royal Society, 2005: pp. 2227–2235. doi:10.1098/rstb.2005.1763.
[48] L.E. Parton, C.P. Ye, R. Coppari, P.J. Enriori, B. Choi, C.Y. Zhang, C. Xu, C.R. Vianna, N. Balthasar, C.E. Lee, J.K. Elmquist, M.A. Cowley, B.B. Lowell, Glucose sensing by POMC neurons regulates glucose homeostasis and is impaired in obesity, Nature. 449 (2007) 228–232. doi:10.1038/nature06098.
[49] B.F. Belgardt, T. Okamura, J.C. Brüning, Hormone and glucose signalling in POMC and AgRP neurons, J. Physiol. 587 (2009) 5305–5314. doi:10.1113/jphysiol.2009.179192.
[50] M.D. Klok, S. Jakobsdottir, M.L. Drent, The role of leptin and ghrelin in the regulation of food intake and body weight in humans: A review, Obes. Rev. 8 (2007) 21–34. doi:10.1111/j.1467-789X.2006.00270.x.
[51] M. Kojima, H. Hosoda, Y. Date, M. Nakazato, H. Matsuo, K. Kangawa, Ghrelin is a growth-hormone-releasing acylated peptide from stomach, Nature. 402 (1999) 656–660. doi:10.1038/45230.
[52] S.-R. Chen, H. Chen, J.-J. Zhou, G. Pradhan, Y. Sun, H.-L. Pan, D.-P. Li, Ghrelin receptors mediate ghrelin-induced excitation of agouti-related protein/neuropeptide Y but not pro-opiomelanocortin neurons, J. Neurochem. 142 (2017) 512–520. doi:10.1111/jnc.14080.
[53] Y. Yang, D. Atasoy, H.H. Su, S.M. Sternson, Hunger States Switch a Flip-Flop Memory Circuit via a Synaptic AMPK-Dependent Positive Feedback Loop, Cell. 146 (2011) 992–1003. doi:10.1016/J.CELL.2011.07.039.
[54] Q. Wang, C. Liu, A. Uchida, J.-C. Chuang, A. Walker, T. Liu, S. Osborne-Lawrence, B.L. Mason, C. Mosher, E.D. Berglund, J.K. Elmquist, J.M. Zigman, Arcuate AgRP neurons mediate orexigenic and glucoregulatory actions of ghrelin, Mol. Metab. 3 (2014) 64–72. doi:10.1016/j.molmet.2013.10.001.
[55] J. Kamegai, H. Tamura, T. Shimizu, S. Ishii, H. Sugihara, I. Wakabayashi, Chronic central infusion of ghrelin increases hypothalamic neuropeptide Y and Agouti-related protein mRNA levels and body weight in rats., Diabetes. 50 (2001) 2438–43.
[56] J. German, F. Kim, G.J. Schwartz, P.J. Havel, C.J. Rhodes, M.W. Schwartz, G.J. Morton,

Hypothalamic Leptin Signaling Regulates Hepatic Insulin Sensitivity via a Neurocircuit Involving the Vagus Nerve, Endocrinology. 150 (2009) 4502–4511. doi:10.1210/en.2009-0445.
[57] H.C. Denroche, J. Levi, R.D. Wideman, R.M. Sequeira, F.K. Huynh, S.D. Covey, T.J. Kieffer, Leptin Therapy Reverses Hyperglycemia in Mice With Streptozotocin-Induced Diabetes, Independent of Hepatic Leptin Signaling, (n.d.). doi:10.2337/db10-0958.
[58] P. Cohen, C. Zhao, X. Cai, J.M. Montez, S.C. Rohani, P. Feinstein, P. Mombaerts, J.M. Friedman, Selective deletion of leptin receptor in neurons leads to obesity, J. Clin. Invest. 108 (2001) 1113–1121. doi:10.1172/JCI13914.
[59] G.N. Luheshi, J.D. Gardner, D.A. Rushforth, A.S. Loudon, N.J. Rothwell, Leptin actions on food intake and body temperature are mediated by IL-1., Proc. Natl. Acad. Sci. U. S. A. 96 (1999) 7047–52. doi:10.1073/PNAS.96.12.7047.
[60] Y. Minokoshi, C. Toda, S. Okamoto, Regulatory role of leptin in glucose and lipid metabolism in skeletal muscle., Indian J. Endocrinol. Metab. 16 (2012) S562-8. doi:10.4103/2230-8210.105573.
[61] Y.-H. Choi, C. Li, D.L. Hartzell, D.E. Little, M.A. Della-Fera, C.A. Baile, ICV leptin effects on spontaneous physical activity and feeding behavior in rats, Behav. Brain Res. 188 (2008) 100–108. doi:10.1016/j.bbr.2007.10.024.
[62] T. Kitamura, Y. Feng, Y. Ido Kitamura, S.C. Chua, A.W. Xu, G.S. Barsh, L. Rossetti, D. Accili, Forkhead protein FoxO1 mediates Agrp-dependent effects of leptin on food intake, Nat. Med. 12 (2006) 534–540. doi:10.1038/nm1392.
[63] A. Pocai, K. Morgan, C. Buettner, R. Gutierrez-Juarez, S. Obici, L. Rossetti, Central leptin acutely reverses diet-induced hepatic insulin resistance., Diabetes. 54 (2005) 3182–9.
[64] S.M. Harlan, D.-F. Guo, D.A. Morgan, C. Fernandes-Santos, K. Rahmouni, Hypothalamic mTORC1 Signaling Controls Sympathetic Nerve Activity and Arterial Pressure and Mediates Leptin Effects, Cell Metab. 17 (2013) 599–606. doi:10.1016/J.CMET.2013.02.017.
[65] J. Korner, E. Savontaus, S.C. Chua, R.L. Leibel, S.L. Wardlaw, Leptin Regulation of Agrp and Npy mRNA in the Rat Hypothalamus, J. Neuroendocrinol. 13 (2008) 959–966. doi:10.1046/j.1365-2826.2001.00716.x.
[66] H. Huang, D. Kong, K.H. Byun, C. Ye, S. Koda, D.H. Lee, B.-C. Oh, S.W. Lee, B. Lee, J.M. Zabolotny, M.S. Kim, C. Bjørbæk, B.B. Lowell, Y.-B. Kim, Rho-kinase regulates energy balance by targeting hypothalamic leptin receptor signaling, Nat. Neurosci. 15 (2012) 1391–1398. doi:10.1038/nn.3207.
[67] L. Gong, F. Yao, K. Hockman, H.H. Heng, G.J. Morton, K. Takeda, S. Akira, M.J. Low, M. Rubinstein, R.G. MacKenzie, Signal transducer and activator of transcription-3 is required in hypothalamic agouti-related protein/neuropeptide Y neurons for normal energy homeostasis, Endocrinology. 149 (2008) 3346–3354. doi:10.1210/en.2007-0945.
[68] K. Rahmouni, W.G. Haynes, D.A. Morgan, A.L. Mark, Intracellular mechanisms involved in leptin regulation of sympathetic outflow., Hypertension. 41 (2003) 763–7. doi:10.1161/01.HYP.0000048342.54392.40.
[69] Y. Lin, Z. Sun, In vivo pancreatic β-cell-specific expression of antiaging gene Klotho: a novel approach for preserving β-cells in type 2 diabetes., Diabetes. 64 (2015) 1444–58. doi:10.2337/db14-0632.
[70] W. Tao, J. Wu, B.X. Xie, Y.Y. Zhao, N. Shen, S. Jiang, X.X. Wang, N. Xu, C. Jiang, S.

Chen, X. Gao, B. Xue, C.J. Li, Lipid-induced muscle insulin resistance is mediated by GGPPS via modulation of the RhoA/Rho kinase signaling pathway, J. Biol. Chem. 290 (2015) 20086–20097. doi:10.1074/jbc.M115.657742.
[71] S. Liu, G. Marcelin, C. Blouet, J.H. Jeong, Y.-H. Jo, G.J. Schwartz, S. Chua, Jr., A gut-brain axis regulating glucose metabolism mediated by bile acids and competitive fibroblast growth factor actions at the hypothalamus., Mol. Metab. 8 (2018) 37–50. doi:10.1016/j.molmet.2017.12.003.
[72] C.-Y. Lin, D.A. Higginbotham, R.L. Judd, A.B.D. White, B. Douglas, Central leptin increases insulin sensitivity in streptozotocin-induced diabetic rats, (n.d.).
[73] H. Al-Qassab, M.A. Smith, E.E. Irvine, J. Guillermet-Guibert, M. Claret, A.I. Choudhury, C. Selman, K. Piipari, M. Clements, S. Lingard, K. Chandarana, J.D. Bell, G.S. Barsh, A.J.H. Smith, R.L. Batterham, M.L.J. Ashford, B. Vanhaesebroeck, D.J. Withers, Dominant Role of the p110β Isoform of PI3K over p110α in Energy Homeostasis Regulation by POMC and AgRP Neurons, Cell Metab. 10 (2009) 343–354. doi:10.1016/J.CMET.2009.09.008.
[74] J.C. Brüning, D. Gautam, D.J. Burks, J. Gillette, M. Schubert, P.C. Orban, R. Klein, W. Krone, D. Müller-Wieland, C.R. Kahn, Role of brain insulin receptor in control of body weight and reproduction., Science. 289 (2000) 2122–5.
[75] M.-S. Kim, Y.K. Pak, P.-G. Jang, C. Namkoong, Y.-S. Choi, J.-C. Won, K.-S. Kim, S.-W. Kim, H.-S. Kim, J.-Y. Park, Y.-B. Kim, K.-U. Lee, Role of hypothalamic Foxo1 in the regulation of food intake and energy homeostasis, Nat. Neurosci. 9 (2006) 901–906. doi:10.1038/nn1731.
[76] H.E. Raybould, Mechanisms of CCK signaling from gut to brain, Curr. Opin. Pharmacol. 7 (2007) 570–574. doi:10.1016/j.coph.2007.09.006.
[77] I.G. Halatchev, R.D. Cone, Peripheral administration of PYY3–36 produces conditioned taste aversion in mice, Cell Metab. 1 (2005) 159–168. doi:10.1016/j.cmet.2005.02.003.
[78] R.L. Batterham, H. Heffron, S. Kapoor, J.E. Chivers, K. Chandarana, H. Herzog, C.W. Le Roux, E.L. Thomas, J.D. Bell, D.J. Withers, Critical role for peptide YY in protein-mediated satiation and body-weight regulation, Cell Metab. 4 (2006) 223–233. doi:10.1016/j.cmet.2006.08.001.
[79] E. Karra, K. Chandarana, R.L. Batterham, The role of peptide YY in appetite regulation and obesity, in: J. Physiol., Blackwell Publishing Ltd, 2009: pp. 19–25. doi:10.1113/jphysiol.2008.164269.
[80] T.D. Müller, B. Finan, S.R. Bloom, D. D'Alessio, D.J. Drucker, P.R. Flatt, A. Fritsche, F. Gribble, H.J. Grill, J.F. Habener, J.J. Holst, W. Langhans, J.J. Meier, M.A. Nauck, D. Perez-Tilve, A. Pocai, F. Reimann, D.A. Sandoval, T.W. Schwartz, R.J. Seeley, K. Stemmer, M. Tang-Christensen, S.C. Woods, R.D. DiMarchi, M.H. Tschöp, Glucagon-like peptide 1 (GLP-1), Mol. Metab. 30 (2019) 72–130. doi:10.1016/j.molmet.2019.09.010.
[81] A.J. Sipols, D.G. Baskin, M.W. Schwartz, Effect of Intracerebroventricular Insulin Infusion on Diabetic Hyperphagia and Hypothalamic Neuropeptide Gene Expression, Diabetes. 44 (1995) 147–151. doi:10.2337/diab.44.2.147.
[82] G.W.C. Cheung, A. Kokorovic, C.K.L. Lam, M. Chari, T.K.T. Lam, Intestinal Cholecystokinin Controls Glucose Production through a Neuronal Network, Cell Metab. 10 (2009) 99–109. doi:10.1016/j.cmet.2009.07.005.
[83] M. Balaskó, S.Z. Soós, A. Párniczky, M. Koncsecskó-Gáspár, M. Székely, E. Pétervári,

Anorexic effect of peripheral cholecystokinin (CCK) varies with age and body composition (Short communication), Acta Physiol. Hung. 99 (2012) 166–172. doi:10.1556/APhysiol.99.2012.2.10.
[84] M. Mesgari-Abbasi, M. Abbasalizad Farhangi, Serum concentrations of cholecystokinin, peptide yy, ghrelin and high sensitive c-reactive protein in association with metabolic syndrome ingredients in obese individuals, Acta Endocrinol. (Copenh). 16 (2020) 37–42. doi:10.4183/aeb.2020.37.
[85] P.D. Raposinho, D.D. Pierroz, P. Broqua, R.B. White, T. Pedrazzini, M.L. Aubert, Chronic administration of neuropeptide Y into the lateral ventricle of C57BL/6J male mice produces an obesity syndrome including hyperphagia, hyperleptinemia, insulin resistance, and hypogonadism, Mol. Cell. Endocrinol. 185 (2001) 195–204. doi:10.1016/S0303-7207(01)00620-7.
[86] R.C. Frederich, A. Hamann, S. Anderson, B. Löllmann, B.B. Lowell, J.S. Flier, Leptin levels reflect body lipid content in mice: Evidence for diet-induced resistance to leptin action, Nat. Med. 1 (1995) 1311–1314. doi:10.1038/nm1295-1311.
[87] S.-H. Lee, H. Huang, K. Choi, D.H. Lee, J. Shi, T. Liu, K.H. Chun, J.A. Seo, I.S. Lima, J.M. Zabolotny, L. Wei, Y.-B. Kim, ROCK1 isoform-specific deletion reveals a role for diet-induced insulin resistance, Am. J. Physiol. Metab. 306 (2014) E332–E343. doi:10.1152/ajpendo.00619.2013.
[88] C. Niederau, K. Meereis-Schwanke, H. Klonowski-Stumpe, L. Herberg, CCK-resistance in Zucker obese versus lean rats, Regul. Pept. 70 (1997) 97–104. doi:10.1016/S0167-0115(97)00014-1.
[89] X. Zhang, G. Zhang, H. Zhang, M. Karin, H. Bai, D. Cai, Hypothalamic IKKβ/NF-κB and ER Stress Link Overnutrition to Energy Imbalance and Obesity, Cell. 135 (2008) 61–73. doi:10.1016/j.cell.2008.07.043.
[90] M. Kuro-o, Y. Nabeshima, Y. Matsumura, H. Aizawa, H. Kawaguchi, T. Suga, T. Utsugi, Y. Ohyama, M. Kurabayashi, T. Kaname, E. Kume, H. Iwasaki, A. Iida, T. Shiraki-Iida, S. Nishikawa, R. Nagai, Mutation of the mouse klotho gene leads to a syndrome resembling ageing., Nature. 390 (1997) 45–51. doi:10.1038/36285.
[91] H. Kurosu, M. Yamamoto, J.D. Clark, J. V Pastor, A. Nandi, P. Gurnani, O.P. McGuinness, H. Chikuda, M. Yamaguchi, H. Kawaguchi, I. Shimomura, Y. Takayama, J. Herz, C.R. Kahn, K.P. Rosenblatt, M. Kuro-o, Suppression of Aging in Mice by the Hormone Klotho, Science (80-.). 309 (2005) 1829–1833. doi:10.1126/science.1112766.
[92] J. Leon, A.J. Moreno, B.I. Garay, R.J. Chalkley, A.L. Burlingame, D. Wang, D.B. Dubal, Peripheral Elevation of a Klotho Fragment Enhances Brain Function and Resilience in Young, Aging, and α-Synuclein Transgenic Mice., Cell Rep. 20 (2017) 1360–1371. doi:10.1016/j.celrep.2017.07.024.
[93] T. Baluchnejadmojarad, S.-M. Eftekhari, N. Jamali-Raeufy, S. Haghani, H. Zeinali, M. Roghani, The anti-aging protein klotho alleviates injury of nigrostriatal dopaminergic pathway in 6-hydroxydopamine rat model of Parkinson's disease: Involvement of PKA/CaMKII/CREB signaling, Exp. Gerontol. 100 (2017) 70–76. doi:10.1016/j.exger.2017.10.023.
[94] E. Zeldich, C.-D. Chen, T.A. Colvin, E.A. Bove-Fenderson, J. Liang, T.B. Tucker Zhou, D.A. Harris, C.R. Abraham, The Neuroprotective Effect of Klotho is Mediated via Regulation of Members of the Redox System, J. Biol. Chem. 289 (2014) 24700–24715.
[95] C.-D. Chen, J.A. Sloane, H. Li, N. Aytan, E.L. Giannaris, E. Zeldich, J.D. Hinman, A.

Dedeoglu, D.L. Rosene, R. Bansal, J.I. Luebke, M. Kuro-o, C.R. Abraham, The Antiaging Protein Klotho Enhances Oligodendrocyte Maturation and Myelination of the CNS, J. Neurosci. 33 (2013) 1927–1939.
[96] S. Adeli, M. Zahmatkesh, G. Tavoosidana, M. Karimian, G. Hassanzadeh, Simvastatin enhances the hippocampal klotho in a rat model of streptozotocin-induced cognitive decline, Prog. Neuro-Psychopharmacology Biol. Psychiatry. 72 (2017) 87–94. doi:10.1016/j.pnpbp.2016.09.009.
[97] Z. Rao, T. Landry, P. Li, W. Bunner, B.T. Laing, Y. Yuan, H. Huang, Administration of alpha klotho reduces liver and adipose lipid accumulation in obese mice, Heliyon. 5 (2019) e01494. doi:10.1016/j.heliyon.2019.e01494.
[98] Y. Lin, Z. Sun, Antiaging gene Klotho enhances glucose-induced insulin secretion by up-regulating plasma membrane levels of TRPV2 in MIN6 β-cells., Endocrinology. 153 (2012) 3029–39. doi:10.1210/en.2012-1091.
[99] Y. Lin, Z. Sun, Antiaging Gene Klotho Attenuates Pancreatic β-Cell Apoptosis in Type 1 Diabetes., Diabetes. 64 (2015) 4298–311. doi:10.2337/db15-0066.
[100] K. Mori, K. Yahata, M. Mukoyama, T. Suganami, H. Makino, T. Nagae, H. Masuzaki, Y. Ogawa, A. Sugawara, Y. Nabeshima, K. Nakao, Disruption of klotho Gene Causes an Abnormal Energy Homeostasis in Mice, Biochem. Biophys. Res. Commun. 278 (2000) 665–670.
[101] G.J. Prud'homme, Y. Glinka, M. Kurt, W. Liu, Q. Wang, The anti-aging protein Klotho is induced by GABA therapy and exerts protective and stimulatory effects on pancreatic beta cells, Biochem. Biophys. Res. Commun. (2017).
[102] G.J. Prud'homme, Y. Glinka, M. Kurt, W. Liu, Q. Wang, Systemic Klotho therapy protects against insulitis and enhances beta-cell mass in NOD mice, Biochem. Biophys. Res. Commun. (2020). doi:10.1016/j.bbrc.2020.02.123.
[103] L. Xing, H. Guo, S. Meng, B. Zhu, J. Fang, J. Huang, J. Chen, Y. Wang, L. Wang, X. Yao, H. Wang, Klotho ameliorates diabetic nephropathy by activating Nrf2 signaling pathway in podocytes, Biochem. Biophys. Res. Commun. (2020). doi:10.1016/j.bbrc.2020.11.061.
[104] T. Matsubara, A. Miyaki, N. Akazawa, Y. Choi, S.-G. Ra, K. Tanahashi, H. Kumagai, S. Oikawa, S. Maeda, Aerobic exercise training increases plasma Klotho levels and reduces arterial stiffness in postmenopausal women, Am. J. Physiol. Circ. Physiol. 306 (2014) H348–H355. doi:10.1152/ajpheart.00429.2013.
[105] R.D. Semba, A.R. Cappola, K. Sun, S. Bandinelli, M. Dalal, C. Crasto, J.M. Guralnik, L. Ferrucci, Plasma klotho and cardiovascular disease in adults., J. Am. Geriatr. Soc. 59 (2011) 1596–601.
[106] X. Li, Z. Li, B. Li, X. Zhu, X. Lai, Klotho improves diabetic cardiomyopathy by suppressing the NLRP3 inflammasome pathway, Life Sci. 234 (2019) 116773. doi:10.1016/J.LFS.2019.116773.
[107] L.-J. Chen, M.-F. Cheng, P.-M. Ku, J.-T. Cheng, Cerebral Klotho Protein as a Humoral Factor for Maintenance of Baroreflex, Horm. Metab. Res. 47 (2014) 125–132. doi:10.1055/s-0034-1375689.
[108] N. Kuwahara, S. Sasaki, M. Kobara, T. Nakata, T. Tatsumi, H. Irie, H. Narumiya, T. Hatta, K. Takeda, H. Matsubara, S. Hushiki, HMG-CoA reductase inhibition improves anti-aging klotho protein expression and arteriosclerosis in rats with chronic inhibition of nitric oxide synthesis, Int. J. Cardiol. 123 (2008) 84–90. doi:10.1016/j.ijcard.2007.02.029.

[109] P. Ravikumar, J. Ye, J. Zhang, S.N. Pinch, M.C. Hu, M. Kuro-o, C.C.W. Hsia, O.W. Moe, α-Klotho protects against oxidative damage in pulmonary epithelia., Am. J. Physiol. Lung Cell. Mol. Physiol. 307 (2014) L566-75.
[110] E.J. Rhee, K.W. Oh, W.Y. Lee, S.Y. Kim, C.H. Jung, B.J. Kim, K.C. Sung, B.S. Kim, J.H. Kang, M.H. Lee, S.W. Kim, J.R. Park, The differential effects of age on the association of KLOTHO gene polymorphisms with coronary artery disease, Metabolism. 55 (2006) 1344–1351. doi:10.1016/j.metabol.2006.05.020.
[111] A. Imamura, K. Okumura, Y. Ogawa, R. Murakami, M. Torigoe, Y. Numaguchi, T. Murohara, Klotho gene polymorphism may be a genetic risk factor for atherosclerotic coronary artery disease but not for vasospastic angina in Japanese, Clin. Chim. Acta. 371 (2006) 66–70. doi:10.1016/j.cca.2006.02.021.
[112] Y. Kim, J.H. Kim, Y.J. Nam, M. Kong, Y.J. Kim, K.H. Yu, B.C. Lee, C. Lee, Klotho is a genetic risk factor for ischemic stroke caused by cardioembolism in Korean females, Neurosci. Lett. 407 (2006) 189–194. doi:10.1016/j.neulet.2006.08.039.
[113] D.E. Arking, D.M. Becker, L.R. Yanek, D. Fallin, D.P. Judge, T.F. Moy, L.C. Becker, H.C. Dietz, KLOTHO allele status and the risk of early-onset occult coronary artery disease, Am. J. Hum. Genet. 72 (2003) 1154–1161. doi:10.1086/375035.
[114] H. Tsujikawa, Y. Kurotaki, T. Fujimori, K. Fukuda, Y.-I. Nabeshima, Klotho, a Gene Related to a Syndrome Resembling Human Premature Aging, Functions in a Negative Regulatory Circuit of Vitamin D Endocrine System, Mol. Endocrinol. 17 (2003) 2393–2403. doi:10.1210/me.2003-0048.
[115] C.-L. Huang, O.W. Moe, Klotho: a novel regulator of calcium and phosphorus homeostasis, Pflügers Arch. - Eur. J. Physiol. 462 (2011) 185–193. doi:10.1007/s00424-011-0950-5.
[116] J.A. Duce, S. Podvin, W. Hollander, D. Kipling, D.L. Rosene, C.R. Abraham, Gene profile analysis implicates Klotho as an important contributor to aging changes in brain white matter of the rhesus monkey, Glia. 56 (2008) 106–117. doi:10.1002/glia.20593.
[117] T. Nakatani, B. Sarraj, M. Ohnishi, M.J. Densmore, T. Taguchi, R. Goetz, M. Mohammadi, B. Lanske, M.S. Razzaque, In vivo genetic evidence for klotho-dependent, fibroblast growth factor 23 (Fgf23) -mediated regulation of systemic phosphate homeostasis, FASEB J. 23 (2009) 433–441. doi:10.1096/fj.08-114397.
[118] I. Wolf, S. Levanon-Cohen, S. Bose, H. Ligumsky, B. Sredni, H. Kanety, M. Kuro-o, B. Karlan, B. Kaufman, H.P. Koeffler, T. Rubinek, Klotho: a tumor suppressor and a modulator of the IGF-1 and FGF pathways in human breast cancer, Oncogene. 27 (2008) 7094–7105. doi:10.1038/onc.2008.292.
[119] M.C. Hu, M. Shi, J. Zhang, T. Addo, H.J. Cho, S.L. Barker, P. Ravikumar, N. Gillings, A. Bian, S.S. Sidhu, M. Kuro-O, O.W. Moe, Renal Production, Uptake, and Handling of Circulating αklotho, J. Am. Soc. Nephrol. 27 (2016) 79–90. doi:10.1681/ASN.2014101030.
[120] Y. Matsumura, H. Aizawa, T. Shiraki-Iida, R. Nagai, M. Kuro-O, Y.I. Nabeshima, Identification of the human klotho gene and its two transcripts encoding membrane and secreted klotho protein, Biochem. Biophys. Res. Commun. 242 (1998) 626–630. doi:10.1006/bbrc.1997.8019.
[121] T. Shiraki-Iida, H. Aizawa, Y. Matsumura, S. Sekine, A. Iida, H. Anazawa, R. Nagai, M. Kuro-o, Y. Nabeshima, Structure of the mouse *klotho* gene and its two transcripts encoding membrane and secreted protein [1], FEBS Lett. 424 (1998) 6–10.

doi:10.1016/S0014-5793(98)00127-6.
[122] O. Tohyama, A. Imura, A. Iwano, J.N. Freund, B. Henrissat, T. Fujimori, Y.I. Nabeshima, Klotho Is a Novel β-Glucuronidase Capable of Hydrolyzing Steroid β-Glucuronides, J. Biol. Chem. 279 (2004) 9777–9784. doi:10.1074/jbc.M312392200.
[123] C.-D. Chen, S. Podvin, E. Gillespie, S.E. Leeman, C.R. Abraham, Insulin stimulates the cleavage and release of the extracellular domain of Klotho by ADAM10 and ADAM17, Proc. Natl. Acad. Sci. 104 (2007) 19796–19801. doi:10.1073/pnas.0709805104.
[124] A. Imura, A. Iwano, O. Tohyama, Y. Tsuji, K. Nozaki, N. Hashimoto, T. Fujimori, Y.I. Nabeshima, Secreted Klotho protein in sera and CSF: Implication for post-translational cleavage in release of Klotho protein from cell membrane, FEBS Lett. 565 (2004) 143–147. doi:10.1016/j.febslet.2004.03.090.
[125] E.P.M. van Loon, W.P. Pulskens, E.A.E. van der Hagen, M. Lavrijsen, M.G. Vervloet, H. van Goor, R.J.M. Bindels, J.G.J. Hoenderop, Shedding of klotho by ADAMs in the kidney, Am. J. Physiol. Physiol. 309 (2015) F359–F368. doi:10.1152/ajprenal.00240.2014.
[126] L. Bloch, O. Sineshchekova, D. Reichenbach, K. Reiss, P. Saftig, M. Kuro-o, C. Kaether, Klotho is a substrate for α-, β- and γ-secretase, FEBS Lett. 583 (2009) 3221–3224. doi:10.1016/j.febslet.2009.09.009.
[127] H. Mitani, N. Ishizaka, T. Aizawa, M. Ohno, S. Usui, T. Suzuki, T. Amaki, I. Mori, Y. Nakamura, M. Sato, M. Nangaku, Y. Hirata, R. Nagai, In Vivo *klotho* Gene Transfer Ameliorates Angiotensin II-Induced Renal Damage, Hypertension. 39 (2002) 838–843. doi:10.1161/01.HYP.0000013734.33441.EA.
[128] T. Utsugi, T. Ohno, Y. Ohyama, T. Uchiyama, Y. Saito, Y. Matsumura, H. Aizawa, H. Itoh, M. Kurabayashi, S. Kawazu, S. Tomono, Y. Oka, T. Suga, M. Kuro-o, Y. Nabeshima, R. Nagai, Decreased insulin production and increased insulin sensitivity in the klotho mutant mouse, a novel animal model for human aging, Metabolism. 49 (2000) 1118–1123. doi:10.1053/meta.2000.8606.
[129] M. Hasannejad, S.Z. Samsamshariat, A. Esmaili, A. Jahanian-Najafabadi, Klotho induces insulin resistance possibly through interference with GLUT4 translocation and activation of Akt, GSK3β, and PFKfβ3 in 3T3-L1 adipocyte cells, Res. Pharm. Sci. 14 (2019) 369–377. doi:10.4103/1735-5362.263627.
[130] H. Olauson, R. Mencke, J.-L. Hillebrands, T.E. Larsson, Tissue expression and source of circulating αKlotho, Bone. 100 (2017) 19–35. doi:10.1016/j.bone.2017.03.043.
[131] H. Zhang, Y. Li, Y. Fan, J. Wu, B. Zhao, Y. Guan, S. Chien, N. Wang, Klotho is a target gene of PPAR-γ, Kidney Int. 74 (2008) 732–739. doi:10.1038/ki.2008.244.
[132] Y. Chihara, H. Rakugi, K. Ishikawa, M. Ikushima, Y. Maekawa, J. Ohta, I. Kida, T. Ogihara, Klotho Protein Promotes Adipocyte Differentiation, Endocrinology. 147 (2006) 3835–3842. doi:10.1210/en.2005-1529.
[133] O.K. Öz, A. Hajibeigi, K. Howard, C.L. Cummins, M. van Abel, R.J. Bindels, R.A. Word, M. Kuro-o, C.Y. Pak, J.E. Zerwekh, Aromatase Deficiency Causes Altered Expression of Molecules Critical for Calcium Reabsorption in the Kidneys of Female Mice, J. Bone Miner. Res. 22 (2007) 1893–1902. doi:10.1359/jbmr.070808.
[134] T.O. Carpenter, K.L. Insogna, J.H. Zhang, B. Ellis, S. Nieman, C. Simpson, E. Olear, C.M. Gundberg, Circulating Levels of Soluble Klotho and FGF23 in X-Linked Hypophosphatemia: Circadian Variance, Effects of Treatment, and Relationship to Parathyroid Status, J. Clin. Endocrinol. Metab. 95 (2010) E352–E357.

doi:10.1210/jc.2010-0589.
[135] S.-J. Tan, E.R. Smith, T.D. Hewitson, S.G. Holt, N.D. Toussaint, Diurnal variation and short-term pre-analytical stability of serum soluble α-klotho in healthy volunteers: a pilot study., Ann. Clin. Biochem. 52 (2015) 506–9. doi:10.1177/0004563214563415.
[136] L. Pedersen, S.M. Pedersen, C.L. Brasen, L.M. Rasmussen, Soluble serum Klotho levels in healthy subjects. Comparison of two different immunoassays, Clin. Biochem. 46 (2013) 1079–1083. doi:10.1016/j.clinbiochem.2013.05.046.
[137] Y. Yamazaki, A. Imura, I. Urakawa, T. Shimada, J. Murakami, Y. Aono, H. Hasegawa, T. Yamashita, K. Nakatani, Y. Saito, N. Okamoto, N. Kurumatani, N. Namba, T. Kitaoka, K. Ozono, T. Sakai, H. Hataya, S. Ichikawa, E.A. Imel, M.J. Econs, Y.I. Nabeshima, Establishment of sandwich ELISA for soluble alpha-Klotho measurement: Age-dependent change of soluble alpha-Klotho levels in healthy subjects, Biochem. Biophys. Res. Commun. 398 (2010) 513–518. doi:10.1016/j.bbrc.2010.06.110.
[138] R.D. Semba, A.R. Cappola, K. Sun, S. Bandinelli, M. Dalal, C. Crasto, J.M. Guralnik, L. Ferrucci, Plasma klotho and mortality risk in older community-dwelling adults., J. Gerontol. A. Biol. Sci. Med. Sci. 66 (2011) 794–800. doi:10.1093/gerona/glr058.
[139] F. Liu, S. Wu, H. Ren, J. Gu, Klotho suppresses RIG-I-mediated senescence-associated inflammation, Nat. Cell Biol. 13 (2011) 254–262. doi:10.1038/ncb2167.
[140] M. Yamamoto, J.D. Clark, J. V Pastor, P. Gurnani, A. Nandi, H. Kurosu, M. Miyoshi, Y. Ogawa, D.H. Castrillon, K.P. Rosenblatt, M. Kuro-O, Regulation of Oxidative Stress by the Anti-aging Hormone Klotho * □, (2005). doi:10.1074/jbc.M509039200.
[141] Y. Saito, T. Nakamura, Y. Ohyama, T. Suzuki, A. Iida, T. Shiraki-Iida, M. Kuro-o, Y. ichi Nabeshima, M. Kurabayashi, R. Nagai, In vivo klotho gene delivery protects against endothelial dysfunction in multiple risk factor syndrome, Biochem. Biophys. Res. Commun. 276 (2000) 767–772. doi:10.1006/bbrc.2000.3470.
[142] Y. Saito, T. Yamagishi, T. Nakamura, Y. Ohyama, H. Aizawa, T. Suga, Y. Matsumura, H. Masuda, M. Kurabayashi, M. Kuro-O, Y.I. Nabeshima, R. Nagai, Klotho protein protects against endothelial dysfunction, Biochem. Biophys. Res. Commun. 248 (1998) 324–329. doi:10.1006/bbrc.1998.8943.
[143] S. Devaraj, B. Syed, A. Chien, I. Jialal, Validation of an Immunoassay for Soluble Klotho Protein, Am. J. Clin. Pathol. 137 (2012) 479–485. doi:10.1309/AJCPGPMAF7SFRBO4.
[144] Q. Wan, Y. He, M. Yuan, Klotho in diabetes and diabetic nephropathy: a brief update review, Int J Clin Exp Med. 10 (2017) 4342–4349.
[145] F. Nie, D. Wu, H. Du, X. Yang, M. Yang, X. Pang, Y. Xu, Serum klotho protein levels and their correlations with the progression of type 2 diabetes mellitus, J. Diabetes Complications. 31 (2017) 594–598. doi:10.1016/J.JDIACOMP.2016.11.008.
[146] J.M. Oswiecimska, M. Pys-Spychala, E. Swietochowska, Z. Ostrowska, A. Szymlak, A. Mikolajczak, Z. Malczyk, M. Chyra, Serum alpha-klotho concentrations in girls with anorexia nervosa., Neuro Endocrinol. Lett. 36 (2015) 539–44.
[147] S.K. Kunert, H. Hartmann, D. Haffner, M. Leifheit-Nestler, Klotho and fibroblast growth factor 23 in cerebrospinal fluid in children, J. Bone Miner. Metab. 35 (2017) 215–226. doi:10.1007/s00774-016-0746-y.
[148] R.D. Semba, A.R. Moghekar, J. Hu, K. Sun, R. Turner, L. Ferrucci, R. O'Brien, Klotho in the cerebrospinal fluid of adults with and without Alzheimer's disease, Neurosci. Lett. 558 (2014) 37–40. doi:10.1016/j.neulet.2013.10.058.
[149] M.S. Emami Aleagha, B. Siroos, M. Ahmadi, M. Balood, A. Palangi, A.N. Haghighi,

M.H. Harirchian, Decreased concentration of Klotho in the cerebrospinal fluid of patients with relapsing-remitting multiple sclerosis, J. Neuroimmunol. 281 (2015) 5–8. doi:10.1016/j.jneuroim.2015.02.004.
[150] I. Urakawa, Y. Yamazaki, T. Shimada, K. Iijima, H. Hasegawa, K. Okawa, T. Fujita, S. Fukumoto, T. Yamashita, Klotho converts canonical FGF receptor into a specific receptor for FGF23, Nature. 444 (2006) 770–774. doi:10.1038/nature05315.
[151] G. Chen, Y. Liu, R. Goetz, L. Fu, S. Jayaraman, M.-C. Hu, O.W. Moe, G. Liang, X. Li, M. Mohammadi, α-Klotho is a non-enzymatic molecular scaffold for FGF23 hormone signalling, Nature. 553 (2018) 461–466. doi:10.1038/nature25451.
[152] M. Mohammadi, S.K. Olsen, O.A. Ibrahimi, Structural basis for fibroblast growth factor receptor activation, Cytokine Growth Factor Rev. 16 (2005) 107–137. doi:10.1016/j.cytogfr.2005.01.008.
[153] T. Yoshida, T. Fujimori, Y.-I. Nabeshima, Mediation of Unusually High Concentrations of 1,25-Dihydroxyvitamin D in Homozygous *klotho* Mutant Mice by Increased Expression of Renal 1α-Hydroxylase Gene, Endocrinology. 143 (2002) 683–689. doi:10.1210/endo.143.2.8657.
[154] E. Lewin, K. Olgaard, Klotho, an important new factor for the activity of Ca2+ channels, connecting calcium homeostasis, ageing and uraemia., Nephrol. Dial. Transplant. 21 (2006) 1770–2. doi:10.1093/ndt/gfl178.
[155] A. Martin, V. David, L. Darryl Quarles, Regulation and function of the FGF23/klotho endocrine pathways, Physiol. Rev. 92 (2012) 131–155. doi:10.1152/physrev.00002.2011.
[156] M. Kuro-o, Klotho as a regulator of fibroblast growth factor signaling and phosphate/calcium metabolism, Curr. Opin. Nephrol. Hypertens. 15 (2006) 437–441. doi:10.1097/01.mnh.0000232885.81142.83.
[157] T. Shimada, M. Kakitani, Y. Yamazaki, H. Hasegawa, Y. Takeuchi, T. Fujita, S. Fukumoto, K. Tomizuka, T. Yamashita, Targeted ablation of Fgf23 demonstrates an essential physiological role of FGF23 in phosphate and vitamin D metabolism, J. Clin. Invest. 113 (2004) 561–568. doi:10.1172/jci19081.
[158] Q. Chang, S. Hoefs, A.W. van der Kemp, C.N. Topala, R.J. Bindels, J.G. Hoenderop, The ß-Glucuronidase Klotho Hydrolyzes and Activates the TRPV5 Channel, Science (80-.). 310 (2005).
[159] X. Tang, Y. Wang, Z. Fan, G. Ji, M. Wang, J. Lin, S. Huang, S.J. Meltzer, Klotho: A tumor suppressor and modulator of the Wnt/β-catenin pathway in human hepatocellular carcinoma, Lab. Investig. 96 (2016) 197–205. doi:10.1038/labinvest.2015.86.
[160] H. Liu, M.M. Fergusson, R.M. Castilho, J. Liu, L. Cao, J. Chen, D. Malide, I.I. Rovira, D. Schimel, C.J. Kuo, J.S. Gutkind, P.M. Hwang, T. Finkel, Augmented Wnt Signaling in a Mammalian Model of Accelerated Aging, Science (80-.). 317 (2007) 803–806. doi:10.1126/science.1143578.
[161] L. Zhou, Y. Li, D. Zhou, R.J. Tan, Y. Liu, Loss of Klotho Contributes to Kidney Injury by Derepression of Wnt/β-Catenin Signaling, J. Am. Soc. Nephrol. 24 (2013).
[162] J. Lee, B. Tsogbadrakh, S.H. Yang, H. Ryu, E. Kang, M. Kang, H.G. Kang, C. Ahn, K.H. Oh, Klotho ameliorates diabetic nephropathy via LKB1-AMPK-PGC1α-mediated renal mitochondrial protection, Biochem. Biophys. Res. Commun. (2020). doi:10.1016/j.bbrc.2020.10.040.
[163] E. Zeldich, C.-D. Chen, T.A. Colvin, E.A. Bove-Fenderson, J. Liang, T.B. Tucker Zhou, D.A. Harris, C.R. Abraham, The neuroprotective effect of Klotho is mediated via

regulation of members of the redox system., J. Biol. Chem. 289 (2014) 24700–15. doi:10.1074/jbc.M114.567321.
[164] H. Gu, W. Jiang, N. You, X. Huang, Y. Li, X. Peng, R. Dong, Z. Wang, Y. Zhu, K. Wu, J. Li, L. Zheng, Soluble Klotho Improves Hepatic Glucose and Lipid Homeostasis in Type 2 Diabetes, Mol. Ther. - Methods Clin. Dev. 18 (2020) 811–823. doi:10.1016/j.omtm.2020.08.002.
[165] Y. Lin, M. Kuro-o, Z. Sun, Genetic Deficiency of Anti-Aging Gene Klotho Exacerbates Early Nephropathy in STZ-Induced Diabetes in Male Mice, Endocrinology. 154 (2013) 3855–3863. doi:10.1210/en.2013-1053.
[166] A. Corcillo, N. Fountoulakis, A. Sohal, F. Farrow, S. Ayis, J. Karalliedde, Low levels of circulating anti-ageing hormone Klotho predict the onset and progression of diabetic retinopathy, Diabetes Vasc. Dis. Res. 17 (2020) 147916412097090. doi:10.1177/1479164120970901.
[167] H.J. Kim, J. Lee, D.W. Chae, K.B. Lee, S.A. Sung, T.H. Yoo, S.H. Han, C. Ahn, K.H. Oh, Serum klotho is inversely associated with metabolic syndrome in chronic kidney disease: Results from the KNOW-CKD study, BMC Nephrol. 20 (2019) 119. doi:10.1186/s12882-019-1297-y.
[168] B. Ji, H. Wei, Y. Ding, H. Liang, L. Yao, H. Wang, H. Qu, H. Deng, Protective potential of klotho protein on diabetic retinopathy: Evidence from clinical and *in vitro* studies, J. Diabetes Investig. 11 (2020) 162–169. doi:10.1111/jdi.13100.
[169] O. Lorenzi, C. Veyrat-Durebex, C.B. Wollheim, P. Villemin, F. Rohner-Jeanrenaud, A. Zanchi, U.M. Vischer, Evidence against a direct role of klotho in insulin resistance, Pflugers Arch. Eur. J. Physiol. 459 (2010) 465–473. doi:10.1007/s00424-009-0735-2.
[170] J. van Ark, H.-P. Hammes, M.C.R.F. van Dijk, M.G. Vervloet, B.H.R. Wolffenbuttel, H. van Goor, J.-L. Hillebrands, Circulating alpha-klotho levels are not disturbed in patients with type 2 diabetes with and without macrovascular disease in the absence of nephropathy, Cardiovasc. Diabetol. 12 (2013) 116.
[171] Y. Chihara, H. Rakugi, K. Ishikawa, M. Ikushima, Y. Maekawa, J. Ohta, I. Kida, T. Ogihara, Klotho Protein Promotes Adipocyte Differentiation, Endocrinology. 147 (2006) 3835–3842. doi:10.1210/en.2005-1529.
[172] J. Xu, D.J. Lloyd, C. Hale, S. Stanislaus, M. Chen, G. Sivits, S. Vonderfecht, R. Hecht, Y.-S. Li, R.A. Lindberg, J.-L. Chen, D.Y. Jung, Z. Zhang, H.-J. Ko, J.K. Kim, M.M. Véniant, Fibroblast growth factor 21 reverses hepatic steatosis, increases energy expenditure, and improves insulin sensitivity in diet-induced obese mice., Diabetes. 58 (2009) 250–9. doi:10.2337/db08-0392.
[173] I.N. Foltz, S. Hu, C. King, X. Wu, C. Yang, W. Wang, J. Weiszmann, J. Stevens, J.S. Chen, N. Nuanmanee, J. Gupte, R. Komorowski, L. Sekirov, T. Hager, T. Arora, H. Ge, H. Baribault, F. Wang, J. Sheng, M. Karow, M. Wang, Y. Luo, W. McKeehan, Z. Wang, M.M. Veniant, Y. Li, Treating Diabetes and Obesity with an FGF21-Mimetic Antibody Activating the Klotho/FGFR1c Receptor Complex, Sci. Transl. Med. 4 (2012) 162ra153-162ra153. doi:10.1126/scitranslmed.3004690.
[174] P.J. Antonellis, B.A. Droz, R. Cosgrove, L.S. O'Farrell, T. Coskun, J.W. Perfield, S. Bauer, M. Wade, T.E. Chouinard, J.T. Brozinick, A.C. Adams, R.J. Samms, The anti-obesity effect of FGF19 does not require UCP1-dependent thermogenesis, Mol. Metab. 30 (2019) 131–139. doi:10.1016/j.molmet.2019.09.006.
[175] R. Samms, P. Antonellis, S. Bauer, D. Smith, L. O'Farrell, A. Culver, M. Hamang, J.

Perfield, T. Coskun, B. Yaden, R. Gimeno, J. Brozinick, A. Adams, The anti-obesity effect of FGF19 occurs independent of the thermogenic protein UCP1 | The FASEB Journal, FASEB. (2017).
[176] M.M. Kwon, S.M. O'Dwyer, R.K. Baker, S.D. Covey, T.J. Kieffer, FGF21-Mediated Improvements in Glucose Clearance Require Uncoupling Protein 1, Cell Rep. 13 (2015) 1521–1527. doi:10.1016/j.celrep.2015.10.021.
[177] L. Mutsnaini, C.S. Kim, J. Kim, Y. Joe, H.T. Chung, H.S. Choi, E. Roh, M.S. Kim, R. Yu, Fibroblast growth factor 21 deficiency aggravates obesity-induced hypothalamic inflammation and impairs thermogenic response, Inflamm. Res. 68 (2019) 351–358. doi:10.1007/s00011-019-01222-2.
[178] K.L. Vinales, B. Begaye, C. Bogardus, M. Walter, J. Krakoff, P. Piaggi, FGF21 is a hormonal mediator of the human "thrifty" metabolic phenotype, Diabetes. 68 (2019) 318–323. doi:10.2337/db18-0696.
[179] C.M. Hill, T. Laeger, M. Dehner, D.C. Albarado, B. Clarke, D. Wanders, S.J. Burke, J.J. Collier, E. Qualls-Creekmore, S.M. Solon-Biet, S.J. Simpson, H.R. Berthoud, H. Münzberg, C.D. Morrison, FGF21 Signals Protein Status to the Brain and Adaptively Regulates Food Choice and Metabolism, Cell Rep. 27 (2019) 2934-2947.e3. doi:10.1016/j.celrep.2019.05.022.
[180] J. Yie, W. Wang, L. Deng, L.-T. Tam, J. Stevens, M.M. Chen, Y. Li, J. Xu, R. Lindberg, R. Hecht, M. Véniant, C. Chen, M. Wang, Understanding the Physical Interactions in the FGF21/FGFR/β-Klotho Complex: Structural Requirements and Implications in FGF21 Signaling, Chem. Biol. Drug Des. 79 (2012) 398–410. doi:10.1111/j.1747-0285.2012.01325.x.
[181] S. Lee, J. Choi, J. Mohanty, L.P. Sousa, F. Tome, E. Pardon, J. Steyaert, M.A. Lemmon, I. Lax, J. Schlessinger, Structures of β-klotho reveal a 'zip code'-like mechanism for endocrine FGF signalling, Nature. 553 (2018) 501–505. doi:10.1038/nature25010.
[182] M. Kuro-o, Klotho and βKlotho, in: Springer, New York, NY, 2012: pp. 25–40. doi:10.1007/978-1-4614-0887-1_2.
[183] A. Satoh, S. iee Han, M. Araki, Y. Nakagawa, H. Ohno, Y. Mizunoe, K. Kumagai, Y. Murayama, Y. Osaki, H. Iwasaki, M. Sekiya, M. Konishi, N. Itoh, T. Matsuzaka, H. Sone, H. Shimano, CREBH Improves Diet-Induced Obesity, Insulin Resistance, and Metabolic Disturbances by FGF21-Dependent and FGF21-Independent Mechanisms, IScience. 23 (2020). doi:10.1016/j.isci.2020.100930.
[184] F.F. Fisher, S. Kleiner, N. Douris, E.C. Fox, R.J. Mepani, F. Verdeguer, J. Wu, A. Kharitonenkov, J.S. Flier, E. Maratos-Flier, B.M. Spiegelman, FGF21 regulates PGC-1α and browning of white adipose tissues in adaptive thermogenesis, Genes Dev. 26 (2012) 271–281. doi:10.1101/gad.177857.111.
[185] R.J. Samms, C.C. Cheng, A. Kharitonenkov, R.E. Gimeno, A.C. Adams, Overexpression of β-Klotho in Adipose Tissue Sensitizes Male Mice to Endogenous FGF21 and Provides Protection From Diet-Induced Obesity, Endocrinology. 157 (2016) 1467–1480. doi:10.1210/en.2015-1722.
[186] L. Lynch, A.E. Hogan, D. Duquette, C. Lester, A. Banks, K. LeClair, D.E. Cohen, A. Ghosh, B. Lu, M. Corrigan, D. Stevanovic, E. Maratos-Flier, D.J. Drucker, D. O'Shea, M. Brenner, iNKT Cells Induce FGF21 for Thermogenesis and Are Required for Maximal Weight Loss in GLP1 Therapy, Cell Metab. 24 (2016) 510–519. doi:10.1016/j.cmet.2016.08.003.

[187] D. V. Chartoumpekis, I.G. Habeos, P.G. Ziros, A.I. Psyrogiannis, V.E. Kyriazopoulou, A.G. Papavassiliou, Brown adipose tissue responds to cold and adrenergic stimulation by induction of FGF21, Mol. Med. 17 (2011) 736–740. doi:10.2119/molmed.2011.00075.
[188] L.-J. Chen, M.-F. Cheng, P.-M. Ku, J.-T. Cheng, Cerebral Klotho Protein as a Humoral Factor for Maintenance of Baroreflex, Horm. Metab. Res. 47 (2014) 125–132.
[189] E. Zeldich, C.-D. Chen, R. Avila, S. Medicetty, C.R. Abraham, The Anti-Aging Protein Klotho Enhances Remyelination Following Cuprizone-Induced Demyelination, J. Mol. Neurosci. 57 (2015) 185–196. doi:10.1007/s12031-015-0598-2.
[190] C.-D. Chen, H. Li, J. Liang, K. Hixson, E. Zeldich, C.R. Abraham, The Anti-Aging and Tumor Suppressor Protein Klotho Enhances Differentiation of a Human Oligodendrocytic Hybrid Cell Line, J. Mol. Neurosci. 55 (2015) 76–90. doi:10.1007/s12031-014-0336-1.
[191] M. Shiozaki, K. Yoshimura, M. Shibata, M. Koike, N. Matsuura, Y. Uchiyama, T. Gotow, Morphological and biochemical signs of age-related neurodegenerative changes in klotho mutant mice, Neuroscience. 152 (2008) 924–941. doi:10.1016/j.neuroscience.2008.01.032.
[192] N. Hensel, A. Schön, T. Konen, V. Lübben, B. Förthmann, O. Baron, C. Grothe, M. Leifheit-Nestler, P. Claus, D. Haffner, Fibroblast growth factor 23 signaling in hippocampal cells: impact on neuronal morphology and synaptic density, J. Neurochem. 137 (2016) 756–769.
[193] G. Marcelin, Y.-H. Jo, X. Li, G.J. Schwartz, Y. Zhang, N.J. Dun, R.-M. Lyu, C. Blouet, J.K. Chang, S. Chua, Central action of FGF19 reduces hypothalamic AGRP/NPY neuron activity and improves glucose metabolism, Mol. Metab. 3 (2014) 19–28. doi:10.1016/j.molmet.2013.10.002.
[194] D.A. Sarruf, J.P. Thaler, G.J. Morton, J. German, J.D. Fischer, K. Ogimoto, M.W. Schwartz, Fibroblast Growth Factor 21 Action in the Brain Increases Energy Expenditure and Insulin Sensitivity in Obese Rats, (n.d.). doi:10.2337/db09-1878.
[195] G.J. Morton, M.E. Matsen, D.P. Bracy, T.H. Meek, H.T. Nguyen, D. Stefanovski, R.N. Bergman, D.H. Wasserman, M.W. Schwartz, FGF19 action in the brain induces insulin-independent glucose lowering., J. Clin. Invest. 123 (2013) 4799–808. doi:10.1172/JCI70710.
[196] K.K. Ryan, R. Kohli, R. Gutierrez-Aguilar, S.G. Gaitonde, S.C. Woods, R.J. Seeley, Fibroblast growth factor-19 action in the brain reduces food intake and body weight and improves glucose tolerance in male rats, Endocrinology. 154 (2013) 9–15. doi:10.1210/en.2012-1891.
[197] T. Lan, D.A. Morgan, K. Rahmouni, J. Sonoda, X. Fu, S.C. Burgess, W.L. Holland, S.A. Kliewer, D.J. Mangelsdorf, FGF19, FGF21, and an FGFR1/β-Klotho-Activating Antibody Act on the Nervous System to Regulate Body Weight and Glycemia, Cell Metab. 26 (2017) 709-718.e3. doi:10.1016/J.CMET.2017.09.005.
[198] J.M. Rojas, M.E. Matsen, T.O. Mundinger, G.J. Morton, D. Stefanovski, R.N. Bergman, K.J. Kaiyala, G.J. Taborsky, M.W. Schwartz, Glucose intolerance induced by blockade of central FGF receptors is linked to an acute stress response, Mol. Metab. 4 (2015) 561–568. doi:10.1016/J.MOLMET.2015.05.005.
[199] K.K. Ryan, R. Kohli, R. Gutierrez-Aguilar, S.G. Gaitonde, S.C. Woods, R.J. Seeley, Fibroblast Growth Factor-19 Action in the Brain Reduces Food Intake and Body Weight and Improves Glucose Tolerance in Male Rats, Endocrinology. 154 (2013) 9–15. doi:10.1210/en.2012-1891.

[200] B.M. Owen, X. Ding, D.A. Morgan, K.C. Coate, A.L. Bookout, K. Rahmouni, S.A. Kliewer, D.J. Mangelsdorf, FGF21 Acts Centrally to Induce Sympathetic Nerve Activity, Energy Expenditure, and Weight Loss, Cell Metab. 20 (2014) 670–677. doi:10.1016/J.CMET.2014.07.012.
[201] R.J. Samms, J.E. Lewis, A. Lory, M.J. Fowler, S. Cooper, A. Warner, P. Emmerson, A.C. Adams, J.C. Luckett, A.C. Perkins, D. Wilson, P. Barrett, K. Tsintzas, F.J.P. Ebling, Antibody-Mediated Inhibition of the FGFR1c Isoform Induces a Catabolic Lean State in Siberian Hamsters, Curr. Biol. 25 (2015) 2997–3003. doi:10.1016/j.cub.2015.10.010.
[202] H.D. Sun, M. Malabunga, J.R. Tonra, R. DiRenzo, F.E. Carrick, H. Zheng, H.-R. Berthoud, O.P. McGuinness, J. Shen, P. Bohlen, R.L. Leibel, P. Kussie, Monoclonal antibody antagonists of hypothalamic FGFR1 cause potent but reversible hypophagia and weight loss in rodents and monkeys, Am. J. Physiol. Metab. 292 (2007) E964–E976. doi:10.1152/ajpendo.00089.2006.
[203] M. Ameka, K.R. Markan, D.A. Morgan, L.D. BonDurant, S.O. Idiga, M.C. Naber, Z. Zhu, L. V. Zingman, J.L. Grobe, K. Rahmouni, M.J. Potthoff, Liver Derived FGF21 Maintains Core Body Temperature During Acute Cold Exposure, Sci. Rep. 9 (2019) 1–10. doi:10.1038/s41598-018-37198-y.
[204] B.M. Owen, X. Ding, D.A. Morgan, K.C. Coate, A.L. Bookout, K. Rahmouni, S.A. Kliewer, D.J. Mangelsdorf, FGF21 Acts Centrally to Induce Sympathetic Nerve Activity, Energy Expenditure, and Weight Loss, Cell Metab. 20 (2014) 670–677.
[205] H. Kurosu, Y. Ogawa, M. Miyoshi, M. Yamamoto, A. Nandi, K.P. Rosenblatt, M.G. Baum, S. Schiavi, M.-C. Hu, O.W. Moe, M. Kuro-o, Regulation of Fibroblast Growth Factor-23 Signaling by Klotho, J. Biol. Chem. 281 (2006) 6120–6123. doi:10.1074/jbc.C500457200.
[206] O.E. Pardo, J. Latigo, R.E. Jeffery, E. Nye, R. Poulsom, B. Spencer-Dene, N.R. Lemoine, G.W. Stamp, E.O. Aboagye, M.J. Seckl, The Fibroblast Growth Factor Receptor Inhibitor PD173074 Blocks Small Cell Lung Cancer Growth In vitro and In vivo, Cancer Res. 69 (2009) 8645–8651. doi:10.1158/0008-5472.CAN-09-1576.
[207] B.T. Laing, K. Do, T. Matsubara, D.W. Wert, M.J. Avery, E.M. Langdon, D. Zheng, H. Huang, Voluntary exercise improves hypothalamic and metabolic function in obese mice., J. Endocrinol. 229 (2016) 109–22. doi:10.1530/JOE-15-0510.
[208] B.T. Laing, P. Li, C.A. Schmidt, W. Bunner, Y. Yuan, T. Landry, A. Prete, J.M. McClung, H. Huang, AgRP/NPY Neuron Excitability Is Modulated by Metabotropic Glutamate Receptor 1 During Fasting, Front. Cell. Neurosci. 12 (2018) 276. doi:10.3389/fncel.2018.00276.
[209] J.T. Ting, T.L. Daigle, Q. Chen, G. Feng, Acute brain slice methods for adult and aging animals: application of targeted patch clamp analysis and optogenetics., Methods Mol. Biol. 1183 (2014) 221–42. doi:10.1007/978-1-4939-1096-0_14.
[210] J. Qiu, H.M. Rivera, M.A. Bosch, S.L. Padilla, T.L. Stincic, R.D. Palmiter, M.J. Kelly, O.K. Rønnekleiv, Estrogenic-dependent glutamatergic neurotransmission from kisspeptin neurons governs feeding circuits in females, (n.d.). doi:10.7554/eLife.35656.001.
[211] J. Katayama, N. Akaike, J. Nabekura, Characterization of pre- and post-synaptic metabotropic glutamate receptor-mediated inhibitory responses in substantia nigra dopamine neurons, Neurosci. Res. 45 (2003) 101–115. doi:10.1016/S0168-0102(02)00202-X.
[212] P.L. Mellon, J.J. Windle, P.C. Goldsmith, C.A. Padula, J.L. Roberts, R.I. Weiner,

Immortalization of hypothalamic GnRH by genetically targeted tumorigenesis, Neuron. 5 (1990) 1–10. doi:10.1016/0896-6273(90)90028-E.
[213] G.J. Chen, B. Weylie, C. Hu, J. Zhu, R. Forough, FGFR1/PI3K/AKT signaling pathway is a novel target for antiangiogenic effects of the cancer drug Fumagillin (TNP-470), J. Cell. Biochem. 101 (2007) 1492–1504. doi:10.1002/jcb.21265.
[214] B. Ahren, N. Wierup, F. Sundler, Neuropeptides and the Regulation of Islet Function, Diabetes. 55 (2006) S98–S107. doi:10.2337/db06-S013.
[215] S.Y. Gil, B.-S. Youn, K. Byun, H. Huang, C. Namkoong, P.-G. Jang, J.-Y. Lee, Y.-H. Jo, G.M. Kang, H.-K. Kim, M.-S. Shin, C.U. Pietrzik, B. Lee, Y.-B. Kim, M.-S. Kim, Clusterin and LRP2 are critical components of the hypothalamic feeding regulatory pathway, Nat. Commun. 4 (2013) 1862. doi:10.1038/ncomms2896.
[216] M. Park, H. Oh, D.A. York, Enterostatin affects cyclic AMP and ERK signaling pathways to regulate Agouti-related Protein (AgRP) expression, Peptides. 30 (2009) 181–190.
[217] J.M. Brown, J.M. Scarlett, M.E. Matsen, H.T. Nguyen, A. Secher, R. Jorgensen, G.J. Morton, M.W. Schwartz, The Hypothalamic Arcuate Nucleus-Median Eminence is a Target for Sustained Diabetes Remission Induced by Fibroblast Growth Factor 1, Diabetes. 68 (2019) db190025. doi:10.2337/DB19-0025.
[218] T. Landry, B.T. Laing, P. Li, W. Bunner, Z. Rao, A. Prete, J. Sylvestri, H. Huang, Central α-Klotho Suppresses NPY/AgRP Neuron Activity and Regulates Metabolism in Mice, Diabetes. 69 (2020) db190941. doi:10.2337/db19-0941.
[219] D. Wang, X. He, Z. Zhao, Q. Feng, R. Lin, Y. Sun, T. Ding, F. Xu, M. Luo, C. Zhan, Whole-brain mapping of the direct inputs and axonal projections of POMC and AgRP neurons, Front. Neuroanat. 9 (2015) 40. doi:10.3389/fnana.2015.00040.
[220] C. García-Cáceres, E. Balland, V. Prevot, S. Luquet, S.C. Woods, M. Koch, T.L. Horvath, C.X. Yi, J.A. Chowen, A. Verkhratsky, A. Araque, I. Bechmann, M.H. Tschöp, Role of astrocytes, microglia, and tanycytes in brain control of systemic metabolism, Nat. Neurosci. 22 (2019) 7–14. doi:10.1038/s41593-018-0286-y.
[221] Y. Yasumoto, H. Miyazaki, M. Ogata, Y. Kagawa, Y. Yamamoto, A. Islam, T. Yamada, H. Katagiri, Y. Owada, Glial Fatty Acid-Binding Protein 7 (FABP7) Regulates Neuronal Leptin Sensitivity in the Hypothalamic Arcuate Nucleus, Mol. Neurobiol. 55 (2018) 9016–9028. doi:10.1007/s12035-018-1033-9.
[222] E. Balland, J. Dam, F. Langlet, E. Caron, S. Steculorum, A. Messina, S. Rasika, A. Falluel-Morel, Y. Anouar, B. Dehouck, E. Trinquet, R. Jockers, S.G. Bouret, V. Prévot, Hypothalamic tanycytes are an ERK-gated conduit for leptin into the brain, Cell Metab. 19 (2014) 293–301. doi:10.1016/j.cmet.2013.12.015.
[223] S.C. Robins, I. Stewart, D.E. McNay, V. Taylor, C. Giachino, M. Goetz, J. Ninkovic, N. Briancon, E. Maratos-Flier, J.S. Flier, M. V. Kokoeva, M. Placzek, α-Tanycytes of the adult hypothalamic third ventricle include distinct populations of FGF-responsive neural progenitors, Nat. Commun. 4 (2013) 1–13. doi:10.1038/ncomms3049.
[224] B.T. Laing, H. Huang, Exercise improves hypothalamic function induced by high-fat diet, Immunoendocrinology. 3 (2016). doi:10.14800/ie.1446.
[225] Z. Jiang, S. Rajamanickam, N.J. Justice, Local corticotropin-releasing factor signaling in the hypothalamic paraventricular nucleus, J. Neurosci. 38 (2018) 1874–1890. doi:10.1523/JNEUROSCI.1492-17.2017.
[226] C. Zhu, Z. Jiang, Y. Xu, Z.L. Cai, Q. Jiang, Y. Xu, M. Xue, B.R. Arenkiel, Q. Wu, G. Shu, Q. Tong, Profound and redundant functions of arcuate neurons in obesity

development, Nat. Metab. (2020) 1–12. doi:10.1038/s42255-020-0229-2.
[227] B.Y.H. Lam, I. Cimino, J. Polex-Wolf, S. Nicole Kohnke, D. Rimmington, V. Iyemere, N. Heeley, C. Cossetti, R. Schulte, L.R. Saraiva, D.W. Logan, C. Blouet, S. O'Rahilly, A.P. Coll, G.S.H. Yeo, Heterogeneity of hypothalamic pro-opiomelanocortin-expressing neurons revealed by single-cell RNA sequencing, Mol. Metab. 6 (2017) 383–392. doi:10.1016/j.molmet.2017.02.007.
[228] C.H. Mazucanti, E.M. Kawamoto, M.P. Mattson, C. Scavone, S. Camandola, Activity-dependent neuronal Klotho enhances astrocytic aerobic glycolysis, J. Cereb. Blood Flow Metab. 39 (2019) 1544–1556. doi:10.1177/0271678X18762700.
[229] A. Hussain, I. Ali, W.A. Kaleem, F. Yasmeen, Correlation between body mass index and lipid profile in patients with type 2 diabetes attending a tertiary care hospital in Peshawar, Pakistan J. Med. Sci. 35 (2019) 591–597. doi:10.12669/pjms.35.3.7.
[230] Y.-N. Kim, S. Kim, Y.-O. Cho, Body mass index was positively correlated with blood triglyceride and total cholesterol levels, FASEB J. 26 (n.d.) lb356–lb356. doi:10.1096/FASEBJ.26.1_SUPPLEMENT.LB356.
[231] A.G. Bakari, C. Onyemelukwe, B.G. Sani, S. Aliyu, S.S. Hassan, T.M. Aliyu, Relationship between casual blood sugar and body mass index in a suburban northern Nigerian population: a short communication., Niger. J. Med. 16 (2007) 77–78. doi:10.4314/njm.v16i1.37287.
[232] N. Satoh, Y. Ogawa, G. Katsuura, Y. Numata, T. Tsuji, M. Hayase, K. Ebihara, H. Masuzaki, K. Hosoda, Y. Yoshimasa, K. Nakao, Sympathetic activation of leptin via the ventromedial hypothalamus: Leptin-induced increase in catecholamine secretion, Diabetes. 48 (1999) 1787–1793. doi:10.2337/diabetes.48.9.1787.
[233] Q. Wang, M. Zhang, G. Ning, W. Gu, T. Su, M. Xu, B. Li, W. Wang, Brown Adipose Tissue in Humans Is Activated by Elevated Plasma Catecholamines Levels and Is Inversely Related to Central Obesity, PLoS One. 6 (2011) e21006. doi:10.1371/journal.pone.0021006.
[234] A.M. Laszczyk, S. Fox-Quick, H.T. Vo, D. Nettles, P.C. Pugh, L. Overstreet-Wadiche, G.D. King, Klotho regulates postnatal neurogenesis and protects against age-related spatial memory loss, Neurobiol. Aging. 59 (2017) 41–54. doi:10.1016/j.neurobiolaging.2017.07.008.
[235] J. Qiu, C. Zhang, A. Borgquist, C.C. Nestor, A.W. Smith, M.A. Bosch, S. Ku, E.J. Wagner, O.K. Rønnekleiv, M.J. Kelly, Insulin excites anorexigenic proopiomelanocortin neurons via activation of canonical transient receptor potential channels, Cell Metab. 19 (2014) 682–693. doi:10.1016/j.cmet.2014.03.004.
[236] C. Blouet, S.-M. Liu, Y.-H. Jo, S. Chua, G.J. Schwartz, TXNIP in Agrp neurons regulates adiposity, energy expenditure, and central leptin sensitivity., J. Neurosci. 32 (2012) 9870–7. doi:10.1523/JNEUROSCI.0353-12.2012.
[237] C. Blouet, G.J. Schwartz, Nutrient-sensing hypothalamic TXNIP links nutrient excess to energy imbalance in mice., J. Neurosci. 31 (2011) 6019–27.

Appendix A: IACUC Approval – AUP 101

EAST CAROLINA UNIVERSITY
ANIMAL USE PROTOCOL (AUP) FORM
LATEST REVISION APRIL, 2017

Project Title: The central role of α-klotho in regulation of metabolism - experimental

	Principal Investigator	Secondary Contact
Name	Hu Huang,	Taylor Landry
Dept.	Kinesiology and Physiology	Kinesiology
Office Ph #	252-737-2879	Click here to enter text.
Cell Ph #	857-540-1871	6039301004
Pager #	Click here to enter text.	Click here to enter text.
Home Ph #	Click here to enter text.	Click here to enter text.
Email	huangh@ecu.edu	landryt17@students.ecu.edu

For IACUC Use Only

AUP #	P101		
New/Renewal	10/3/2019		
Full Review/Date	DR/Date		
Approval Date	12/18/2018		
Study Type	metabolism		
Pain/Distress Category	D		
Surgery - yes	Survival - yes	Multiple - yes	
Prolonged Restraint			
Food/Fluid Regulation			
Other			
Hazard Approval/Dates	Rad	IBC 10/3/2019	EHS 9/5/2019
OHP Enrollment			
Mandatory Training			
Amendments Approved	#1 11/26/2019	#2 4/27/2020	#3 6/25/2020
	#4 10/23/2020		

Appendix B: IACUC Approval – AUP 085

East Carolina University

Animal Care and Use Commitee
212 Ed Warren Life Sciences Building
East Carolina University
Greenville, NC 27834

252-744-2436 office
252-744-2355 fax

October 23, 2013

Hu Huang, Ph.D.
Department of Kinesiology
Ward Sports Medicine Bldg.
ECU Brody School of Medicine

Dear Dr. Huang:

Your Animal Use Protocol entitled, "Central Nervous System Control of Metabolism Responses to Exercise and Diet - Experiments" (AUP #P085) was reviewed by this institution's Animal Care and Use Committee on 10/23/13. The following action was taken by the Committee:

"Approved as submitted"

Please contact Dale Aycock at 744-2997 prior to hazard use

A copy is enclosed for your laboratory files. Please be reminded that all animal procedures must be conducted as described in the approved Animal Use Protocol. Modifications of these procedures cannot be performed without prior approval of the ACUC. The Animal Welfare Act and Public Health Service Guidelines require the ACUC to suspend activities not in accordance with approved procedures and report such activities to the responsible University Official (Vice Chancellor for Health Sciences or Vice Chancellor for Academic Affairs) and appropriate federal Agencies.

Sincerely yours,

Susan McRae, Ph.D.
Chair, Animal Care and Use Committee

SM/jd

Enclosure